Genetic analysis of heading cabbage traits

Performing a genome wide association study in a *Brassica oleracea* collection

Name: Twan Groot
Registration number: 921217285040
Supervisor: dr. ir. A.B. Bonnema
Examiners: dr. ir. A.B. Bonnema
P.F.P. Arens

March 2017

Front image:

VN plants (2017). VN Plants Plantenkwekerij – Mix naar eigen keuze. [online] Available at: <https://www.vnplants.be/producten/kolen/assortiment/> [Accessed 19 March 2017]

Wageningen University

Plant Breeding Department
Growth and Development group

Genetic analysis of heading cabbage traits

Performing a genome wide association study in a *Brassica oleracea* collection

Name: Twan Groot

Registration number: 921217285040

Thesis code: PBR – 80436 | MSc Thesis Plant Breeding

Supervisor: dr. ir. A.B. Bonnema

Examiners: dr. ir. A.B. Bonnema
P.F.P. Arens

March 2017

Abstract

Brassica oleracea is an economically important plant species with a large variation in morphotypes. The genetic regulation of leaf morphology is not fully understood. This study focusses on the genetic basis behind the heading cabbage morphotype. First a population structure was calculated over three iterations with 100.000 burn-in and 50.000 MCMC calculations using STRUCTURE software. The result was a population structure with eight subgroups. TASSEL software was used to calculate marker-trait associations. Three phenotypic datasets, WURField2015, Companies2015 and ZonMW2016, served as phenotypic input in the association analysis. Furthermore, genotypic data was gathered by Sequence Based Genotyping, which resulted in 18.580 Single Nucleotide Polymorphisms. TASSEL calculated many significant marker-trait associations after FDR correction. Due to time constraints, interesting regions for Head Length, Blistering and Head Weight were further analysed in the BolBase genome browser. A search window of 100 Kb around the peak marker identified multiple candidate genes. Candidate genes of Head Length (*CUC2*), Blistering (*CYCU2-1, EXP4/6* and *CUC1*) and Head Weight (*TMK1/4, APUM5, MKK5, GTE4* and *CHC1*) were proposed for further research.

Table of Contents

1. Introduction

In this chapter, the Brassicaceae family and their ancestry is introduced. Furthermore, some background about *B. oleracea* is given and followed up by knowledge on leaf growth. Finally, genes associated with leafy head formation in cabbages are introduced.

1.1. *Brassicaceae* and their ancestry

Brassica is a plant genus which is part of the *Brassicaceae* family and consists of 3709 species and 338 genera of which 308 can be assigned to 44 tribes (Warwick *et al.,* 2006; Warwick *et al.,* 2010). Furthermore, cytogenetic studies confirmed large variation in chromosome number for species within the Brassicaceae family ranging from four to 128 (Appel & Al-Shehbaz, 2003). The *Brassicaceae* family includes many widely cultivated crops. Known products involve vegetable food, oil, condiments and animal feed (Cartea *et al.*, 2011). Furthermore, brassica is an economically important genus with a production of more than 99 million tonnes of vegetable food and 70 million tonnes of oil and in 2013. (FAOSTAT, 2015; Labana *et al., 1993*). Brassica vegetables are known for their nutritional characteristics such as low fat and protein content, high amount of fibre, vitamins and minerals. Besides the standard characteristics, brassicas possess glucosinolates which aid the plant in defence against fungal and bacterial pathogens (Halkier & Gershenzon, 2006) and have antioxidant and anticarcinogenic properties after consumption (Khwaja *et al.,* 2009; Li *et al.,* 2010; Higdon *et al.,* 2007).The six most important cultivated brassica species are given in the 'Triangle of U' and are interrelated (*figure 1*). The diploid species *Brassica rapa* (AA, n=10), *Brassica nigra* (BB, n=8) and *Brassica oleracea* (CC, n=9) are hybridized to the allotetraploid species *Brassica juncea* (AB, n=18), *Brassica napus* (AC, n=19) and *Brassica carinata* (BC, n=17) (Nagaharu, 1935; Prakash & Hinata, 1980).

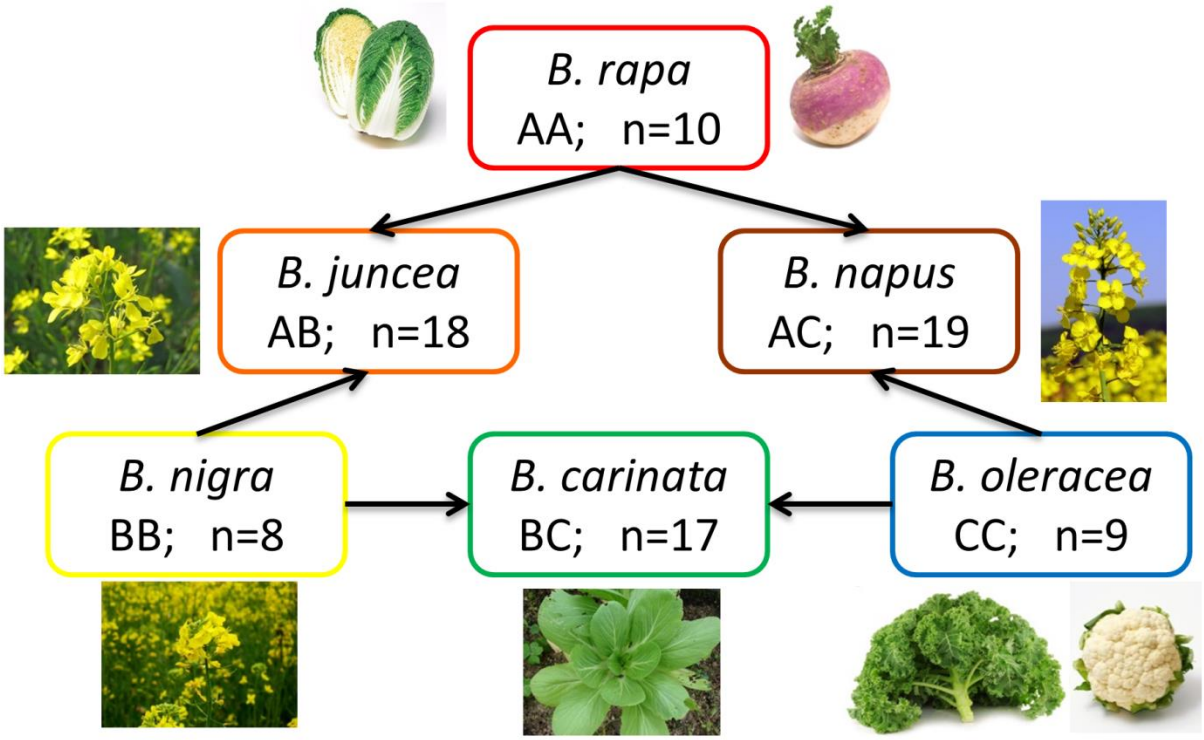

Figure 1: The triangle of U with examples of each species. Diploid genomes of *B. rapa* (AA, Chinese cabbage and turnip), *B. nigra* (BB, black mustard) and *B. oleracea* (CC, curly kale and cauliflower) hybridize to the allotetraploid species *B. juncea* (AB, Ethiopian mustard), *B. napus* (AC, rapeseed) and *B. carinata* (BC, mustard greens) (Fit&Nourished, 2016; REAL, 2016; Toxicologycentre, 2016; Pinterest, 2016; GardensOnline, 2016; Takii seed, 2016; MSU, 2016; Wikipedia, 2016)

Many different morphotypes are present in each species and different organs are consumed as vegetable (*figure 1*). For example, the floral organs of caixin (*B. rapa*) and cauliflower (*B. oleracea*), the leafy head of cabbage (*B. oleracea*), Chinese cabbage *(B. rapa*) and head mustard (*B. juncea*) and the tuberous parts of kohlrabi (*B. oleracea*), turnip (*B. rapa*) and rutabaga (*B. napus*). Besides vegetables for consumption, vegetable oil can be extracted from rapeseed (*B. napus*), sarsons (*B. rapa*) black mustard (*B. nigra*) and Indian mustard (*b. juncea*. Furthermore, Indian mustard (*B. juncea*), black mustard (*B. nigra*) and the related species white mustard (*Sinapis alba*), are used as condiment.

As can be seen in *figure 1*, different brassica species have different chromosome numbers. *B. rapa* has ten pairs of chromosomes whereas *B. oleracea* has nine chromosome pairs. The allopolyploid derived form of *B. rapa* and *B. oleracea*, *B. napus* contains the sum of their chromosomes, 19 in total. Furthermore, 24 large genomic regions were identified, also known as genomic blocks (GB). The GB are arranged in eight, nine or ten chromosomes and are syntenic between genomes of Brassicaceae. (Cheng *et al.,* 2014; Parkin *et al.,* 2005; Schranz *et al.,* 2006; Lysak *et al.,* 2007). Genomes of *Brassicaceae* that contain one set of 24 GB are considered diploid species whereas genomes with more than one set of 24 GB is considered a paleopolyploid species (Cheng *et al.,* 2014). The six species from 'the triangle of U' share a whole genome triplication (WGT) event (Wang *et al.,* 2011; Cheng *et al.,* 2012; Liu *et al.,* 2014; Panjabi *et al.,* 2014). This event took place after the divergence of the brassica ancestor (translocation Proto-Calepineae Karyotype (tPCK)) and *Arabidopsis thaliana* approximately 13 to 17 million years ago (MYA) (Cheng *et al.,* 2013). The WGT event most likely happened in two steps (*figure 2)*.

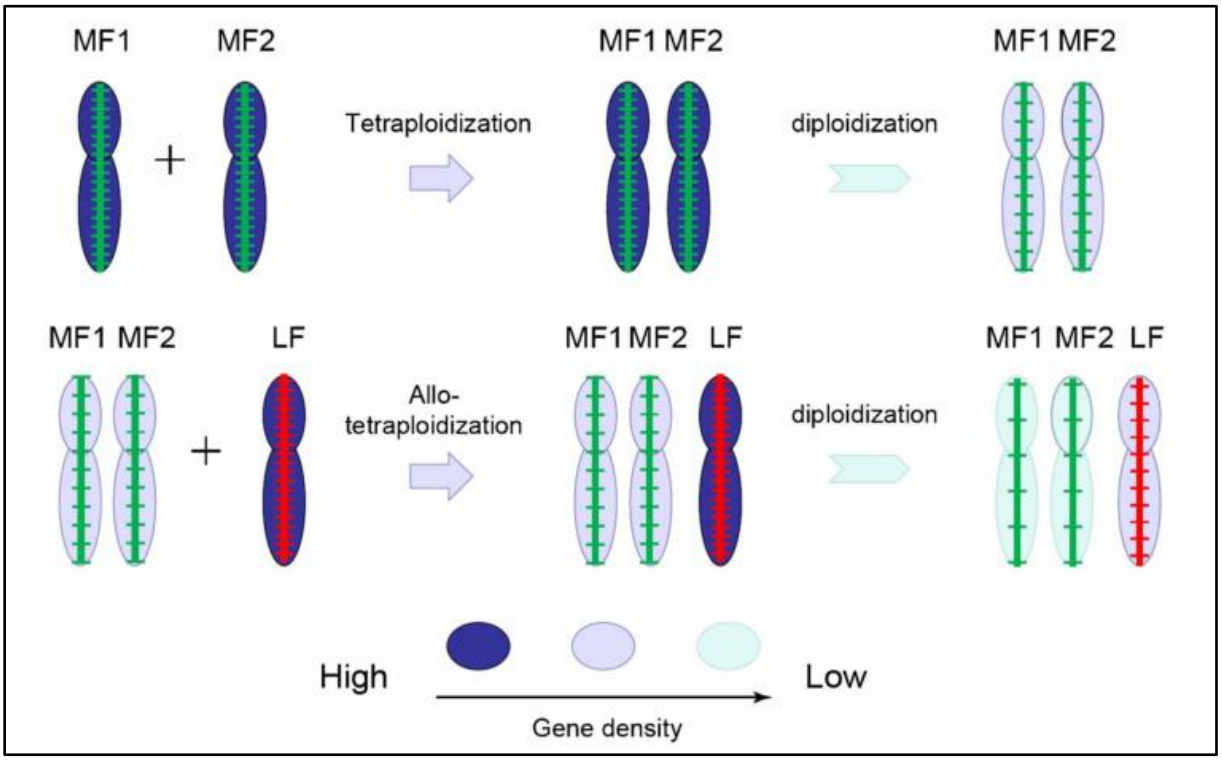

Figure 2: WGT event in two steps, reproduced from Cheng *et al.,* 2014. Two ancestral tPCK genomes combined into a new diploid. Subsequently, a third tPCK genome combined into the ancestor of modern Brassica species. Because MF1 and MF2 merged earlier than MF1MF2 and LF, the MF1 and MF2 are 'more fractioned' than the LF: 'least fractioned'.

In the first step, two tPCK genomes (MF1 and MF2) were combined and due to gene fractioning and genomic reshuffling a new diploid was formed. In the second step, the new

diploid was combined with a third tPCK genome (LF). After a second round of gene fractioning and genomic reshuffling the ancestor of Brassica was formed (Wang *et al.,* 2011; Cheng *et al.,* 2012). The three subgenomes consist of the least fractionated subgenome (LF) and the more fractionated subgenomes (MF1 and MF2). The LF subgenome is higher expressed than the MF subgenomes, which resulted in more fractionation and thus gene loss in the MF subgenomes. The LF subgenome has therefore more functional genes than the MF subgenomes (Cheng *et al.,* 2012). The WGT event and associated gene retention contributed to the large variety of Brassica morphotypes (Cheng *et al.,* 2016).

1.2. *Brassica oleracea*

A species within the *Brassica* genus including many morphotypes is *B. oleracea*. *B. oleracea* is a self-incompatible crop. Therefore, old races are heterogeneous due to open pollination. However, modern hybrids are made from two homozygous parental lines which are crossed to make a hybrid which is heterozygous on many loci with a homogeneous phenotype. Debate has been going on about the origin of wild *B. oleracea*, also known as wild cabbage (Smyth, 1995). The north Atlantic region was proposed (Song *et al.,* 1980) versus the Mediterranean region (Maggioni *et al.,* 2010; Arias *et al.,* 2014). The centres of domestication and genetic diversity are in Europe and wild *B. oleracea* exist along the Atlantic and English Channel coasts (Cartea *et al.,* 2011; Bonnema *et al.,* 2011). By the process of crop domestication, various morphotypes were selected within this species (Gómez-Campo & Prakash, 1999). *B. oleracea* can be divided into nine morphotypes: white, pointed and red cabbage (*B. oleracea* spp*. capitata*), savoy cabbage (*B. oleracea* spp*. sabauda*), Tronchuda cabbage (*B. oleracea* spp*. costata*), cauliflower (*B. oleracea* spp*. botrytis*), broccoli (*B. oleracea* spp*. italica*), kale/collards (*B. oleracea* spp*. acephala*), Chinese kale (*B. oleracea* spp*. alboglabra*), Brussels sprouts (*B. oleracea* spp*. gymnifera*) and kohlrabi (*B. oleracea* spp*. gongylodes*) (*figure 3*).

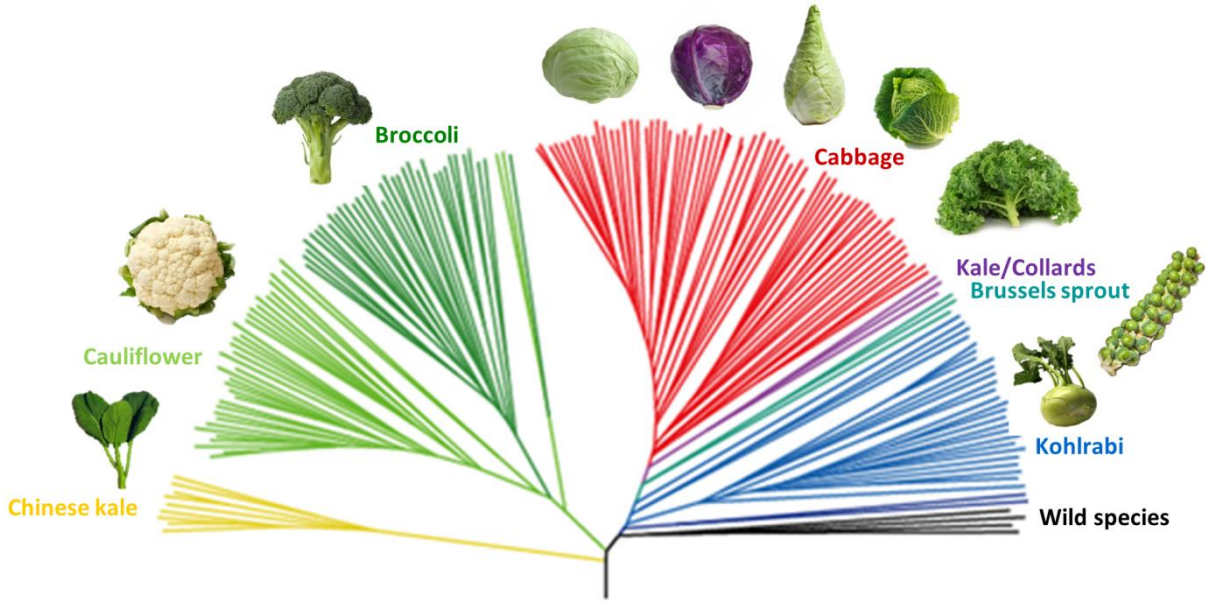

Figure 3: Phylogenetic tree of *B. oleracea*, adapted from Cheng *et al.,* 2016. Each colour resembles a morphotype and eight colours can be discriminated. Yellow: Chinese kale, light green: cauliflower, green: broccoli, red: white/red/pointed/savoy cabbage, purple: kale, light blue: Brussels sprout, blue: kohlrabi and wild species in black (Senome Layang, unknown; Fit&Nourished, 2016; LaoDong, 2016; FruttaWeb, 2016; JordanSeeds, 2016; VanBijOns, 2016; Grillo Services, 2016; REAL, 2016; FoodsWithJudes, 2013; OpenFotos, 2016).

Different plant organs are consumed for many of these morphotypes. Inflorescence are consumed for broccoli and cauliflower whereas the swollen stem is consumed for kohlrabi and axillary buds for Brussels sprouts. Furthermore, leafs are consumed for kale and Chinese kale. Besides loose leafs, folded leaves form a head which is the consumed part of cabbage (Bonnema *et al.,* 2011). A large variation in leaf shape, colour, size and texture is observed when all morphotypes are compared with each other. Furthermore, leaves can aid the crop in improving the quality of edible parts. For instance: the inward folding leaves of cauliflower protect the curd from physical damage and ensures the white colour of the curd by blocking sunlight. Therefore, breeders aim to improve these traits in their crops. However, the genetic regulation of leaf morphology of *B. oleracea* is not fully understood. It is still unknown why certain morphotypes form heads whereas others form a rosette. This makes leaf traits and the genetics behind them interesting to study.

1.3. Leaf development

Plant leaves determine the light capturing area, sense light spectra, temperature, host-plant interactions, tolerance to abiotic stress and day length (Dhkar & Pareek, 2014). To reach a better understanding in leaf morphology, leaf traits should be studied and therefore leaf development is an important starting point. Leaf development is well studied in model species *A. thaliana*, a family member of the *Brassicaceae* family. Leaf development starts in the shoot apical meristem (SAM) where stem cells lose their identity. This is followed by leaf initiation by formation of the leaf primordium. The adaxial/abaxial sides of the leaf are determined by leaf polarity control. Furthermore, leaf width and length are defined by leaf polarity control genes. Subsequently, leaf growth is driven by cytoplasmic growth, cell division and cell expansion. Finally, cell differentiation causes cells to form stomata, vascular tissue or trichomes. The different developmental stages are controlled by various regulatory pathways having hormonal and genetic compounds (Braybrook & Kuhlemeier, 2010; Kalve *et al.,* 2014; Bar & Ori, 2014).

1.3.1. Leaf initiation

The SAM consists of three layers (L1, L2 and L3) and has three zones. The central zone (CZ) consist of undifferentiated cells dividing at a low rate. The peripheral zone (PZ) is faster dividing and cells differentiate in plant organs (Satina *et al*., 1940; Braybrook & Kuhlemeier, 2010). This starts within the rib-zone (RZ) where cells lose their stem cell fate and start dividing. This is regulated by the regulatory loop of *WUSCHEL* (*WUS*) and *CLAVATA* gene products (*CLV1*, *CLV2* and *CLV3*). *WUS* promotes stem cell fate by activating *CLV3* in CZ. Subsequently, *CLV3* binds to *CLV1/2* which inhibit *WUS* activity (*figure 4*). This mechanism makes sure there is a stable number of cells in the SAM and therefore a controlled number of plant organs are formed (Schoof *et al.,* 2000; Carles and Fletcher, 2003; Kalve *et al.,* 2014; Braybrook & Kuhlemeier, 2010).

To form a leaf primordium, the antagonistic relation between KNOTTED-like homeobox (KNOX1) and *ASYMMETRIC LEAF1(AS1)/ROUGH SHEATH2(RS2)/PHANTASTICA(PHAN)* (*ARP* family) plays an important role. KNOX1 makes sure that cells do not differentiate in the SAM by maintaining the cytokinine (CK) biosynthesis. Hereby, the cytokinine/gibberellin (CK/GB) ratio remains constant and stem cell fate is retained (Scofield & Murray, 2006; Yanai *et al*., 2005; Braybrook & Kuhlemeier, 2010; Barkoulas *et al.,* 2007). An auxin maximum is created by auxin influx carrier *AUXIN RESISTANT* (*AUX1*) and efflux transporter *PIN-FORMED1* (*PIN1*). The higher auxin levels downregulate KNOX1 and the cytokinine

biosynthesis is restrained. The leaf primordia is induced by *ARP* genes being expressed (Bayer *et al*., 2009; Geunot *et al*., 2012; Su *et al*., 2011; Byrne *et al*., 2002).

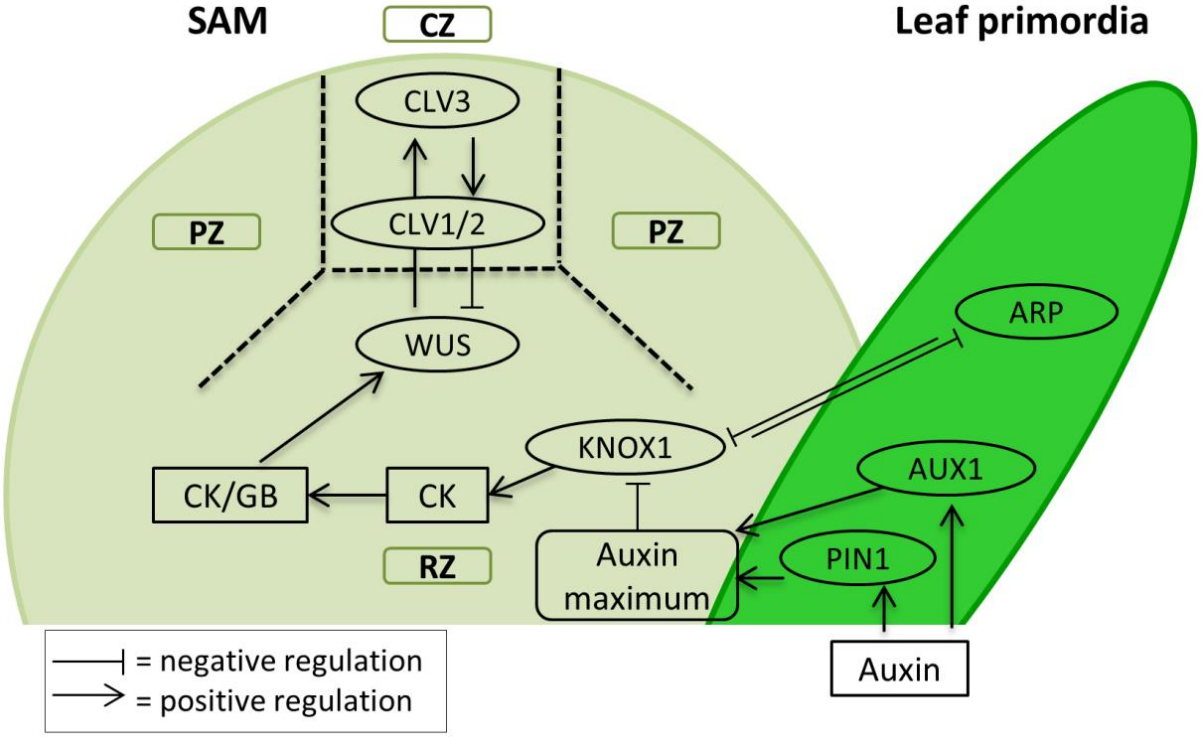

Figure 4: Schematic overview of the shoot apical meristem (SAM) and the leaf primordia. Within the SAM, three zones are present. The central zone (CZ), peripheral zone (PZ) and the rib zone (RZ). Stem cell maintenance is regulated by WUS. High auxin levels supress KNOX1 which triggers ARP to form a leaf primordia.

1.3.2. Adaxial/abaxial leaf polarity

After initiation of the leaf primordia, it is important for the leaf to develop a polarity gradient. Without the adaxial and abaxial side of the leaf defined, the leaf will be malformed because the leaf blade is missing (Waites & Hudson, 1995). Adaxial cell fate is determined by *PHABULOSA* (*PHB*), *PHAVOLUTA* (*PHV*) and *REVOLUTA* (*REV*) genes that encode class III homeodomain-leucine zipper (HD-ZIPIII) proteins (McConnell *et al.,* 2001) (*figure 5*). The abaxial cell fate is determined by expression of the *KANADI* (*KAN*) gene family, *AUXIN RESPONSE FACTOR* (*ARF3* and *4*) gene family members and members of the *YABBY* gene family (Eshed *et al.,* 2004; Siegfried *et al.,* 1999). *KAN, ARF3* and *ARF4* are activated by auxin and positively regulate the expression of *YABBY* genes. In return, *FILAMENTOUS FLOWER/YABBY3* (*FIL/YAB3*) creates a positive feedback loop by stimulating *KAN* and *ARF4* (Bonaccorso *et al.*, 2012).

The above described domains have an antagonistic function. *PHB*/*PHV*/*REV* genes in the abaxial domain are repressed by *KAN* and *KAN* and *YABBY* genes are in the adaxial domain repressed by *PHB*/*PHV*/*REV* (Tsukaya, 2013). Besides the domains, two small RNA also have a function in determining leaf polarity. 21-nucleotide microRNA (miRNA165/166) and 24-nucleotide transacting small interfering RNA (ta-siRNA) have an antagonistic role as well. MiR165/166 stimulates the cleavage of HD-ZIPIII on the adaxial side and is regulated by *ARGONAUTE1* (*AGO1*). Ta-siR-ARF targets *ARF3* and *ARF4* for cleavage and degradation on the abaxial side and is regulated by *AGO7* and *TRANS-ACTING SIRNA3* (*TAS3*) (Kidner & Martienssen, 2004; Adenot *et al.,* 2006).

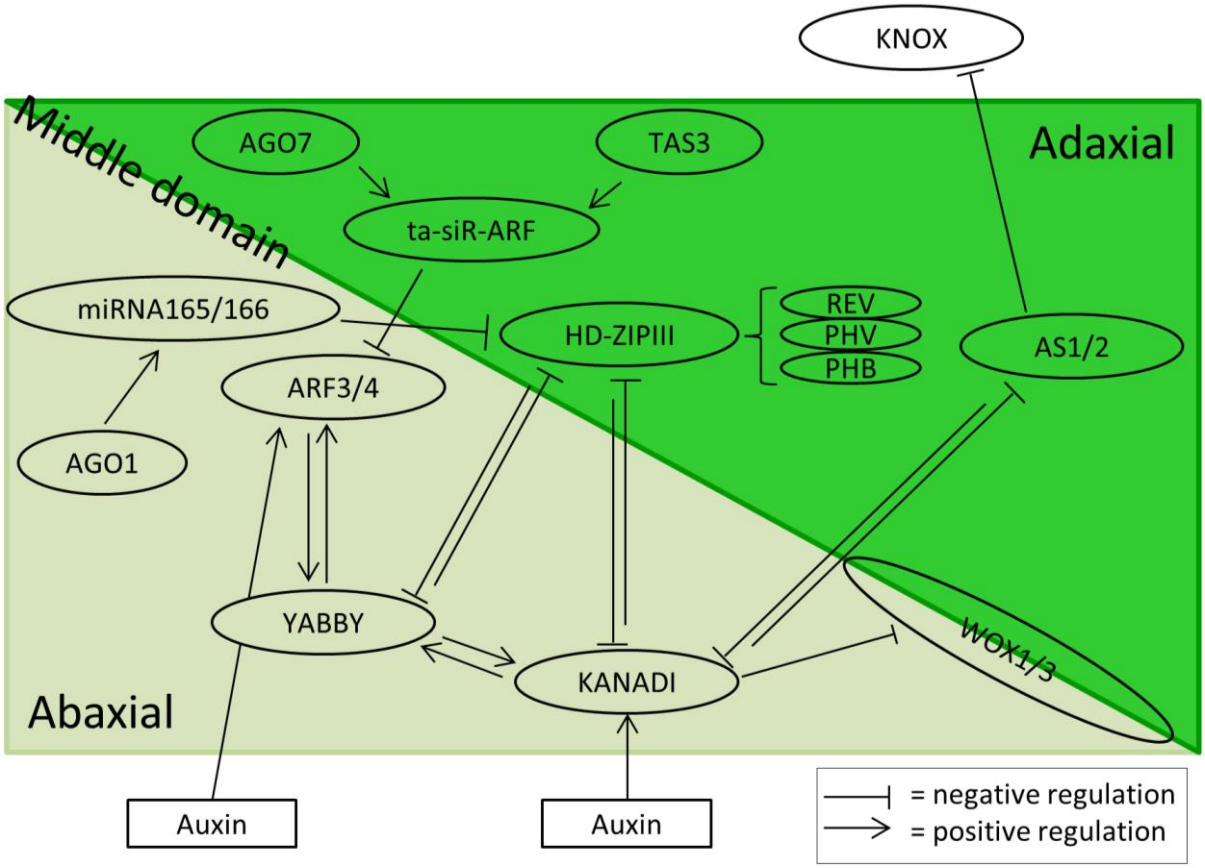

Figure 5: Schematic overview of leaf polarity control. Three domains can be distinguished: the adaxial, abaxial and middle domain.

At the gradient created by the adaxial and abaxial side, *WUS-RELATED HOMEOBOX* (*WOX*) genes are involved in blade growth and margin specific development. In this middle domain, *WOX1* and *WOX3* are repressed by *KAN* (Nakata *et al.,* 2012). In conclusion, this leads to three pathways for leaf polarity (Cheng *et al.,* 2016).

1. *TAS3* - ta-siRNA - *ARF3/ARF4*
   TAS3 downregulates expression of *ARF3/ARF4*, which leads to adaxial cell fate.
2. miR-166 - HD-ZIPIII
   miR-166 downregulates HD-ZIPIII for abaxial cell fate
3. KNOX - *AS1/AS2* - *KAN*
   KNOX expression is repressed by *AS1*/*AS2* for adaxial cell fate. In turn, *AS1*/*AS2* is repressed by *KAN* for abaxial cell fate.

1.3.3. Cell growth: division and expansion

The leaf can start growing after the establishment of the adaxial and abaxial axis. Leaf growth is accomplished by cell division and expansion. To begin cell division, cytoplasmic growth is necessary and the Target of Rapamycin (TOR) pathway supplies the macromolecules (Zhang *et al.,* 2013). Plant hormones auxin, cytokinine, brassinosteroids and gibberellin activate D-type cyclin (CYCD) which in turn activates A-type dependent kinase (CDKA). CDKA is a key protein in cell division throughout the cell cycle (Inzé & de Veylder, 2006; Gaamouche *et al.,* 2010). Auxin plays an important role to make the transition from cell division to cell expansion. Auxin induces the expression of *AUXIN-REGULATED GENE INVOLVED IN ORGAN SIZE* (*ARGOS*). In turn, *ARGOS* regulates the DNA binding protein AINTEGUMENTA (ANT). Besides the ANT family, GROWTH REGULATING FACTOR (GRF) and TEOSINTE BRANCHED/CYCLOIDEA/PCF (TCP) transcription factor

families regulate cell growth (Hu *et al.,* 2003; Kalve *et al.,* 2014). GRF5 has an interaction with GRF-INTERACTING FACTOR1 (GIF1) and both are negatively regulated by miR396. Subsequently, *CINCINNATA* (*CIN-TCP*) negatively regulates miR396 and is involved in a cell cycle checkpoint (Horiguchi *et al.,* 2005; Liu *et al.,* 2009; Rodriguez *et al.,* 2010; Platnik *et al.,* 2003). Besides transcription factors, multiple genes play a role in cell expansion. The putative ubiquitin receptor DA1, that restricts cell proliferation, and E3 ubiquitin ligase BIG BROTHER, that limits organ size, are restricting the duration of cell growth. Furthermore, DA1 cooperates with mediator complex subunit 25 (MED25) to restrict cell growth (Li *et al.,* 2008; Xu & Li, 2011). *KLUH* (*KLU/CYP78A5*) is a regulator of leaf size control (Anastasiou *et al.,* 2007). Moreover, *STRUWWELPETER* (*SWP*) has a function in defining the period of cell growth and acts similar to MED25 (Autran *et al.,* 2002). For cell expansion, the cell wall is loosened by various proteins and this process is vacuole and turgor driven (Scheuring *et al*., 2016). Auxin and brassinoline, a brassinosteroid, induce the activity of P-type plasma membrane proton ATPase (AHA). In turn, AHA activates expansins (EXP), xyloglucanendotransglucosylase/hydrolase (XTH), xyloglucan endohydrolase (XEH) and xyloglucan endotransglucosylase (XET) which results in cell wall loosening (Wolf *et al.,* 2012; Yokoyama & Nishitani, 2001). Genes that are possibly related to cell expansion are *ANGUSTIFOLIA* (*AN3*), *ROTUNDIFOLIA3* (*ROT3*) and *JAGGED* (*JAG*) (Horiguchi *et al.,* 2011; Tsunge *et al.,* 1996; Dinneny *et al.,* 2004).

The final step in the development of a leaf is cell differentiation. Main groups are defined as guard cells, vascular tissue and trichomes. Each of these types have separate genetic pathways which are extensively described in Kalve *et al.,* 2014.

1.4. Current knowledge on leaf and heading traits in *B. oleracea*

The knowledge of leaf development, mainly obtained in *A. thaliana*, as described in the previous paragraphs can be applied to study leaf development of another member of the Brassicaceae family: *B. oleracea*. Few studies have been conducted on leaf morphology in Brassica's. Lan and Paterson, 2001 looked at the F_2 population derived from crosses between rapid cycling *B. oleracea* and three cauliflower varieties: Cantanese, Pusa Katki and Bugh Kana. Traits were correlated to quantitative trait loci (QTLs). However, the WTL have not been fine-mapped and genes underlying the traits were not discovered. In another research project from Sebastian *et al.,* 2002, Brussel sprouts were crossed to cauliflower. Leaf, flowering, axillary bud and stem traits were correlated to QTL regions but no genes were identified.

In a recent study conducted by the Brassica groups of Wageningen Plant Breeding and the Institute of Vegetables of Flowers of the Chinese Academy of Agricultural Sciences, genome resequence data from many genotypes were compared to identify regions of selection for leafy head formation in cabbages. They identified three candidate genes for leaf heading traits: *BoATHB15.2*, *BoKAN2.2* and *BoBRX.2*. *BoATHB15.2* is an orthologue of *ARABIDOPSIS HOMEOBOX 15* and belongs to the HD-ZIPIII gene family. Furthermore, *BoKAN2.2* is an orthologue of the KANADI gene family and *BoBRX.2* is an orthologue of *BREVIS RADIX* (*BRX*). *BRX* plays a role in auxin signalling, brassinosteroid biosynthesis and cytokinine signalling which regulates cell growth and cell size (Mouchel *et al.,* 2006; Li *et al.,* 2009). In addition to *B. oleracea*, Cheng *et al.,* 2016 found either orthologues of these candidate genes or other genes in the same molecular pathway in *B. rapa*. Genes from the ARF family were found besides *KAN* and *BRX* genes.

It is likely that leaf polarity genes play an important role in differentiating heading *B. oleracea* from other *B. oleracea* crop types. Knowledge on leaf formation and leaf growth has been

studies extensively in *A. thaliana*. However, little knowledge on leafy head formation, in for example cabbage (*B. oleracea*), Chinese cabbage (*B. rapa*) and lettuce (*Lactuca sativa*) exists. Leafy head formation is a clear domestication trait and is therefore interesting to study. An approach to identify possible genes is a genome wide association study (GWAS). In addition, leaf formation and regulation has to be studied and accurately described to define traits than can be used in an association analysis.

1.5. GWAS and population structure

A genomic wide association study is an association analysis that can link a phenotypic trait to a location on the genome in large collections of genotypes belonging to a species. An important aspect of this method is that allelic variation is distributed over the genome. Furthermore, prior knowledge about regions or genes is not necessary since a GWAS will identify regions linked to the trait of interest. Association analysis uses the natural variation and historical recombination of the mapping populations (Nordborg & Tavaré, 2002; Risch & Merikangas, 1996). Therefore, it is important to have a sufficient large sample population that effectively provides genetically information (Cantor *et al.,* 2010).

In this study, the mapping population consists of many accessions representing various morphotypes of *B. oleracea*. The *B. oleracea* population is not homogeneous because breeding efforts occurred more within morphotypes than between morphotypes. The breeding efforts resulted in a population structure which can lead to false positives. Especially, when the variation of the trait of interest is strongly associated with a subpopulation. Therefore, it is important to correct the GWAS with a population structure to reduce false positives. A population structure uses allelic information from random molecular markers across the genome to account for genetic relatedness in an association analysis (Zhu *et al.,* 2008). When false positives are accounted for, overcorrection can cause the introduction of false negatives. This is caused by the removal of candidate genes associated with the morphological trait and the population structure. *Figure 6* gives an overview of the steps to perform a GWAS. The germplasm has to be grown to phenotype certain traits. Additionally, germplasm has to be genotyped, for example by sequencing. After sequencing, genome-wide polymorphisms can be called and a population structure can be made. The phenotypic and genotypic data can be combined for association analysis in various association analysis software.

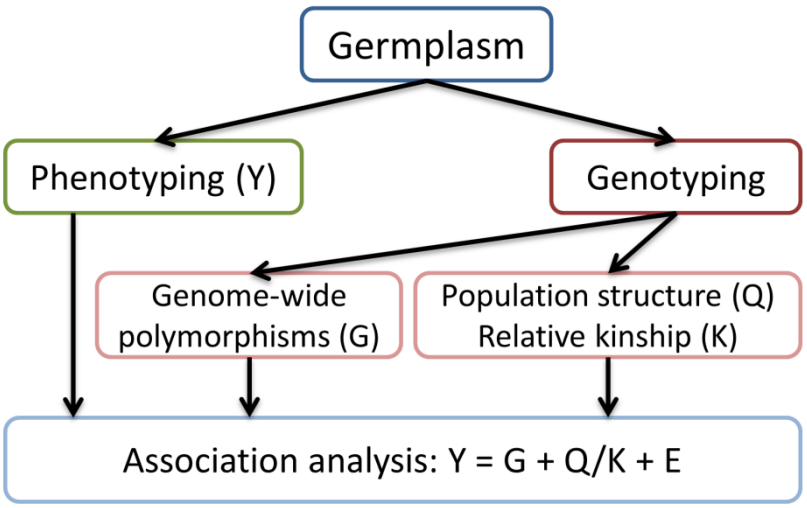

Figure 6: Overview of GWAS adapted from Zhu *et al.,* 2008. The association analysis is performed by finding associations between the phenotype (Y) and the genotype (G) corrected with population structure (Q) and/or kinship correction (K). Residual variance (E) also plays a role in finding associations.

2. Aim

The aim of this thesis will be to study the genetic basis behind leaf morphology in *B. oleracea* and in particular the heading cabbage morphotype. This will be done by performing a GWAS on a collection of *B. oleracea*, representing all morphotypes and consisting of modern hybrids, old landraces and wild species. In order to do so, genotypic data obtained by SBG has to be analysed to call Single Nucleotide Polymorphisms that serve as input to build a population structure and for the association analysis. Furthermore, multiple phenotypic datasets have to be collected and analysed to serve as input for the association analysis.

The following objectives are addressed in this thesis (*figure 7*):

- Organise and analyse phenotypic data from Companies2015
- Collect, organise and analyse phenotypic data from ZonMW2016
- Determine the overlap between three phenotypic datasets (WURField2015, Companies2015 and ZonMW2016)
- Create a population structure from SBG data originating from the TKI 1000 genome project with STRUCTURE software.
- Perform three association analyses with SBG data, population structure and three phenotypic datasets with TASSEL software.
- Screen significant marker trait associations and select regions for candidate gene searches in the *Brassica* database (BolBase/BRAD).

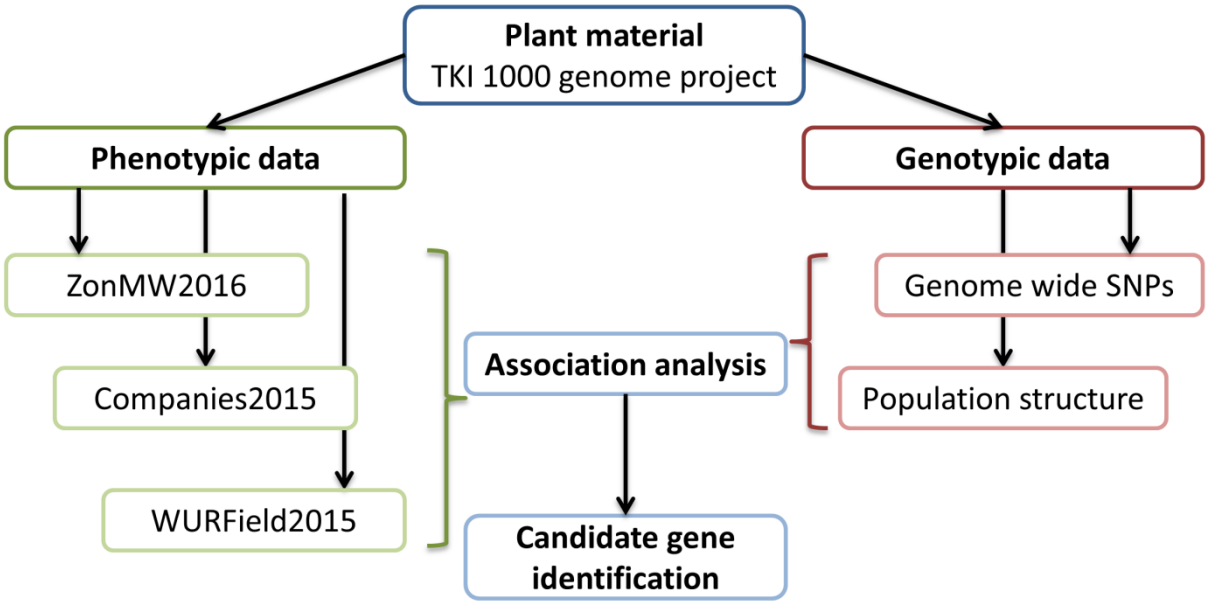

Figure 7: Overview of the thesis. The foundation lies with the plant material of the TKI project. Three phenotypic datasets are derived from the plant material. Furthermore, genotypic data is based on the plant material. These phenotypic and genotypic data combined allows an association analysis.

3. Materials and methods

All data, genomic and phenotypic, originate from a TKI project: 1000 *B. oleracea* genomes which started in 2015. The project has the goal to genotype 1000 different *B. oleracea* genomes to reveal the genetic diversity in modern hybrids, genebank accessions and wild accessions across different morphotypes. The group of Guusje Bonnema is cooperating in this project with 7 other companies. Bejo, Hazera, Rijk Zwaan, Syngenta, Enza and Takii as breeding companies and KeyGene as molecular marker provider. For the genomic data, Sequence based genotyping (SBG) was performed and was used to determine the population structure. Furthermore, it served as genomic input for the GWAS. Three phenotypic datasets were collected in multiple years on multiple sites which served as input for the GWAS.

3.1. Plant material

In the TKI 1000 genomes project, 936 unique modern hybrids (380) and genebank material (556) which consist of landraces and wild material were send for genotyping. For the ease of communication the modern hybrids, landraces and wild material will be called accessions. In *figure 8*, the 936 accessions are shown divided over 11 morphotypes. Heading cabbage (orange) is the largest group which can be separated in sub-morphotypes. Furthermore, cauliflower and broccoli are represented in larger numbers. Kale, kohlrabi, Brussels sprouts and C9 *Brassica* species are represented in medium quantities. The rest of the morphotypes are represented in small numbers.

White cabbage is represented in large numbers compared to red, savoy and pointed cabbage. This is due to the fact that white cabbage has the largest variation compared to other heading cabbage types.

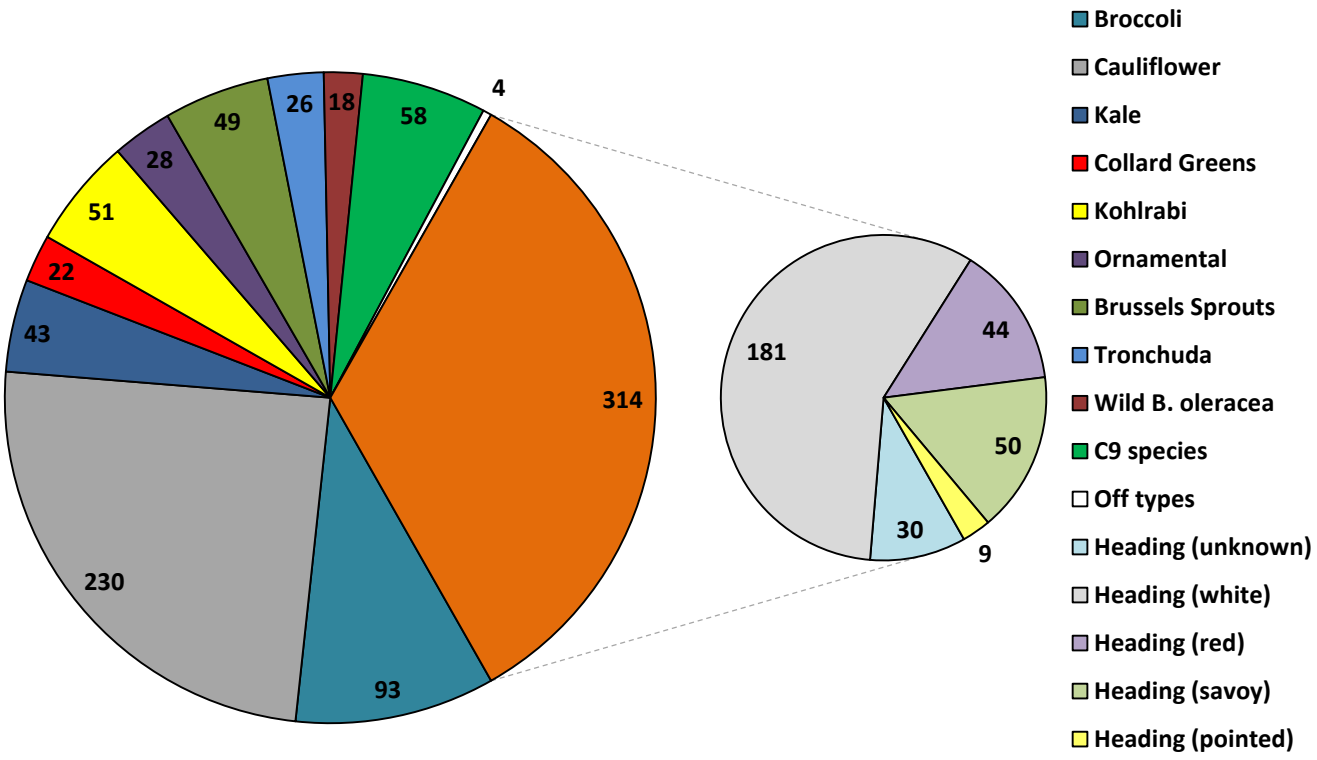

Figure 8: Overview of the plant material in the TKI 1000 genome project (n=936). 11 morphotypes can be distinguished in the left pie chart with a total of 936 unique accessions. The right pie chart shows the morphotype of heading cabbage (orange, 314) divided into sub-morphotypes.

3.2. Genomic data

In this section, the genotypic data will be explained. SBG was performed on the plant material described above. For hybrids, which are homogeneous, DNA was isolated from the hypocotyls and cotyledons of 50-100 seedlings. For genebank accessions and accessions representing wild Brassica's, DNA was isolated from single plants representing the heterogeneous accession. After processing by a bioinformatician, this genotypic data served as input for a population structure and subsequent association analysis.

3.2.1. Sequence Based Genotyping

Sequence based genotyping is a genotyping method developed by KeyGene N.V. A genome reduction step is performed by cutting the genome with two restriction enzymes. PstI (5'-CTGCA/G-3') and MseI (5'-T/TAA-3') were chosen to cut the DNA which have a recognition site of six and four nucleotides long. Furthermore, two selective nucleotides (GC) were attached to the MseI end to control the amount of cuts made. The fragment flanked by PstI-MseI sites plus the two selective nucleotides was sequenced from the PstI site by Illumina sequencing resulting in sequence data with an approximate length of 120 base pairs.
SEED software was used for variant calling on the Binary Alignment/Map (BAM) files. Loci were selected that occur in at least 800 of the 1008 accessions and have at least two reads coverage. Only Single Nucleotide Polymorphism (SNPs) were retained, InDels were not considered for this analysis. The reads with a mapping quality of five or higher were mapped to a unique location on reference genome of homozygous white cabbage line 02-12 (Liu *et al.,* 2014) by Theo Borm. The reads mapped to nine chromosomes representing the genome of *B. oleracea* with a length of approximately 500 Mb. The reads that did not map to the reference genome were assigned to fictional chromosome C00 with three times 'N' between reads. The germplasm contained duplicates for a diversity panel which were removed after mapping. This resulted in a dataset of 85.532 loci (SNPs) in 943 accessions in Variant Call Format (VCF).
The dataset is filtered with a genotype call of 80% which resulted in 85.168 remaining loci. Furthermore, a minor allele frequency (MAF) was chosen of 2.5% which resulted in 18.580 loci with an allele frequency > 2.5 %. Accessions with more than 60% missing values were removed from the dataset. This dataset with 18.580 loci in 913 accessions will be used as genotypic input for the association analysis. To calculate a population structure, the dataset was thinned to have a reasonable computational time. Loci were selected with ≥ 250 Kb distance. This resulted in 1376 SNP markers evenly distributed over the genome with an average distance of 0.36 Mb.

3.2.2. Population structure

The population structure was calculated using the 913 accessions and SNP markers described in section 3.1.1. However, due to time and computational limitations 459 SNP markers were used to calculate a population structure. The population structure program STRUCTURE 2.3.4 (Pritchard *et al.,* 2002) was used to perform the calculations. The SNPs were converted from VCF to STRUCTURE format using PGDSpider 2.1.0.3 (Lischer & Excoffier, 2012). PGDSpider was run with only SNP markers and the numeric format has five values: 1 for Guanine, 2 for Cytosine, 3 for Tyrosine, 4 for Adenine and -9 for a missing value.
STRUCTURE was run with a burnin period of 100.000 runs followed up by 50.000 Markov chain Monte Carlo (MCMC) calculations. All calculations were performed three times with the assumption of two to 12 subpopulations (K). The optimal number of subpopulations was

determined by StructureHarvester (Earl, 2012; Evanno *et al.,* 2005). In StructureHarvester, four graphs are shown:

1. L(K) The likelihood per K — Pritchard *et al.,* 2002
2. L'(K) The first rate of change of L(K) — Evanno *et al.,* 2005
3. |L''(K)| The second rate of change of L'(K) — Evanno *et al.,* 2005
4. ΔK |L''(K)| / StDev(L(K)) — Evanno *et al.,* 2005

In the first graph from Pritchard *et al*., 2002, a plateau could indicate the optimal K and is calculated by: $Optimal\ K = (K\ at\ plateau) - 1$
Furthermore, the fourth graph (ΔK) shows a peak at the optimal K. When an optimal K was chosen, the Q matrices from three iterations were compared for data consistency. The goal is to verify if each accession was assigned to the same K. One Q matrix is selected and served as input for the association analysis. Furthermore, STRUCTURE provides bar plots to visualize the results. Q matrix values ≥ 50% were used for the description of the composition of the different populations (K).

3.2.3. GWAS

The association analysis was performed with TASSEL software version 5.2.33 (Bradbury *et al.,* 2007). A General Linear Model (GLM) was chosen to calculate marker-trait associations. The model requires two or three input files. Genotypic data: described in section 3.2.1, an optional population structure: described in section 3.2.2 and phenotypic data: described in paragraph 3.3. The GLM was run with 999 permutations to control the experiment-wise error rate for individual phenotypes (Anderson & ter Braak, 2003). Significant marker-trait associations were determined by the False Discovery Rate (FDR) (Benjamini & Hochberg, 1995; Pike, 2011). The FDR threshold was set at 0.01 which lead to a significant marker-trait association when the q-value ≤ 0.01. Significant associations were visualized by Manhattan plots. From these Manhattan plots, markers were selected that increase in LOD score when we compare the GWAS without and with population structure respectively. Furthermore, markers that are associated with a trait in multiple datasets have a higher possibility to be truly associated. Candidate regions were investigated in BolBase (Yu *et al.,* 2013).

3.3. Phenotypic data

In this section, three datasets will be explained that served as input for the association analysis. In *figure 9*, each dataset: WUR_Field_2015, Companies2015 & ZonMW2016 is depicted in A, B and C respectively. The composition of the datasets is more or less the same with white cabbage as the largest group.

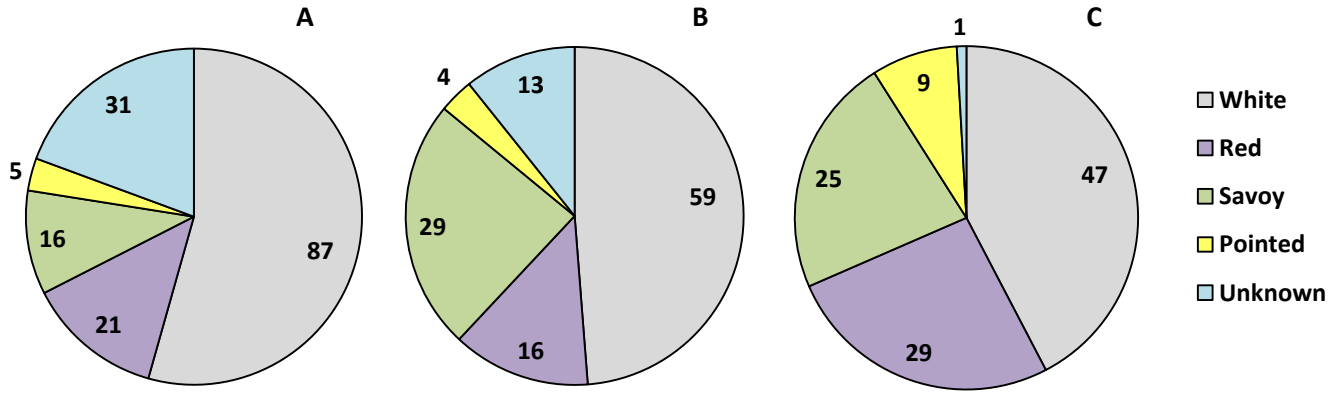

Figure 9: Overview of heading sub-morphotypes in three datasets. A: WUR_Field_2015 (n=160), B: Companies2015 (n=121) and C: ZonMW2016 (n=111)

Some accessions occur in multiple datasets. To gain insight in the overlap between datasets, a Venn-diagram was created (*figure 10*). Dataset ZonMW2016 has 10 unique accessions, 61 shared accessions with WUR_Field_2015 and 40 accessions shared with Companies 2015. Furthermore, WUR_Field_2015 and Comapnies2015 have 20 accessions in common which leads to 79 unique accessions in WUR_Field_2015 and 61 unique accessions in Companies 2015. Only two accessions are shared between all datasets. A large amount of shared accessions between datasets is desirable to estimate the correlation between datasets. If the correlation of similar traits is high, they can be compared with each other. However, small overlap between datasets has advantages as well. When the same association is found in multiple datasets with little overlap, it is a good indication that the association is a true association.

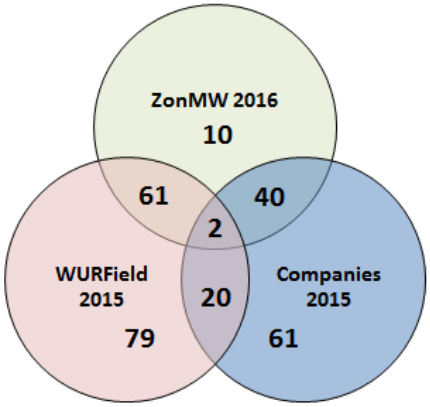

Figure 10: Venn diagram indicating shared accessions between datasets.

3.3.1. WURField2015

In 2015, a trial field was constructed at the Grebbedijk (clay soil) in Wageningen. The goal of this trial field was to generate phenotypic data of leaf and heading traits (a*ppendix 1.1*). 465 accessions from the TKI 1000 genome project were sown in April 2015 and transplanted to the field after four weeks with a total of five plants per accession. 160 accessions were heading cabbage (*figure 10A*) and three cabbage heads per accession were harvested 152 days after sowing. The heads were cleaved and photographed from the frontal side. Subsequently, parameters in *table 1* were measured by visual scoring, weighing and picture analysis with ImageJ.

Table 1: Heading cabbage parameters defined by Slob, 2016.

Trait	Abbreviation	Description	Unit
Head Area	HA	Surface area of the midsection of the head	mm^2
Head Volume	HV	Volume of a fitted spheroid	mm^3
Head Length	HL	Maximum length of the head	mm
Head Width	HWi	Maximum width of the head	mm
Total Weight	TW	Fresh weight of above ground biomass	g
Head Weight	HWe	Fresh weight of the head	g
Head Weight Percentage	HWeP	HWe percentage of TW	%
Head Density	HD	HWe/HV	g/mm^3
Head Index	HI	Ratio of HL/HWi	#
Head Shape	HS	UPOV scale	scale
Head Roundness	HR	4 x (HA/(π x length major axis of a fitted ellipse))	#

3.3.2. Companies2015: Subset TKI 1000 genome project

In 2015, cooperating companies in the TKI 1000 genome project tested 121 genebank and wild accessions at their own facilities for authenticity of the accession. White and pointed cabbage were phenotyped at Rijk Zwaan in De Lier. Red cabbage was phenotyped at Hazera in Tuitjenhorn and savoy cabbage was scored at Syngenta in Enkhuizen. In *figure 10B*, the number of accessions per sub-morphotype is shown. Each cabbage type was

scored by different companies. Furthermore, some traits were not measured in all cabbage types. The traits that were used for association analysis are shown in *table 2* while the whole set of traits is presented in *appendix 1.2*.

Table 2: Selection of parameters from Companies2015.

Trait	Abbreviation	Description	Unit
Head Weight	HWe	Fresh weight of the head	g
Stem Length	SL	Maximum length of the stem of the whole plant	cm
Head Length	HL	Maximum length of the head	cm
Head Width	HWi	Maximum width of the head	cm
Core Length	CL	Maximum length of the core within the head	cm
Uniformity	U	Degree of uniformity between replicates 9=Very uniform | 5=Intermediate | 1=Very heterogeneous	scale
Blistering	B	Degree of Blistering of the leaf 9=Very fine highly blistered | 1=Smooth	scale
Head Density	HD	Density of the cabbage head 9=Solid build-up | 1=Very open	scale

3.3.3. ZonMW2016: ZonMW 3D Digileaf

The ZonMW: 3D Digileaf project initiated in 2016 and is a cooperation between the group of Guusje Bonnema and the department of computer vision & plant phenotyping (WUR Glastuinbouw). The goal of the project is to identify and quantify parameters describing the variation in leafs and cabbage heads from a *B. oleracea* collection. Brassica leaves are known for their curvature and bubbling surfaces. Therefore, 3 dimensional (D) cameras were used. In this thesis only data will be analysed concerning heading cabbage.

Table 3: Overview of measured traits in ZonMW2016. In total, 10 out of 12 traits were measured of which 9 were measured by picture analysis.

Trait	Abbreviation	Description	Unit
Head Length	HL	Maximum length of the head	mm
Head Width	HWi	Maximum width of the head	mm
Core Length	CL	Maximum length of the core within the head	mm
Head Weight	HWe	Fresh weight of the head	g
Head Volume	HV	Volume of the head	mm^3
Head Density	HD	Density of the head	#
Head Shape: Roundness	R	Roundness of the cabbage head	#
Head Shape: AreaRatio	AR	Ratio of area for cabbage upper/lower widths	#
Head Shape: Phi	P	Orientation of ellipse fitted to the cabbage	#
Head Shape: Anisomety	A	Radius y- axis direction/Radius x-axis direction (of fitted ellipse)	#
Head Shape: Maxwidth row over half length	M	HWi / (½HL)	#
Head Shape: Length over Width	LoW	HL/HWi	#

A trial field was constructed at the Grebbedijk (clay soil), Wageningen with a randomized block design with two blocks. In September 2016 after ~150 days of sowing, the heads of heading cabbage were harvested. Three representative cabbages per accession per block were harvested and transferred to Unifarm. On the same day, the cabbage heads were cleaved and pictures were taken from the cross section side and the frontal side with a 3D camera setup. The analysis of the pictures was performed by Danijela Vukadinovic and Gerrit Polder. An overview of the measured traits is shown in *table 3*.

Head Length (HL), Head Width (HWi) and Head Weight (HWe) are straight forward traits which represent the length, width and weight of the cabbage head. Furthermore, Core Length (CL) represents the maximum length of the core or pith in the cabbage head (*figure 11*). Due to time limitations, Head Volume (HV) and Head Density (HD) were not analysed by picture analysis.
The qualitative trait Head Shape was subdivided in six quantitative parameters (*appendix 1.3*). The parameter Roundness (R) is calculated by subtracting the standard deviation over the distance of radii from one:

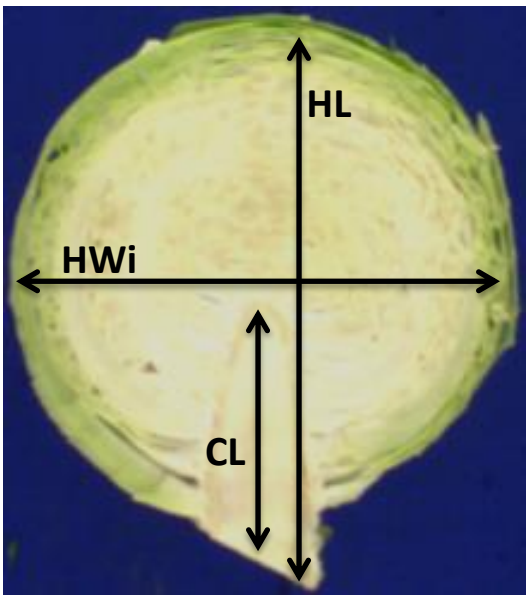

Figure 11: White cabbage head with Head Length, Head Width and Core Length.

$$Roundness\ (R) = 1 - \frac{Sigma}{Distance}$$

For the parameter AreaRatio (AR), the cabbage is divided into two halves. The width of the cabbage is measured from top to bottom for the upper half and lower half. This has resulted in a plot of which the area was calculated for the upper and lower half. The area under the graph of the upper half was called S1 and the area under the lower half was called S2. The AR was calculated by:

$$AreaRatio\ (AR) = \frac{S1}{S2}$$

The parameter Phi (P) holds the orientation of a fitted ellipse on the cabbage. An x-axis is drawn over the image, then an ellipse is fitted to the cabbage head. Two radii are drawn: one radius in y-axis direction (Ra) and one radius in x-axis direction (Rb). The angle between Ra and the x-axis over the image defines P. Furthermore, Anisometry (A) is defined by:

$$Anisometry\ (A) = \frac{Ra}{Rb}$$

The parameter Maxwidth row over half length (M) is calculated by defining the HL and HWi of the cabbage head. Subsequently, the position of HWi (counted from top to bottom) is divided by half HL.

$$Maxwidth\ row\ over\ half\ length\ (M) = \frac{position\ HWi}{\frac{1}{2}HL}$$

The parameter Length over width (LoW) is calculated similar to M. Again, the HL and HWi are defined. Then, the HL is divided by the HWi:

$$Length\ over\ width\ (LoW) = \frac{HL}{HWi}$$

3.3.4. Statistical analysis

The phenotypic data from Companies2015 and ZonMW2016 are analysed with GenStat 18th edition (VSN International, 2015). The Pearson correlation test was used to calculate the correlation between traits within and between datasets. The correlation matrix is shown to visualize the results. Furthermore, normality assumptions were checked by Quantile-Quantile (Q-Q) plots. To identify significant differences between morphotypes for each trait, a one-way ANOVA test was conducted. In addition, a Fisher's Protected LSD was calculated to identify significant differences. The differences were visualized by boxplots.

4. Results

First, phenotypic data from Companies2015 and ZonMW2016 will be presented (*paragraph 4.1*). In *paragraph 4.2*, the population structure is treated and the results of the GWAS is described in *paragraph 4.3*. Finally, some candidate genes for a subset of the marker trait associations will be presented.

4.1. Phenotypic data

Phenotypic data from two datasets will be presented in this section. The third dataset, WURField2015 was already analysied previous year by Slob, 2016. Correlations between traits within datasets are shown and the variance between morphotypes is tested with a one-way ANOVA followed by a Fisher's protected LSD for each trait. Significant differences of traits between different cabbage types (white, red, savoy and pointed) are presented.

4.1.1. Companies2015

In the Companies2015 dataset, 121 heading cabbage accessions were phenotyped belonging to four morphotypes. However, not all eight traits were scored for all cabbage types. Only 46 accessions contained data for all traits. Based on these accessions, a Pearson correlation matrix was calculated. Head Weight and Head Width have a positive correlation (r =0.64). Other correlations involving Blistering, Head Density, Head Length, Core Length, Stem Length and Uniformity were not found in this dataset (*appendix 6.1*). Normality assumptions were checked for the eight traits that were scored. The distribution was analysed by Q-Q plots with a 95% confidence interval (*appendix 6.2*). As can be seen, Blistering, Head Density and Uniformity were scored in a qualitative manner which does not lead to normally distributed data. Significant differences were found between cabbage types for all traits except Core Length (*figure 12 & appendix 6.3 & 6.4*). For Head Density, savoy is less dense than white and red cabbage. Based on Head Weight, savoy is lighter than white and red cabbage (*figure 12*).

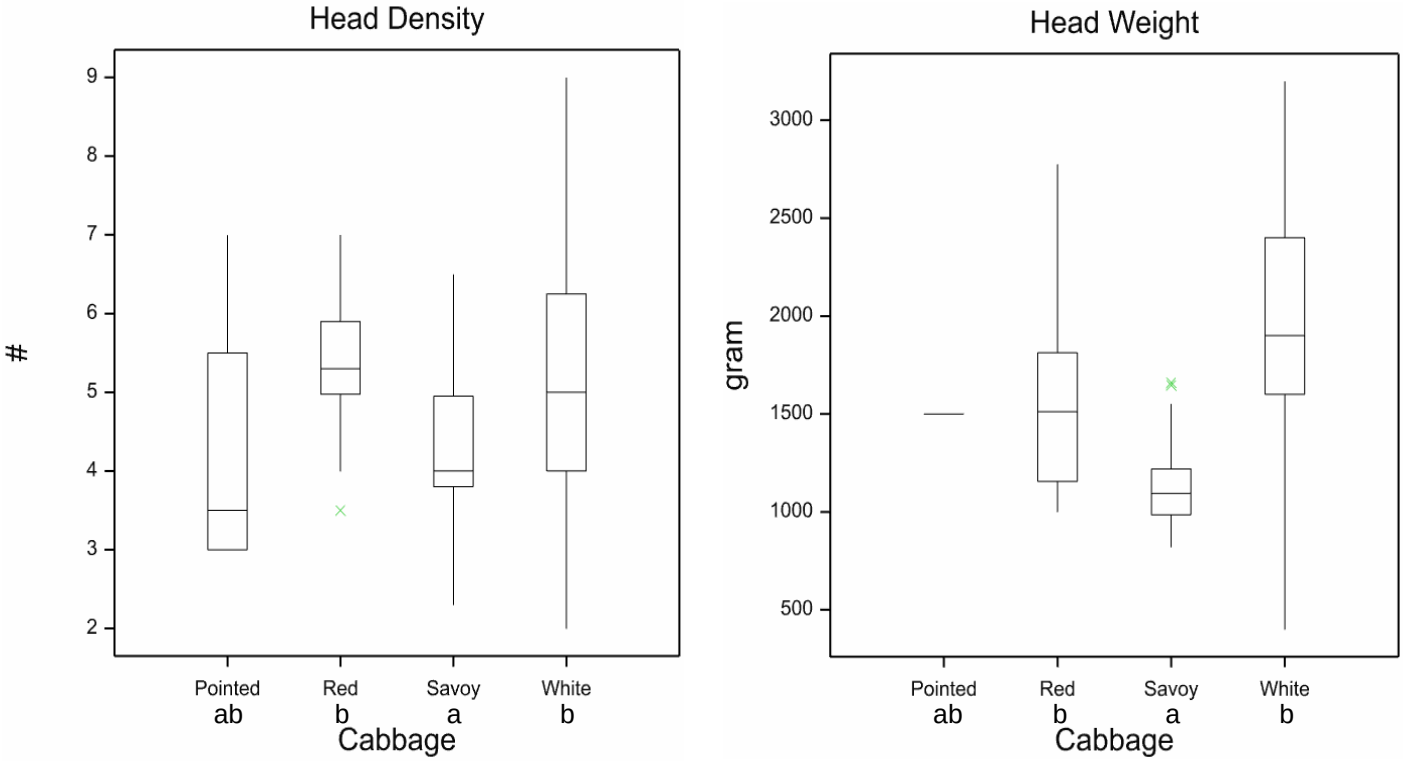

Figure 12: Boxplot for Head Density (left, n=109) and Head Weight (right, n=95). Letters on the x-axis (a or b) indicate significant differences ($p \leq 0.05$) identified by Fishers's Protected LSD.

Leaf blistering is a typical savoy cabbage trait that was not measured in red cabbage. However, it was measured in white and pointed cabbage. Unsurprisingly, savoy has more severe blistering than white and pointed cabbage. Core Length showed no significant differences between cabbage types. For Head Length, pointed is significantly longer than red, savoy and white cabbage. Additionally, white cabbages are on average broader than pointed, red and savoy cabbages for Head Width. Red cabbage is more uniform than white and savoy cabbage (*appendix 6.3 & 6.4*).

4.1.2. ZonMW 3D Digileaf

In the ZonMW2016 dataset, 111 heading cabbage accessions were present. A block effect was identified for HL and LoW (*appendix 5.3 & 5.4*). Therefore, HL and LoW from block A and B were treated as separate traits in the analysis. In the dataset, ten traits were measured and 86 accessions contained information for each trait. The Pearson correlation matrix was based on these accessions (*figure 13*). Values ≥ 0.5 or ≤ -0.5 are considered correlated (*appendix 5.5*).

Core Length is positively correlated with Head Length (r =0.58) and Head Weight (r =0.52). Furthermore, both Head Length and Head Width are positively correlated with Head Weight (r =0.53 & r =0.52). Head Width is also positively correlated with Anisometry (r =0.54). Length over Width (LoW) is positively correlated with Head Length (r =0.52) but negatively correlated with Head Width (r =0.71). Maxwidth over half Length (M) is positively correlated with Anisometry (r =0.59) and Head Width (r =0.53) but negatively correlated with Area Ratio (r =0.85). Phi is positively correlated with LoW (r =0.60). Finally, Roundness is positively correlated with Area Ratio (r =0.50) but negatively correlated with Anisometry (r =0.78) and M (r =0.61).

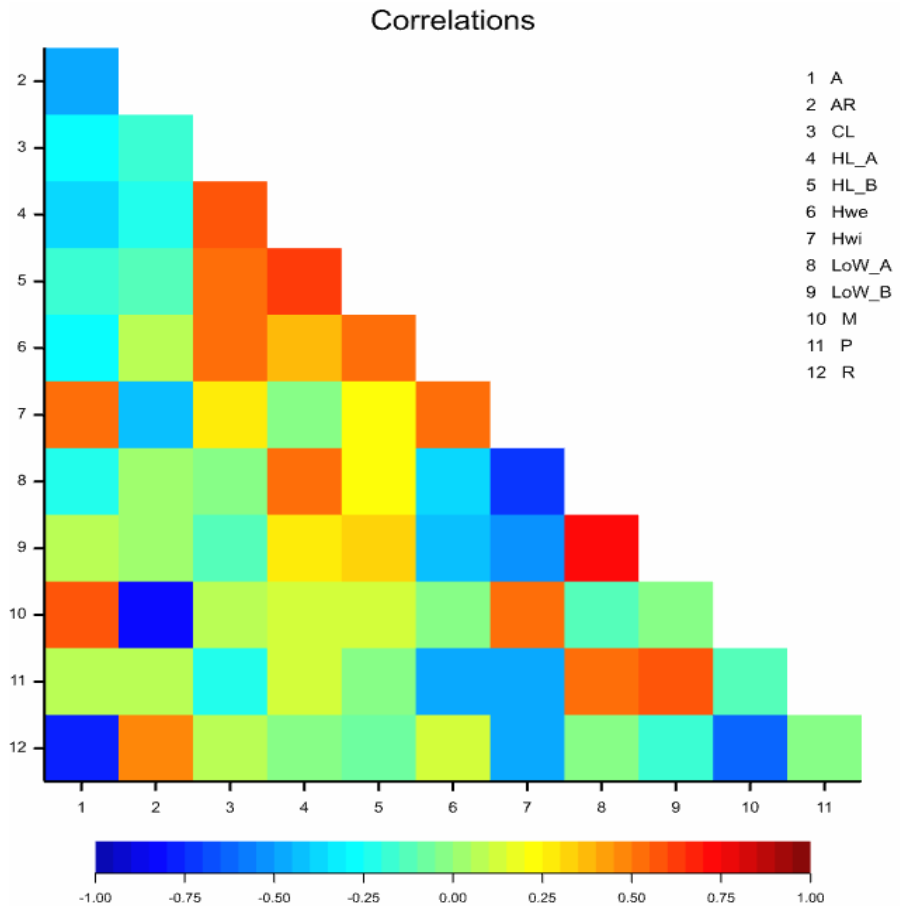

Figure 13: Pearson correlation matrix for traits in ZonMW2016 (n=86). A red/orange colour indicated a positive correlation whereas a blue colour indicates a negative correlation between traits.

Normality assumptions were violated for Anisometry, Phi and Roundness (*appendix 5.6*). Head Length, Head Width, Head Weight, Core Length, Length over Width, AreaRatio and Maxwidth over half Length are around normal distributed in the Q-Q plot. Significant differences were found between morphotypes for all traits except Anisometry (*appendix 5.7 & 5.8*). In contrast to Companies2015, Core Length of pointed cabbage is the largest followed by white, savoy and red cabbage. Furthermore, pointed cabbage has the longest Head Length. White cabbage heads are longer than savoy cabbages whereas red cabbage cannot be distinguished from white and savoy cabbage (*figure 14*).

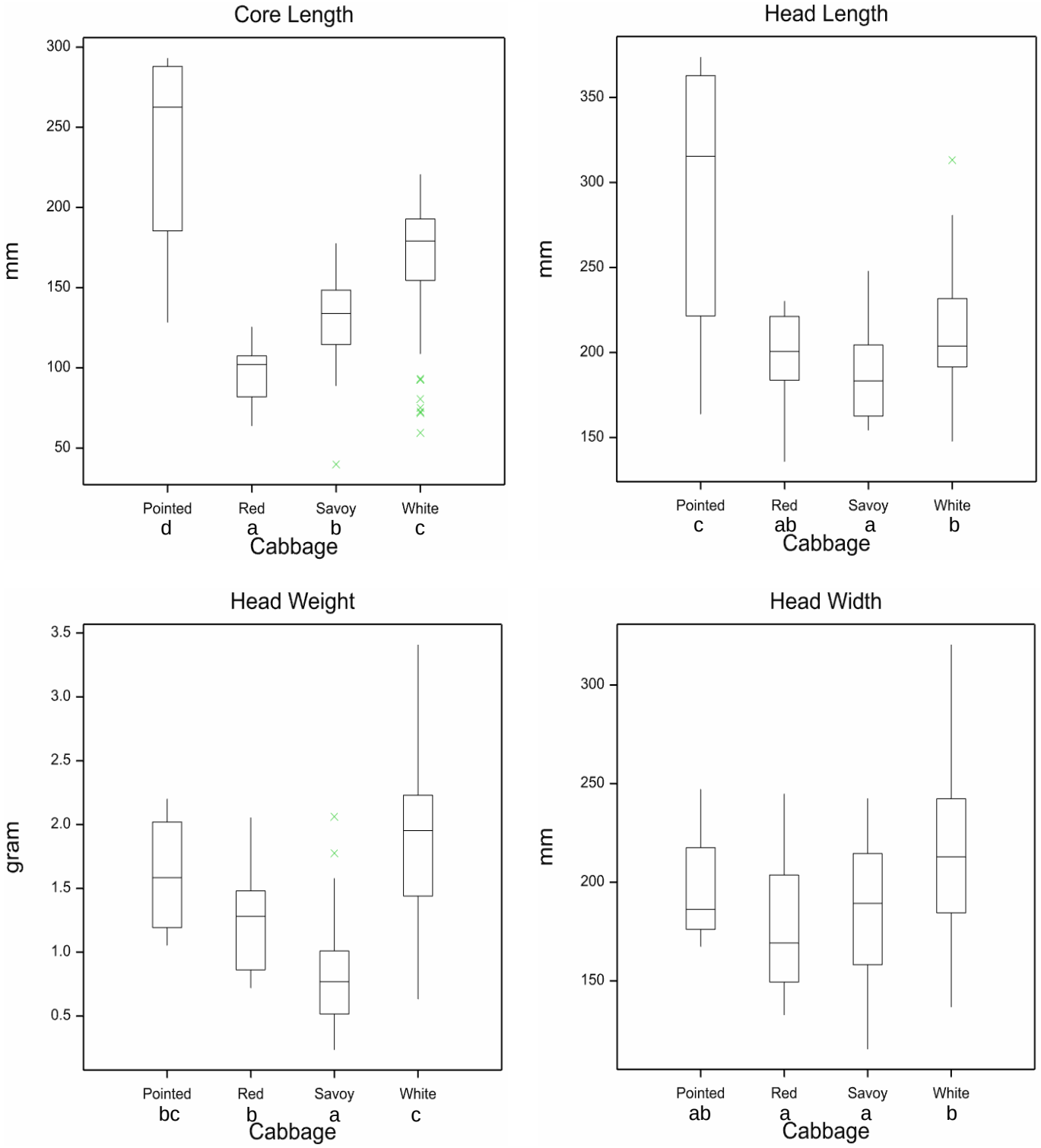

Figure 14: Boxplot for Core Length (upper left, n=110), head Length (upper right, n=102), Head Weight (lower left, n=110) and Head Width (lower right, n=110).

White cabbage has the highest Head Weight. Pointed does not differ from red or savoy but red is heavier than savoy cabbage. White cabbage has a higher Head Width than red and savoy cabbage (*figure 14)*.
Anisometry does not have significant differences between cabbage types. Pointed cabbage has a lower AreaRatio than red, savoy and white cabbage. Length over Width of white and savoy cabbages is lower than red and pointed cabbage. Maxwidth over half Length of red and white cabbages is lower than savoy and pointed cabbages. Phi of white cabbage is lower than red and pointed cabbage whereas pointed is higher than savoy and white cabbage. Roundness of pointed cabbage is lower than savoy and white cabbage and Roundness of white cabbage is higher than red and pointed cabbage (*appendix 5.7* & *5.8*).

4.2. Population structure

The population structure was established with 459 SNP markers genotyped in 913 accessions using three iterations with 100.000 burn-in and 50.000 MCMC calculations. Based on the likelihood of K in the output from Pritchard *et al*., 2002 in *figure 15A*, more or less two plateaus are formed. One plateau at K=9 and another plateau at K=11 which would indicate a righteous K of eight or ten. Error bars indicate the standard deviation over the three iterations. Furthermore, the Evanno *et al.,* 2005 visualisation method shows a clear peak at K=8 in *figure 15B*. Based on these findings, eight subpopulations were chosen as the optimal number of subpopulations.

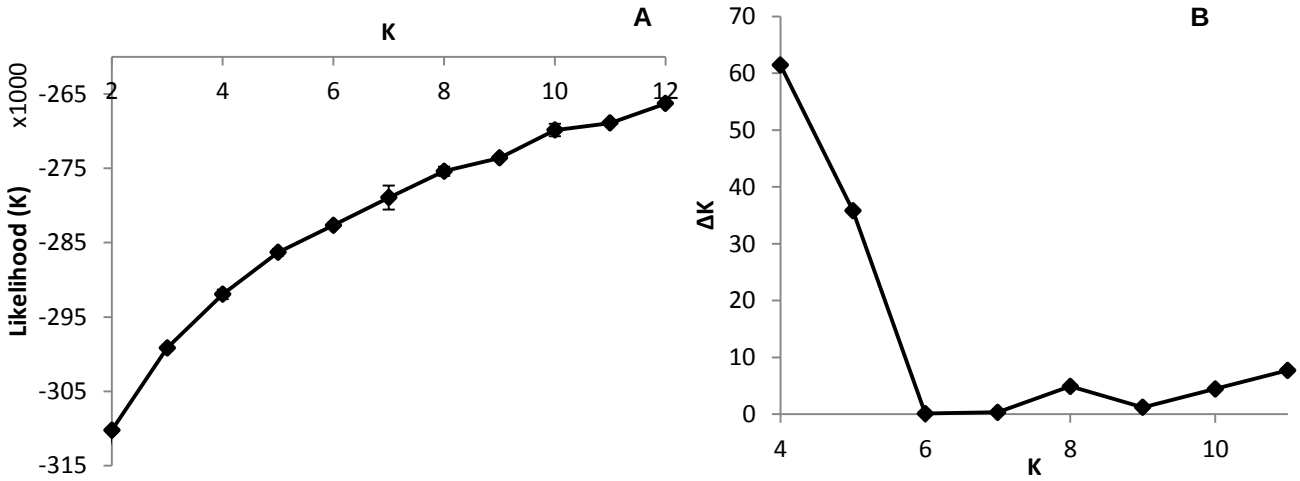

Figure 15: Identification of the optimal K. **A**) L(K) from Pritchard *et al.,* 2002. A plateau is more or less formed at K9. **B)** ΔK from Evanno *et al.,* 2005. A peak is visible at K8.

A graphical representation of the Q-matrix is shown in *figure 16*. Each line in the bar plot represents a single accession. The eight colours represent the eight different subpopulations. If accessions have multiple colours, this means that they are admixed, with subsets of markers having allele frequencies fitting in different subpopulations. This admixture can be observed in all eight groups, especially on the right hand side of each group. Often does the admixture have a light blue colour originating from the rest group.

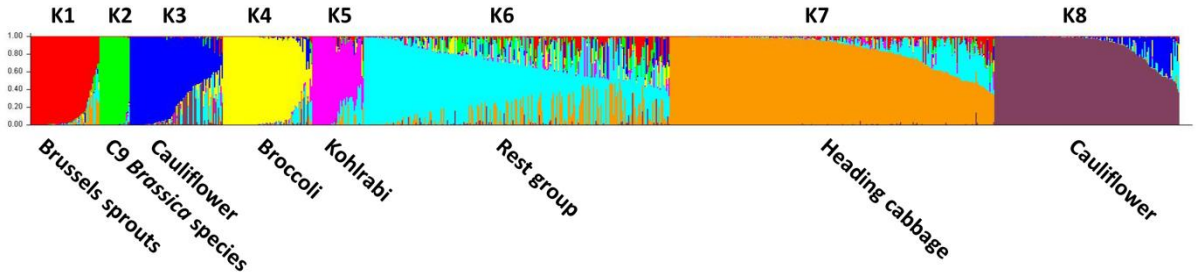

Figure 16: Bar plot of the population structure with eight groups. Rest group K6 has high admixture compared to other groups.

The composition of the eight groups was defined by counting the number of accessions belonging to the morphotypes in each group (≥ 50% membership, *appendix 4*). K1 consists of Brussels sprouts (red) and K2 consists of C9 *Brassica* species (green). Not all C9 *Brassica* species fall in K2 but the group is mainly defined by *Brassica villosa*, *Brassica rupestris*, *Brassica incana* and *Brassica macrocarpa*. K3 consists of winter and Romanesco cauliflowers (blue). The admixed end of the group has similarity with K8 and K6. Group K4 consists of broccoli (yellow) and K5 of kohlrabi (pink). Group K6 has a lot of accessions with high percentages admixture and is therefore considered a rest group (light blue). The group contains all collard greens, tronchuda, kales and ornamentals. Furthermore, some C9 *Brassica* species and wild *B. oleracea* fit in this group. Finally, K6 contains a large part of heading cabbage which are only genebank accessions. These cabbages are generally represented by the orange bars in the lower part of group K6. Group K7 contains all four heading cabbage types (orange). All hybrid cultivars fall in this group. Furthermore, some admixture can be seen at the right hand side, mainly light blue and caused by the large part of heading cabbage in K6. Finally, K8 is a second cauliflower group that consist of summer, autumn and tropical types (brown). Some admixture can be seen which is mainly due to the other cauliflower group in blue.

4.3. GWAS

The genome wide association study was performed using TASSEL software with a GLM and 999 permutations using 18.580 SNP markers. Traits generated in the three different datasets were analysed in GWAS. For each dataset, a GWAS was calculated with and without a population structure (K8). Subsequent FDR analysis (FDR ≤ 0.01) identified significant marker-trait associations. In the WURField2015 dataset, 11 traits were analysed which resulted in 3594 significant marker-trait associations. Markers were associated to multiple traits which lead to 1347 markers associated to one or more traits. For each trait in this dataset (*table 1*), significant marker-trait associations were found. In the Companies2015 dataset, 252 significant marker-trait associations were found in three out of eight traits (Head Length, Blistering, Stem Length; *table 2*). Two markers were associated to more than one trait which results in 250 markers associated to one or more traits. The GWAS of ZonMW2016 identified 1696 significant marker-trait associations in seven out of 12 traits. Associations were found for Head Length, Head Width, Head Weight, Core Length, Length over Width, Anisometry and Roundness (*table 3*). Again, markers were associated to multiple traits which resulted in 1433 significant markers associated to one or more traits. In total, 5542 marker-trait associations were found in the three datasets. These lead to 2301 unique markers associated to one or more traits. The marker-trait associations are visualised in Manhattan plots (*figure 17; appendix 7.2, 7.3* & *7.4*).

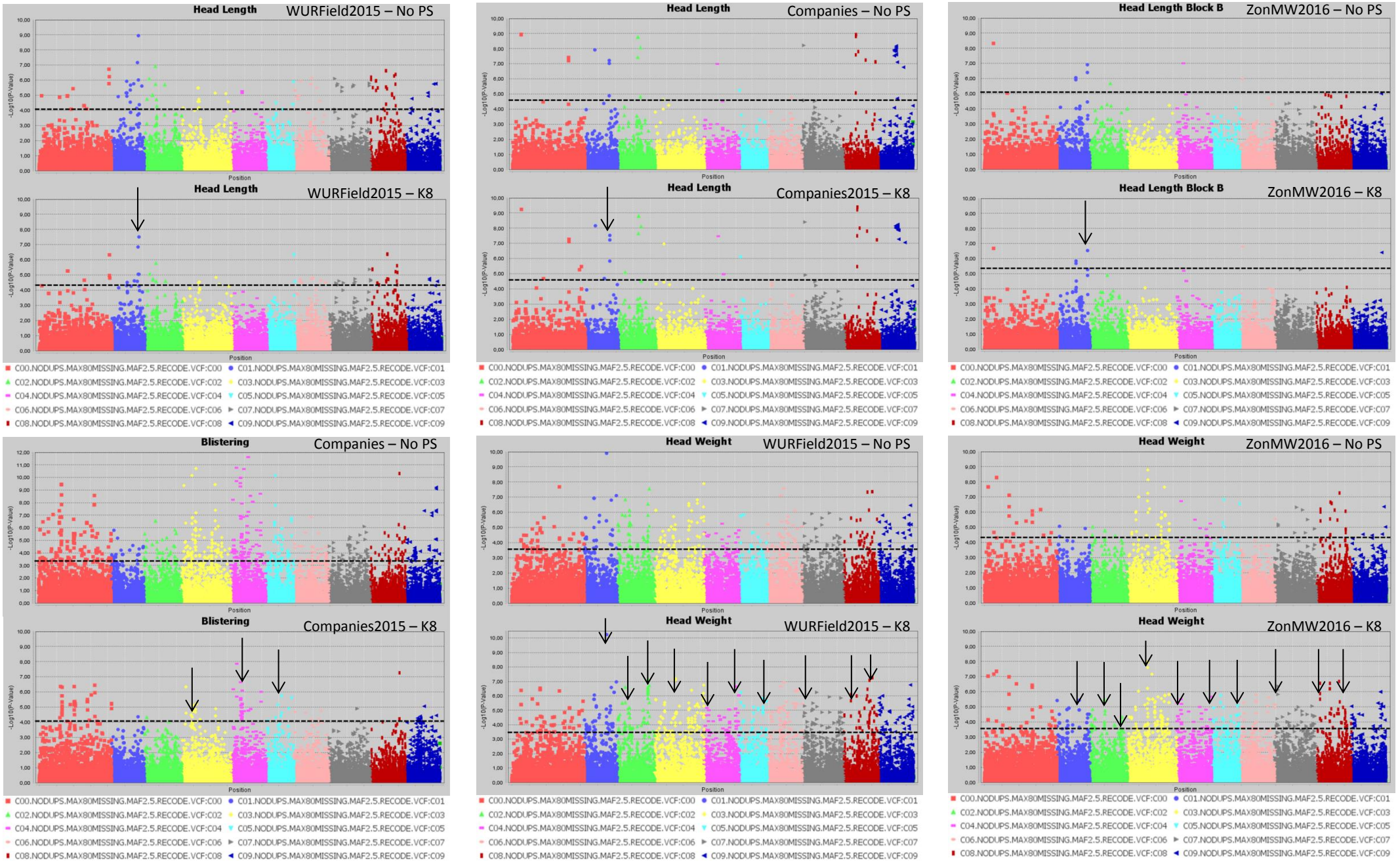

Figure 17: Selection of GWAS output using TASSEL software. Each graph represents a single trait in a dataset with the upper graph association without population structure (No PS) and the lower graph with population structure (K8). The upper six graphs show plots for Head Length from data generated in three datasets. The lower left graph shown Blistering in Companies2015. The middle and right lower graphs show Head Weight in WURField2015 and ZonMW2016. Ten colour blocks can be distinguished of which the first one is fictional chromosome C0, the other nine are *B. oleracea* chromosomes C01-C09. The dotted line represents the FDR significant threshold of FDR ≤ 0.01. Interesting regions are indicated with an arrow.

To identify interesting regions in terms of marker trait associations, certain assumptions have been made. When many significant markers were found, for example for Head Weight in WURField2015 and ZonMW2016, emphasis was laid on markers that form a peak. Furthermore, a peak is considered interesting if the LOD score is increased in the analysis with population structure correction compared to no population structure correction. When a limited number of significant associations was found, the emphasis was on single markers that increased in LOD score when analysed with population structure correction compared to analysis without population structure correction. When markers from the same genomic region are associated with a trait phenotyped in different datasets, the region is considered a candidate region.

Candidate regions associated with traits were identified from the Manhattan plots in *figure 17* and are indicated with an arrow. A limited number of markers are significantly associated with the trait Head Length in all three datasets (upper three graphs). Therefore, single markers are also considered interesting when they occur in multiple datasets and increase in LOD score after population structure correction. The region on C01 (arrow at blue dots) is considered a candidate region, as markers form a peak in both WURField2015 and Companies2015 datasets and in the Companies2015 dataset the LOD score of the associated markers increased from 7.1 without population structure to 7.6 with population structure. This region is selected as candidate region for HL. Blistering in the lower left graph was only measured in Companies 2015 making comparison across datasets impossible. After population structure correction, 130 markers were significantly associated with Blistering. Candidate regions in the form of peaks appear on C03 (yellow), C04 (pink) and C05 (light blue). No significant marker-trait associations were identified for Head Weight in Companies2015. However, many significant marker-trait associations for HWe were found in WURField2015 (569) and ZonMW2016 (291), even after population structure correction. Therefore, peaks were chosen that occur in WURField2015 and ZonMW2016 and increase in LOD score after population structure correction. In total, 14 peak markers were chosen as indicators of candidate regions (*table 4*).

Table 4: Markers selected for candidate gene search. For each marker, the corresponding trait, allele frequency and search region is shown. Furthermore, the marker name holds information about the position (chromosome_nucleotide position).

Trait	Peak marker	Allele frequency		Candidate region (100Kb)
Head Length	C1_31515139	88% T	12% C	31465139..31565139
Blistering	C3_13093205	59% G	41% A	13043205..13143205
Blistering	C4_11126258	75% G	25% A	11076258..11176258
Blistering	C5_11156527	81% C	19% G	11106527..11206527
Head Weight	C1_26101229	92% G	8% C	26051229..26151229
Head Weight	C2_17135516	57% C	43% G	17085516..17185516
Head Weight	C2_35893708	53% C	47% T	35843708..35943708
Head Weight	C3_24041641	76% T	24% A	23991641..24091641
Head Weight	C4_4779806	62% C	38% T	4729806..4829806
Head Weight	C4_36909949	78% G	22% A	36859949..36959949
Head Weight	C5_31650480	65% A	35% G	31600480..31700480
Head Weight	C7_3941239	89% A	11% G	3891239..3991239
Head Weight	C8_4812778	84% C	16% T	4762778..4862778
Head Weight	C8_30305730	58% A	42% G	30255730..30355730

In *table 4,* the frequency of the alleles for the associated markers is shown. Some markers have a high percentage of major allele whereas other markers while the frequency of some markers is similar. *Figure 18* shows variation in Head Length (C1_31515139) for all three datasets organised per allelic composition. Head Length did not vary significantly when comparing the allelic groups for Companies2015 and ZonMw2016. However, Head Length did vary significantly between allelic groups in WURField2015 for this marker. When a C is present, whether it is homozygous or heterozygous, the Head Length is higher. Nevertheless, conclusions have to be drawn with caution. Only three CC accessions were present and 14 CT accessions compared to 75 TT accessions.
Another marker was inspected for its allelic composition. C2_17135516 is associated with Head Weight on C02. It has an allele frequency of 57% C and 47% G. In both WURField2015 and ZonMW2016, the allelic groups varied significantly for this marker. When a C allele is present (homozygous or heterozygous), the cabbage is heavier then when a G allele is present (*figure 18*). The number of accessions analysed for this marker trait combination of C2_17135516 is larger than C1_31515139 and evenly distributed over genotype frequencies. Therefore, the association of C2_17135516 with Head Weight is more trustworthy than the association of C1_17135516 with Head Length.

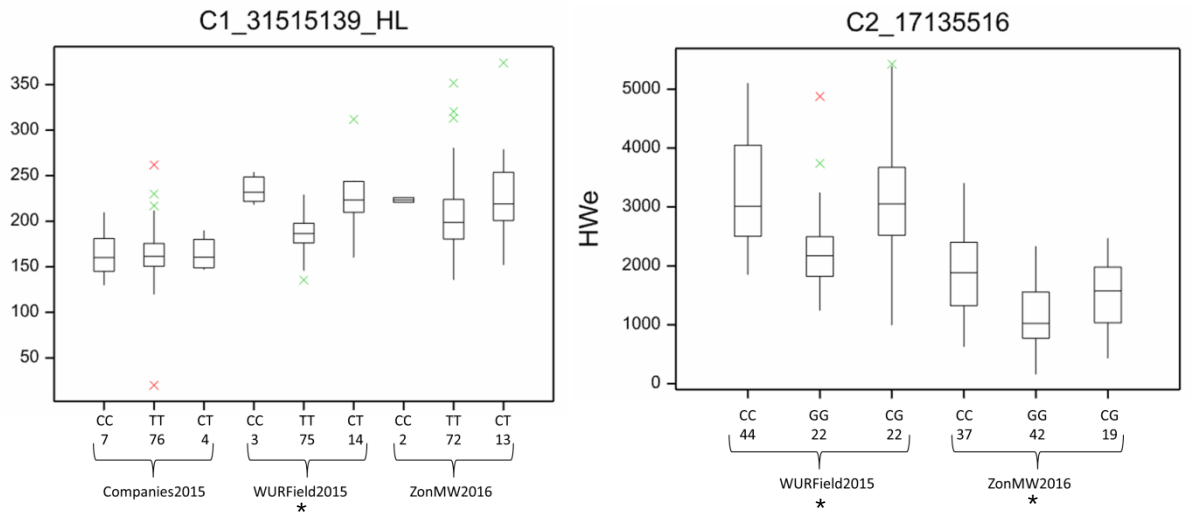

Figure 18: Allelic composition of marker C1_31515139 for Head Length and C2_17135516 associated with Head Weight. The allele frequency of C1_31515139 is compared to HL data of three datasets. WURField2015 showed significant results. The allele frequency of C2_17135516 is compared to WURField2015 and ZonMW2016. Both datasets showed significant difference, indicated with an asterisk.

4.4. Candidate genes

The regions in *table 4* were chosen for candidate gene analysis. A window of 100 Kb around a marker was chosen to search for candidate genes. Each candidate region was entered in the BolBase genome browser to identify genes located in this region. A candidate gene is defined as a gene involved in leaf initiation, leaf polarity or cell growth. Swis-Prot and TrEMBL databases (Apweiler *et al.,* 2004) were used for gene characterisation. Each 100 Kb region revealed more than one gene. In *table 5*, an overview is given of markers and their candidate genes.
For Head Length, two candidate genes were identified in the vicinity C1_31515139. For Blistering, few markers were added to increase the search region because multiple markers were associated with the peaks in *figure 17* (C3_17002635; C4_6657392). Two markers on C03, two markers on C04 and one marker on C05 gave rise to eight candidate genes for

Blistering. In the analysis for Head Weight, four markers were added for the same reason as Blistering (C2_1410548; C3_23629292; C5_2023603; C8_33624272). In total, 12 candidate genes were identified for genomic regions around 14 markers associated with Head Weight.

Table 5: List of markers and candidate genes. The marker name holds information for chromosome and position. The short and full name of the gene is given. Furthermore, the gene model corresponds to a *B. oleracea* code to find the gene in the UniProt database.

Trait	Marker	Gene	Gene (full name)	Gene model
HL	C1_31515139	SG1	SLOW GREEN 1	Bol030944
		NAC098	CUP-SHAPED COTYLEDON 2	Bol030940
B	C3_13093205	CyCu2-1	CYCLIN-U2-1	Bol029526
		EXPB4&6	EAXPANSIN-B4&6	Bol029527
	C3_17002635	NAC054	CUP-SHAPED COTYLEDON 1	Bol025747
	C4_6657392	WSD1	Wax Synthase diacylglycerol acyltransferase1	Bol016269
		AVT1	Vacuolar amino acid transporter 1	Bol016265
	C4_11126258	MYB81/104	Transcription factor MYB81/104	Bol027782
	C5_11156527	CDC48A	Cell division control protein 48 homolog A	Bol022544
		ARF6	Auxin response factor 6	Bol022542
HWe	C1_26101229	TMK1&4	Transmembrane Kinase1&4	Bol028706
		IAA9	Indoleacetic acid induced protein 9	Bol028707
	C2_1410548	TFL1	TERMINAL FLOWER 1	Bol005471
	C2_17135516	-	-	-
	C2_35893708	-	-	-
	C3_23629292	APUM5	PUMILIO homolog 5	Bol026663
	C3_24041641	MKK5	MITOGEN-ACTIVATED protein kinase 5	Bol026625
	C4_4779806	IRX9	IRREGULAR XYLEM 9	Bol025525
	C4_36909949	-	-	-
	C5_2023603	GTE4	GLOBAL TRANSCRIPTION FACTOR GROUP E4	Bol023338
		CLO	CLOTHO	Bol023337
	C5_31650480	CHC1	CLATHRIN HEAVY CHAIN1	Bol005887
		LOB21	LOB domain-containing protein 21	Bol005885
	C7_3941239	SPL10	Squamosa promoter-binding-like protein 10	Bol016006
	C8_4812778	-	-	-
	C8_30305730	-	-	-
	C8_33624272	PIP5K3	Phosphatidylinositol 4-phosphate 5-kinase 3	Bol045728

5. Discussion

5.1. Phenotypic data

First, the quality of phenotypic data will be discussed. Subsequently, the correlation between traits within and between datasets will be discussed. Finally, traits that show significant differences between morphotypes will be discussed. The datasets in this research (WURField2015, Companies2015 and ZonMW2016) are independent from one another. The phenotypic data was gathered at different locations and different years. Furthermore, a collection of different accessions was used with a limited number of overlapping accessions (*figure 10*).

5.1.1. Data quality

The WURField2015 dataset contained a total of 160 accessions of which 140 were modern hybrids and 20 were genebank accessions. A variety of traits were measured by image analysis software ImageJ. Overall, the measurements give a good approximation of the trait values. However, traits such as Head Density, Head Roundness, Head Shape and Head Volume will be measured more accurately with 3D imaging software compared to measurements taken from 2D pictures.

The goal of the ZonMW dataset was to identify and quantify heading parameters using a 3D camera set up. Furthermore, advanced imaging software such as Halcon would be used for the 3D picture analysis. In total 111 accessions were phenotyped of which 65 were modern hybrids and 46 were genebank accessions. The cabbage heads were harvested by cutting them just beneath the attachment of the outer leaves of the cabbage head. Loose leaves that did not wrap around the cabbage head were removed before images were taken. Within the 111 accessions, sub-morphotypes were identified. Most of the accession have a known phenotype, white, red, savoy or pointed cabbage. However, the phenotype of some accessions was still unknown. These accessions could be sown on the field next year to phenotype them correctly. This extra phenotypic information could be incorporated into the analysis. The traits Head Weight, Head Length and Head Width were correctly measured. A correct measurement is a measurement that was performed by an algorithm and gives the same output as a measurement by hand.

Core Length was not correctly measured by the algorithm especially in white and pointed cabbage types. This is due to the inner colour of the cabbage. White, pointed and savoy cabbage have a white core and white/green leaves whereas red cabbage has a white core and purple leaves. An adjustment in the algorithm has to be made to be able to discriminate between core and leaf colour. Halcon is able to separate the images in multiple colour spectra. When the yellow colour spectrum is filtered out, differences in core and leaves can be seen. Core Length is an interesting trait for breeders because a good hybrid has a small core which leads to a larger edible part of the cabbage. Furthermore, it is expected that a smaller Core Length increases the density of the cabbage head, which is also favoured by breeders and consumers. However, the relationship between Core Length and Head Density is unknown because Core Length was not correctly measured and Head Density still has to be measured by the computer vision and robotics group. Because Core Length is important for breeding purposes and selection on the trait must have happened, it would be interesting to identify candidate gens that are involved in defining the Core Length.

The trait Head Shape was divided into six parameters, ranging from an ellipse shape to pointed phenotypes (*appendix 2*). The idea was that these six parameters would be used by an algorithm to define the Head Shape. Later in the project, the decision was made that

quantitative parameters would be better for association analysis than the qualitative trait Head Shape. Phi is not informative as trait parameter but is used by the algorithm to establish the orientation of the cabbage on the image and is used by the software to make a decision if the picture should be turned 90 degrees or not before other parameters could be calculated. The other shape parameters, Anisometry, AreaRatio, Length_over_Width, Roundness and Maxwidth_row_over_half_Length, give information about the heading cabbage shape.

Due to circumstances in the computer vision and robotics department, Head Density and Head Volume were not measured in the analysis. Head Density is a measure for the density or compactness of the cabbage head. This is an interesting trait to study because large variation in the cabbage density is observed. Furthermore, this is an important trait for breeding companies and selection must have happened on this trait. It would be interesting to identify genes that make a difference in a loose or dense cabbage structure. If Head Density is still not measured in future research, an approximation for density can be used. Based on Head Density from the WURField2015 dataset. The Head Weight can be divided by the Head Volume to give an indication for Head Density. Head Volume is an interesting trait because it gives an indication about cabbage size and can be used in parameter calculation described above. One would expect it to be positively correlated with Head Length, Head Width, Core Length and Head Weight. Indeed, in the WURField2015 dataset a positive correlation was found for Head Volume with Head Length, Head Width and Head Weight. Moreover, Head Density is negatively correlated with Head Length and Head Width in WURField2015. This implies that a denser cabbage is shorter and less broad; i.e. smaller.

Based on these hypotheses, it would be a good addition to the ZonMW2016 dataset if Head Density and Head Volume were included based on 3D image analysis.

The Companies2015 dataset contains 121 genebank accessions. Heading types were phenotyped at different breeding companies. This resulted in 26 measured traits of which 14 were real heading cabbage traits (*appendix 1.2*). However, the traits were not scored for each cabbage type. Eight traits were chosen for analysis which were measured in at least two cabbage types (*table 2*). The assumption was made that traits measured by different companies can be compared with each other, on the condition that the same plant part was compared. Head Weight, Head Length, Head Width and Core Length are quantitative traits and are correctly measured. Stem Length was not measured consistently. The trait was not scored in savoy cabbage and in red cabbage very high values were observed. This indicates that different interpretations of Stem Length were applied. Blistering and Head Density were also measured in a qualitative manner. Unfortunately, the cabbage heads were not harvested at the same moment for all cabbage types. Furthermore, it is unknown if the harvest date within a cabbage type was the same. This makes the quality of the measured data hard to judge because it was carried out by other people than the writers of this thesis. It is assumed that noise is introduced by the varying harvest dates and because measurements were takes by different persons.

5.1.2. Correlations within and between datasets

In Companies2015, hardly any correlations between traits were found within the dataset. The only correlation found was between HWe and HWi. When a cabbage is heavier, it is logical that it is broader but it would also make sense that it would be longer or more dense. However, this was not observed within this dataset. The absence of correlations between traits can be due to the fact that Companies2015 contained only genebank accessions. Genebank accessions are heterogeneous, and thus accessions are often not uniform in

appearance. This results in variation within accessions. However, 46 out of 121 accessions were used in the Pearson correlation test because the Pearson correlation test requires accessions that contain data for each trait. If more accessions contained data for all traits there is a possibility that more correlations would be found. Another method to identify correlations would be the use of subsets of traits. For example, Blistering was not measured for red cabbage. Therefore, all red cabbages were omitted in the Pearson correlation test. When Blistering is removed from the traits in the Pearson correlation test, more accessions will be available to calculate the correlation between the remaining traits.
In ZonMW2016, more significant correlations were found. Head Weight is positively correlated with Head Length, Head Width and Core Length. This makes sense because a longer cabbage or broader cabbage is larger and thus heavier. Unsurprisingly Core Length is positively correlated with Head Length because a longer head has a longer core. However, we have to keep in mind that Core Length was not measured correctly in all cases. It would be interesting to find out if the Core Length is still positively correlated to Head Length when the algorithm can identify Core Length correctly or the Core Length is manually calculated. The Head Shape parameters show correlations as well. Length_over_Width is negatively correlated with Head Width and positively correlated with Head Length. This is logical since Head Length is divided by Head Width. Head Width is positively correlated with Anisometry and Maxwidth over half Length because Anisometry and Maxwidth over half Length both use Head Width in their parameter calculation. Subsequently, Anisometry and Maxwidth over half Length are positively correlated as well whereas Maxwidth over half Length and AreaRatio are negatively correlated.
When we compare the relationships of ZonMW2016 and Companies2015 to WURField2015 the same conclusions can be drawn with regard to Head Weight, Head Length and Head Width. The shape parameters of ZonMW2016 cannot be compared to Head Shape of WURField2015.

5.1.3. Differences between morphotypes

Quantitative traits should be analysed with a parametric test and qualitative data should be analysed with a non-parametric test. The comparison between parametric and non-parametric data is hard. Therefore, all data was analysed with parametric tests. Normality assumptions were violated in Companies2015 and ZonMW2016 by qualitative traits (Blistering, Head Density, Uniformity) but also by quantitative traits (Anisometry, Phi, Roundness, Stem Length) (*appendix 5.6 & 6.2*). However, this is not considered a problem because the sample size of 121 and 111 should be large enough for the data to behave as approximately normally distributed data (Central Limit Theorem (Whitlock & Schlutter, 2009)).
Significant differences were found between cabbage types by ANOVA analysis. In the Companies2015 dataset (*appendix 6.3 & 6.4*), pointed cabbage was represented only once in 121 accessions. Therefore, no conclusions can be drawn regarding this cabbage type. Savoy cabbage has the lowest density and weight. This is logical because savoy is known for its looser structure. Moreover, savoy cabbage has higher blistering than white cabbage. This is also logical because savoy is known for the blistering structure of the leaves. Blistering was not measured in red cabbage. No significant differences were found for Core Length. This is remarkable because differences do exist. It may be explained by the absence of pointed cabbage in the dataset because it has in theory the highest Head Length and thus Core Length. Another explanation may be that the genebank accessions did not have had strict selection on Core Length because this material has not extensively been used in breeding. No significant differences were found in Head Length. This is also due to the

absence of pointed cabbage which has in theory the largest Head Length (*appendix 2*). A high standard deviation in Head Length is observed for white cabbage. This is because there is large variation in Head Length for white cabbages. Shape class one to five, which range from transverse narrow elliptic to broad obovate, are observed within the white cabbages. These different shape classes have a large impact on Head Length. Subsequently, this wide variation in white cabbage can be observed for Head Width. White cabbage is significantly broader than the other cabbage types. Uniformity is omitted in further analysis because this trait was measured within accessions and not between accessions.

More significant differences between morphotypes were found in the ZonMW2016 dataset. Results are shown in *figure 14* and *appendix 5.7* and *5.8*. The Head Length of pointed cabbage is significantly longer than that of the other cabbage types. This is in line with HL expectations. Furthermore, Core Length of pointed cabbage is also longer than that of the other cabbage types. This can be explained by the correlation between Head Length and Core Length: the longer the cabbage, the longer the core. Pointed cabbage has a higher Core Length which lead to a larger distance between subsequent leaves within the cabbage head. This larger distance between leaves increase the total Head Length. Furthermore, pointed cabbage is expected to wrap its leaves in a different manner than other cabbage types which also adds to the Head Length. Unfortunately, the hypotheses between Head Length and Core Length cannot be tested in the ZonMW2016 dataset. Core Length was not measured correctly and is therefore omitted in further analysis. White cabbage has a higher Head Width than red and savoy cabbage. This is due to shape class one and two, representing transverse narrow- and transverse elliptic shape classes, which are observed in white cabbages. Moreover, white cabbage has a higher weight than red and savoy cabbage. A reason can be that white cabbage tends to be larger. Both longer and broader than red and savoy cabbage. Another hypothesis can be that white cabbage has a higher density than red and savoy cabbage. In order to test this hypothesis, Head Density should be measured in an accurate manner. This can be done by the algorithm by quantifying Head Density. For example, the looser the cabbage head, the more shadow is visible on the image. The algorithm can quantify this degree of shading. Furthermore, a distinction can be made in upper and lower density of the cabbage head. The lower part of the cabbage head, around the Core Length, tends to be looser of structure than the upper part of the cabbage head.

No significant differences were found for Anisometry. An explanation may be the number of outliers in the dataset which can be caused by the transverse narrow- and transverse elliptic shapes of white cabbage. The algorithm could have switched Ra with Rb which lead to outliers in the data. The Area Ratio for pointed cabbage is smaller than for the other cabbage types. This is logical because the upper half of a pointed cabbage has a smaller area than the lower half of the pointed cabbage. Since upper area is divided by lower area, the AreaRatio will be < 0 whereas the upper and lower area of other cabbage types will be more or less equal which leads to an AreaRatio of approximately 1. Length_over_Width of pointed and red cabbage is larger than savoy and white cabbage. This is logical for pointed cabbage since the Head Length is longer than Head Width (shape class six and seven). In addition, it seems that red cabbage is always longer than broad. This is also logical because red cabbage has shape class four and five wherein Head Length is longer than Head Width. The shape classes one, two and three in white cabbage and two and three in savoy cabbage cause the difference with pointed (broad/angular ovate) and red cabbage (broad obovate). Maxwidth over half Length of red and white cabbage is smaller than pointed and savoy cabbage. This makes sense because shape class five (broad obovate) is observed in white and red cabbage. Broad obovate cabbage results in a smaller position number (counted from

top to bottom) of the maximum width compared to other cabbage types. This position number is divided by half the Head Length and thus Maxwidth over half Length would be a smaller number in shape class five (broad obovate) compared to the other shape classes. Roundness of pointed cabbage is smaller than savoy and white cabbage. This is logical because pointed cabbage is not as round as white and savoy cabbage. Furthermore, white cabbage is more round than red cabbage. This is surprising because more shapes are observed for white cabbage compared to red cabbage. Outliers were observed for red and savoy cabbage which could have skewed the result. This is also an indication that Roundness is not perfectly measured by the algorithm.
The main reasons why the algorithm calculated the parameters incorrectly is indicated in *figure 19*. 1) The Core Length could not be distinguished (A&B). 2) The orientation of the cabbage was wrong in the cabinet (C). 3) Loose leaves cause the algorithm to recognize different Head Lengths and Head Widths (D).

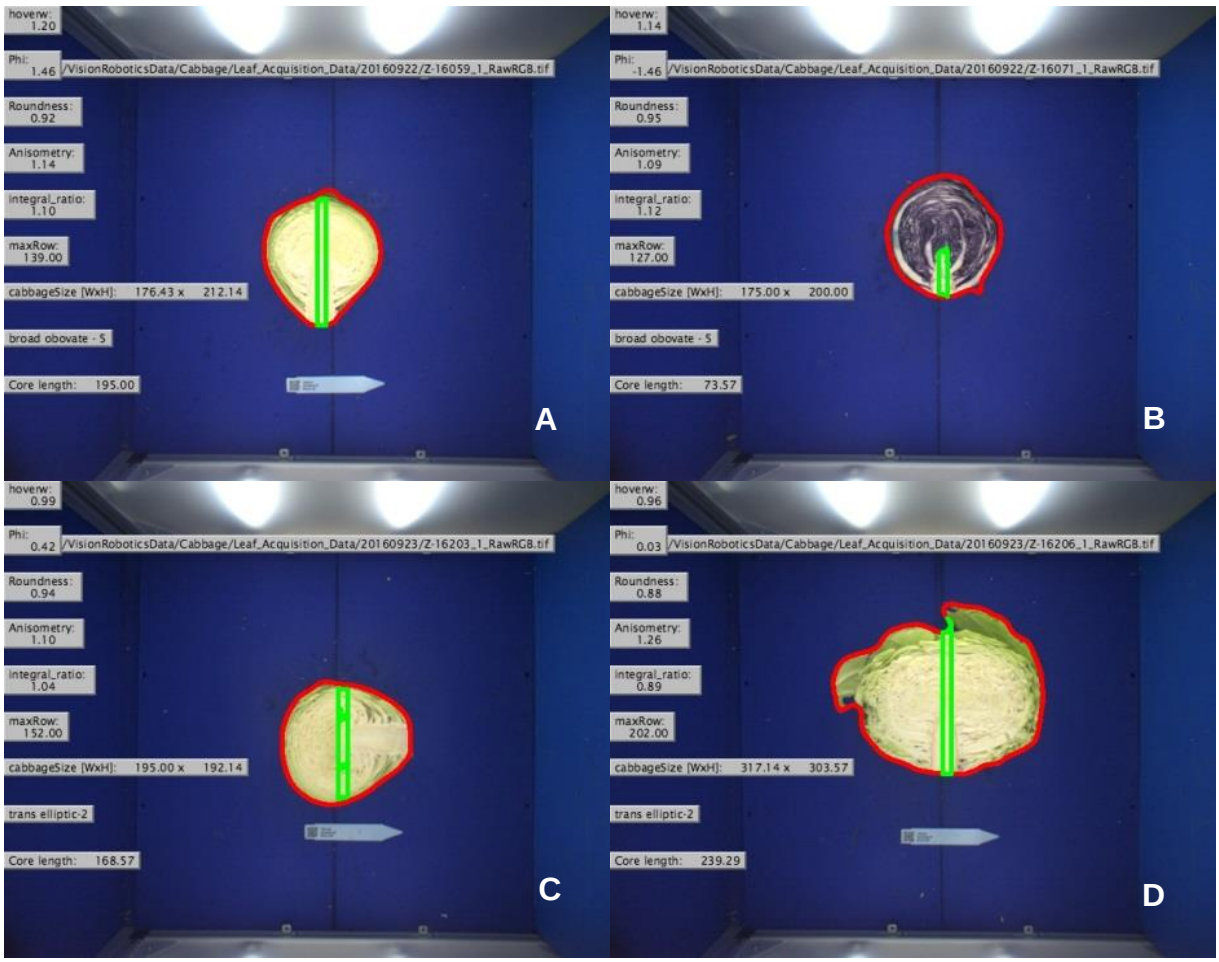

Figure 19: Main errors of the algorithm. Core Length cannot be distinguished in A and B, Orientation is wrong in C and loose leaves cause overrepresentation of cabbage lengths in D.

When the results of Companies2015 and ZonMW2016 are compared to WURField2015, differences and similarities are found. Pointed cabbage is absent from the analysis in WURField2015 which leaves white, red and pointed for analysis. Furthermore, each dataset contains traits which cannot be compared to other datasets because they are unique in their dataset. These traits are Head Area, Head Volume, Total Weight, Head Weight Percentage, Stem Length, Uniformity, Blistering, Anisometry, AreaRatio, Phi and Maxwidth over half Length. Furthermore, Core Length, Head Density and Head Roundness (Roundness) are

measured in a different way across datasets which also makes comparison hard. In other words, Head Length, Head Width, Head Weight and Length_over_Width (Head Index) can be compared across datasets. No large differences in Head Length, Head Width, Head Weight and Length_over_Width were found across datasets.
A large improvement of the ZonMW2016 dataset was the controlled environment in where the images were taken, compared to the images taken of the field in WURField2015. Furthermore, the throughput was increased in ZonMW2016 by the use of an algorithm in Halcon compared to semi-automated measurements in ImageJ in WURField2015. However, al lot of work still has to be done for further analysis. For starters, leaf data still has to be analysed. Leaf parameters have to be defined in cooperation with the computer vision and robotics department. When the leaf traits have been measured, a GWAS can be conducted on this data and compared to the results of WURField2015 GWAS output. Besides leaves, the computer vision and robotics department still has to analyse Head Density and Head Volume. These traits are considered important in breeding and need further research to genetically understand cabbage density and volume. The algorithm, as it is now, is not able to measure all traits correctly in ZonMW2016. Colours have to be split in different channels to discriminate the Core Length from leaves. In future heading cabbage measurement, it is suggested that the imaging is performed on both halves of the cabbage head that was photographed from the cross-section side. This way you will get a good indication of Head Volume because both halves of the cabbage are photographed instead of two times the same half. Additionally, when the cabbage was not perfectly sliced in half, an average can be taken. This approach needs a correction for depth in the image. Thicker cabbages are closer to the camera resulting in an overestimation for cabbage size.

5.2. Genotypic data

In this paragraph, the genotyping will be reviewed followed up by the population structure. Finally, the GWAS and candidate genes will be discussed.

5.2.1. Genotyping

The accessions in the dataset were genotyped by SBG, a Keygene technology. One of the restriction enzymes used, PstI, is methylation sensitive. This excludes sequence information around methylated PstI sites which likely occur around the centromere. The dataset was filtered with a genotype call of 80% which implies that each marker should be scored in at least 80% of the accessions. Furthermore, a MAF of 2.5% was chosen. This means that markers with a minor allele frequency lower or equal than 2.5% will be filtered out. Accessions with more than 60% missing marker values were removed from the dataset because these accessions were not considered informative enough for analysis. The MAF filtering step proved to filter most markers out; from 85.168 to 18.580 markers. Minor alleles can be important in for example finding resistance genes. The resistance genes are expected to occur in low frequencies. To identify these genes, the low frequency markers are especially interesting. However, low frequency markers also tend to be mistakes in the genotypic data, possibly induced by the use of restriction enzymes or by sequencing errors. This research aims to identify heading cabbage traits. The alleles involved in defining leaf morphology are not expected to occur in low allele frequencies. Besides, running a GWAS on 85.168 markers takes longer computational time. A dataset with 18.580 markers is easier to work with but it is expected that marker-trait associations will be missed in the analysis. This is due to a limited amount of markers in a region where the LD is low. The half maximum LD decay in *B. oleracea* was estimated at 36.8 Kb by Cheng *et al.,* 2016.

Furthermore, the reference genome is approximately 500 Mb. Based on these numbers, an indication for a sufficient marker density can be given.

$$\frac{500\ Mb}{36.8\ Kb} = \sim 13.600\ markers$$

The marker density would be sufficient with more than 13.600 markers evenly distributed over the genome. In this research, 18.580 markers were used which is in theory enough. However, the markers are not evenly distributed over the genome (*appendix 7.5*). Especially the upper parts of C07, C09 and C02 as well as the lower part of C02 have a low amount of markers. Further LD analysis is necessary as the LD varies over the genome; some regions have had more recombination that other regions, for example low recombination frequencies at centromeres and telomeres. Therefore, it is recommended that the LD will be calculated over the genome from which haplotypes can be defined. Subsequently, the haplotypes can serve as input for the association analysis rather than SNPs. Haplotypes will be more informative because multiple SNPs can be in LD with each other and define together a haplotype (Brown & Weir, 2010; Gattepaill & Leslie, 2011). The LD analysis was not carried out in this research due to limited time.
Filtering plays an important role in the organisation of genotypic data. In this research, genetic information from 11 morphotypes was used to call SNPs. One would expect many differences between morphotypes but Del Carpio *et al.,* 2011 showed that the diversity within a morphotype is larger than between morphotypes. This is due to the fact that in history, most crosses were made within a morphotype and not between morphotypes and likely means that only a small part of the genome is involved in morphotype specific traits. It would be interesting to call SNPs solely based on the morphotypes of heading cabbage. One would expect that in case all called SNPs are informative, the quality of the population structure will improve and the quality of the association analysis might increase. If SNPs are called based on heading cabbage, it is likely that the genetic information that discriminates a cabbage from other morphotypes will be lost. However, these associations are lost when correcting by population structure as well.

5.2.2. Population structure

For the population structure, 1376 SNP markers were selected which were evenly distributed over the genome with a minimum distance of 250 Kb. Not all 1376 SNP markers were used to build a population structure. The markers were thinned to 459 SNP markers to shorten computational time. In the first run, a burn-in period of 50.000, MCMC calculations of 50.000 and three iterations were chosen as settings. However, the obtained results were not consistent over the three runs. Therefore, the burn-in period was increased to 100.000. The error bars in the Pritchard output in *figure 15* indicate that there is still some deviation between runs. Due to time limitations, this STRUCTURE output was chosen as population structure.
Based on the Pritchard output, two plateaus can be identified at K=9 and K=11. This indicates a righteous K of eight and ten. Since the interpretation of the Pritchard graph is hard, Evanno *et al.,* 2005 developed a method to visualize the STRUCTURE output. The Evanno method is built from the Pritchard output. The first derivative (L'(K)) is obtained by calculating the rate of change of L(K). From this L'(K) the second derivative (L''(K)) is obtained by calculating the rate of change in L'(K). The second derivative can be negative and is therefore calculated as absolute values (|L''(K)|). Finally, |L''(K)| is divided by the

standard error of the Pritchard output. A peak in this graph indicates the righteous K. However, the Evanno method is also not straight forward. Small K's always have very high values in the Evanno graph (*figure 15*). K=2 and K=3 are already removed from the graph to clarify the peak at K8. These high values are due to a large rate of change in L(K) with lower K's. Therefore, the assumption was made that the Evanno graph should first become close to zero before a subsequent peak was chosen as righteous K. Based on the Pritchard manual, the K closest to zero should be chosen as righteous K. Accordingly, eight groups were chosen as population structure.

When the Q matrix of K8 is researched, some accessions were fit into multiple groups based on membership percentages. To make a clear group definition, accessions with a membership of 50% or more were considered in the description. The formed groups are logical and are shown in *figure 16* and *appendix 4*. Surprisingly, cauliflowers are represented by two groups: K3 for winter and Romanesco types and K8 for summer, autumn and tropical types. Furthermore, heading cabbage has their own group including all hybrids and some genebank material. A large proportion of heading cabbage accessions is present in rest group K6 indicated by the orange colour of heading cabbage group K7. These heading cabbages represent all genebank material and thus these accessions are more likely to be assigned to the rest group than hybrids. The germplasm of hybrids nowadays will be used more often than genebank material in breeding, thus is more related and groups together but has lost a lot of variation. Accordingly, the genebank accessions are an important source of genetic variation. Group K2 is a group that contains *Brassica* species with nine chromosomes. Remarkably, not all C9 *Brassica* species group into K2 but also a large proportion is assigned to rest group K6. *B. villosa* and *B. rupestris* are solely assigned to K2 whereas the majority of *B. incana* and *B. macrocarpa* are assigned to K2 and the remaining species (*B. bourgeaui, B. cretica, B. insularis, B. maurorum* and *B. montana*) to K6. An explanation may be that *B. villosa, B. rupestris, B. incana* and *B. macrocarpa* are more related to each other and to *B. oleracea* than to the other *Brassica* C9 species. To confirm this, more research is needed. Overall, rest group K6 seems to be more admixed than other groups which is indicated by many colours which makes sense because all morphotypes are represented in this group.

The population structure can be further improved. More markers (1376) can be used which can improve the quality of the population structure, although the computational time will increase. Besides adding more markers, haplotypes can be defined from the total SNP dataset by LD analysis. Population structure analysis in the human genome showed that a more subtle population structure was captured with the haplotype-based approach (Lawson *et al.,* 2012). The burn-in period and MCMC calculations can be increased to improve the population structure quality, albeit computational time will increase. Based on other literature, burn-in and MCMC calculations of 100.000 and 100.000-300.000 are used respectively (Cheng *et al.,* 2016; Harper *et al.,* 2012; Bus *et al.,* 2011; Hamblin *et al.,* 2010). Moreover, data consistency can be improved by increased iterations which should decrease the standard error.

Besides improving parameters in the software, the selection of accessions to build a populations structure can be altered. In this research, a population structure was made for 11 morphotypes. The ideology behind it is that the population structure can be used for leaf analysis and not only cabbage head analysis. However, the leaf data was not analysed in this thesis due to time constraints and available data. Therefore, it would be interesting to build a population structure with only heading cabbage accessions to reanalyse the data in the GWAS with the new population structure. The resulting correction of heading cabbage is

expected to be stricter than population correction based on population structure calculated over all morphotypes. Furthermore, a split in cabbage types is expected; white cabbage in a different group than red cabbage whereas all cabbage types were in the same group in this research. Researcher Dr. Xuan Xu started working with only heading cabbage material. Preliminary results of the population structure showed that cabbage types are assigned to different groups. Furthermore, the subpopulations are formed based on geographically origins in which a clear group can be formed in Asia, Europe and North America. This suggests that breeding with *B. oleracea* mainly occurred within continents and little plant material across continents was exchanged.
STRUCTURE software has the drawback that the results are hard to interpret. Other programs and methods to calculate a population structure do exist. Principal Component Analysis (PCA) or Principal Coordinate Analysis (PCoA) are used in software packages, for example R (T RC, 2014; Jombar, 2008; Conomos, 2017). The output of PCA and PCoA are matrices just like the Q matrix and can be used as input for a GWAS. A GWAS on candidate genes for water stress tolerance in canola (*B. napus*) showed PCA outperforming STRUCTURE software (Zhang *et al.,* 2015) but in other research on seed quality in *B. napus* and metabolite variation in *B. rapa*, PCA/PCoA and STRUCTURE showed similar results (Gajardo *et al.,* 2015; Del Carpio *et al.,* 2011). Therefore, it would be interesting to see if quality differences could be identified by using the Q or PCA matrix in the GWAS of this research.
Besides population structure correction, kinship correction can be applied. Kinship correction takes genetic distances between populations or relatedness between individuals into account. Because the material in this research was used in breeding, especially the hybrids, one could expect relatedness between accessions. Kinship correction in the form of a K-matrix can be calculated with, for example, SPAGeDi (Spatial Pattern Analysis of Genetic Diversity) software (Hardy & Vekemans, 2002). Research in *B. rapa* showed small effect for kinship correction. However, for *B. oleracea* and in particular this dataset, the kinship is unknown. Q and K matrices are often combined for GWAS, the so called 'QK method' (Yu *et al.,* 2006). Therefore, it would be interesting to compare the outcome of the GWAS when there is no correction applied, population structure correction (Q and PCA), kinship correction (K) and population structure with kinship correction (Q+K and PCA+K).

5.2.3. Genome wide association study

The GWAS was performed with TASSEL software using a GLM with 18.580 SNP markers and 999 permutations. The permutations were done to control the experiment-wise error rate. Because this research chose to correct with a population structure, a GLM was sufficient to analyse the data. However, when kinship is included into the analysis, a Mixed Linear Model (MLM) should be used. This model is more stringent than GLM and can lead to type II errors: false negatives. GLM is mainly prone to type I errors: false positives (Pace *et al.,* 2015). However, it is assumed that false negatives occur in the GWAS. This is because markers that explain leaf development can be associated with a morphotype and are therefore filtered out. To reduce these false positives, the False Discovery Rate was applied (FDR ≤ 0.01). The FDR method by Benjamini and Hochberg controls the false positives among significant results. Other correction methods do exist, for example the Bonferroni Genome Wide Error method. This method is very stringent. The significance threshold (0.01) is divided by the total number of markers (18.580) (Gupta *et al.* 2013),. For each trait a significance threshold of 5.38×10^{-7} would be used whereas the FDR method has a threshold

per trait per dataset (*appendix 7.1*). With the Bonferroni method many traits would not have significant markers because these do not meet the LOD threshold of 6.27.

$$Bonferroni\ LOD\ threshold = -log^{10}\left(\frac{0.01}{18.580} = 5.38 * 10^{-7}\right) = 6.27$$

The FDR method is less stringent than the Bonferroni method which should lead to more false positives. However, it is assumed that this is not considered a major problem because an interesting genomic region in one of the three datasets can be validated in the other two independent datasets. Furthermore, other indicators of marker quality are available. One of these indicators may be the allelic composition of the marker. *Figure 18* only showed two of the 14 markers from *table 4*. It is clear from this figure and table that the allele composition varies between markers. When the difference between major and minor allele is large, for example marker C1_31515139, a large difference in genotype frequency is observed as well. When a limited number of accessions have the minor allele (3), one can wonder if the marker-trait association is trustworthy. As the observed frequency is caused by cabbage specific allelic composition (white, red, savoy and pointed) and because some traits differ among cabbage types (for example red cabbages are smaller and have a specific shape). For marker C1_31515139, the C allele is not observed in red cabbage whereas it is observed in white, savoy and pointed cabbage. The allele frequency of the second marker, C2_17135516, is similar for all cabbage types. This gives an indication that the marker is not cabbage type specific and thus has a lower chance of being a false positive. Each marker in *table 4* should be analysed for its quality by allelic composition and its effect on the associated trait. However, due to time limitations only two out of 14 markers (C1_31515139 & C2_17135516) were analysed.

For each trait in each dataset, a GWAS was calculated two times: with and without population structure correction. In the situation with many significant markers, a marker-trait association was considered interesting if a peak increased in LOD score after population structure correction and when the same region was identified for the same trait in other datasets. In the situation of traits with a limited number of significant marker-trait associations, individual markers that do not form a peak can be considered interesting when they increase in LOD score after population structure correction and when the region reoccurs in other datasets for the same trait. An explanation for these individual significant markers may be a low LD in these regions or a local low marker density.

In WURField2015, the GWAS data are visualised in 22 Manhattan plots for 11 traits. 3594 significant marker-trait associations were found which were identified by 1347 markers. This means that many markers are correlated to multiple traits. This has two explanations. First, some traits are partly defined by other traits. For example: Head Weight is used to determine the Head Weight Percentage; Head Width and Head Length are used as parameters to calculate Head Index/Length_over_width. Second, Head Weight, Head Width, Head Area, Head Index, Head Volume, Head Weight Percentage and Total Weight all have many overlapping significant markers. The FDR method was not stringent for these traits which resulted in a low LOD score which in turn result in many significant markers. Among the significant markers many false positives will be present. If the Bonferroni threshold would be used, less markers would be significant. This may be a solution in further GWAS analyses, when many marker-trait associations are found by FDR correction, the Bonferroni threshold

should be used. Head Shape and Head Roundness did not find noteworthy marker-trait associations. Moreover, Head Density was removed from the analysis because the phenotypic data was not trustworthy. The other traits, Head Length, Head Width, Head Weight, Head Area, Head Index, Head Volume, Head Weight Percentage and Total Weight resulted in many marker-trait associations (*appendix 7.2*).

In the analysis of the Companies2015 data, less significant marker-trait associations after populations structure correction were detected. In the GWAS for Head Weight, Head Width, Core Length, Head Density and Uniformity, no significant marker-trait associations were identified at all. An explanation may be the fact that this dataset contained only genebank accessions. These accessions are known to have variation between plants of the same accession; they are heterogeneous. Therefore, GWAS software may not identify marker-trait associations, as the genotypic data are from single plants that may not be representative. Furthermore, each cabbage type was phenotyped by a different company which used different phenotyping criteria. Moreover, the cabbage types were not harvested on the same date and the different types were grown on different locations. The GWAS for Head Length, Blistering and Stem Length did result in identification of significant marker-trait associations (*appendix 7.3*). Stem Length was not measured consistently for all cabbage types and is therefore ignored for further analysis. Leaf blistering is an interesting trait mainly observed in savoy cabbage. Unfortunately, this trait was only measured in Companies2015 which makes validation across datasets impossible. However, significant marker-trait association peaks were identified after population structure correction (*figure 17*). The marker with the highest LOD score in a peak (peak marker) was chosen for candidate region analysis for leaf blistering (C3_13093205, C4_11126258, C5_11156527; *table 4*).

In ZonMW2016, 1696 marker-trait associations were identified after correction by population structure. Not for all traits significant marker-trait associations were identified. For AreaRatio, Maxwidth over half Length, Phi, Head Length in block A and Length_over_Width in block A no significant associations were identified. Because for Head Length and Length_over_Width, traits that showed an interaction with blocks and thus were analysed in block, in block A no significant associations were identified, analysis was done for Head Length block B and Length over Width block B and the outcome was compared across datasets because these traits have significant marker-trait associations. The GWAS for Head Weight and Core Length resulted in identification of many significant marker-trait associations after FDR analysis. For these traits, the Bonferroni method might give a better indication for significant associations. Furthermore, Core Length was not correctly measured by the algorithm. Therefore, no concrete conclusions can be drawn for this trait. The ZonMW2016 GWAS for Core Length could be repeated with red cabbage data only because these were correctly measured. However, it is advised to improve the algorithm or measure Core Length manually to keep the sample size high and increase the chance to find true associations. Interesting markers were identified for Head Length, Head Weight, Head Width, Anisometry, Length over Width and Roundness (*appendix 7.4*).

When the datasets are compared to one another, few remarks can be made. Head Length is the only trait in which the GWAS identified significant marker-trait associations in each dataset. Furthermore, many marker-trait associations were identified in the same genomic region between WURField2015 and ZonMW2016 for Head Weight, Head Width and Length_over_Width/Head index. However, due to time limitations only few traits were

analysed in more detail. Head Length was chosen because the trait was scored in all datasets. Only one significant region on C01 reoccurred in all datasets. This region was analysed by peak marker C1_31515139. Interesting regions for Blistering are described above. Finally, one trait with many significant marker-trait associations for both WURField2015 and ZonMW2016 was chosen for further analysis. Head Weight was chosen over Head Width and Length_over_Width/Head Index because it contained more significant peaks in ZonMW2016 that increased in LOD score.

5.2.4. Candidate genes

From the GWAS output, 14 markers were chosen that serve as peak markers of candidate regions for candidate gene searches. A search window was established in the BolBase genome browser. The average LD of *B. oleracea* was estimated at 36.8 Kb which would indicate a search window of 2 * 36.8 = 73.6 Kb search window. However, 36.8 Kb is an average and to increase the probability to find a candidate gene, a search window of 2 * 50 Kb = 100 Kb was chosen.

The search window around marker C1_31515139 for Head Length identified two candidate genes. *SLOW GREEN1* is in *A. thaliana* involved in the early stage of chloroplast development (Hu *et al.,* 2014). It is imaginable that the number of chloroplasts has a relation with plant growth and thus Head Length. *NAC058* was identified which is part of the NAC transcription factor family consisting of *NO APICAL MERISTEM* (*NAM*), *Arabidopsis Thaliana ACTIVATING FACTOR* (*ATAF*) and *CUP-SHAPED COTYLEDON* (*CUC*) (Naruzzaman *et al.,* 2015). *NAC058* is coding for *CUC2* that activates *SHOOTMERISTEMLESS* (*STM*) and *KNOTTED-like homeobox protein 6* from *Arabidopsis* (*KNAT6*) which play a role in SAM maintenance (Belles-Boix *et al.,* 2006) . Furthermore, *CUC2* is involved in leaf margin development and leaf serration (Peaucelle *et al.,* 2007; Nikovics *et al.,* 2007). *CUC2* seems to be involved in leaf shape and leaf growth which makes this a real interesting candidate gene.

Based on *table 4,* three regions around markers associated with leaf blistering are selected to search for candidate genes. Three linked significant markers were added to expand the regions; one on C03 and two on C04. This was done because the peaks formed in *figure 16* covered a larger area on C03 and C04 which could not be covered by a 100 Kb region around a single marker per chromosome. Candidate genes involved in cell growth, especially in plant leaves, are considered interesting for the Blistering phenotype.

The search around C3_13093205 identified two candidate genes. *CYCLIN-U2-1* (*CYCU2-1*) might be involved in cell division and is expressed in the shoot apex, leaf primordia and young leaves (Torres-Acosta *et al.,* 2004). *EXPANSIN-B6* and *B4* (*EXPB6/EXPB4*) may cause the loosening and extension of cell walls (Sampedro & Cosgrove, 2005).

Marker C3_17002635 identified *NAC054*, another member of the NAC transcription factor family which encodes *CUC1*. *CUC1* has the same function as *CUC2* in SAM formation, interaction with *STM* & *KNAT6* and leaf margin development (Aida *et al.,* 1999).

Marker C4_6657392 identified two candidate genes. *Wax Synthase diacylglycerol acyltransferase1* (*WSD1*) is involved in cuticular wax biosynthesis (Li *et al*., 2008). *Vacuolar amino acid transporter 1* (AVT1) is required for the vacuolar uptake of large amino acids in yeast (Rusnak *et al.,* 2001). Perhaps it has a similar function in cabbage which causes cells to swell and have a blistering phenotype.

Marker C4_11126258 identified two transcription factors MYB81 and MYB104 which might be involved in cell differentiation, based on their GO annotation. However, this is not

supported by literature yet and needs verification. Marker C5_11156527 identified two candidate genes. *Cell division control protein 48 homolog A* (*CDC48A*) probably has a function in cell division and growth processes (Rancour *et al.,* 2004). *Auxin Response Factor 6* (*ARF6*) is a transcriptional activator that responds to auxin. The gene is known to promote jasmonic acid production and is involved in flower development (Nagpal *et al.,* 2005). Many cell growth processes are regulated by auxin. Perhaps *ARF6* plays a role in cell growth defining the Blistering phenotype. The best candidate genes for blistering are *CYCU2-1*, *EXPB4/6* and *CUC1* based on their described functions in the genes above.

To identify candidate genes for Head Weight, genomic regions around 10 markers were selected for further analysis (*table 4*). Additionally, some regions were expanded with four markers because some region did not contain any genes or the region contained multiple interesting peaks in the Manhattan plots that was better represented by a larger region. Candidate genes for Head Weight are involved in plant growth because this generates biomass and thus weight. Genes involved in cell growth were selected.
The region around marker C1_26101229 identified two candidate genes. *TRANSMEMBRANE KINASE1* and *4* (*TMK1/TMK4*) are involved in cell expansion and proliferation (Dai *et al.,* 2013) and may be involved in brassinosteroid-mediated growth and development auxin signal transduction (Kim *et al.,* 2013). *Indoleacetic acid induced protein 9* (*IAA9*) is a transcriptional faction that acts as a repressor of early auxin response genes and interacts with *ARFs* (Liscum & Reed, 2002). Since auxin is involved in many cell growth processes, *IAA9* may play a role in Head Weight.
The region around two markers on C02 did not contain clear candidate genes (*table 4* & *5*). Another region around marker (C2_1410548) was added and a gene was identified. *TERMINAL FLOWER 1* (*TFL1*) is a repressor of flowering time in the long-day flowering pathway. It controls inflorescence meristem identity and interacts with *APETALA1* and *LEAFY* (Shannon & Meeks-Wagner, 1991). Although this gene has no direct connection to Head Weight, it is still remarkable that a flowering gene is correlated to a marker for Head Weight. An explanation might be that *TFL1* delays flowering which creates time for leafy head growth.
In the region around marker C3_23629292, *PUMILIO homolog 5* from *Arabidopsis* (*APUM5*) was identified which is a RNA binding protein that regulated translation and stability. *APUM5* has interaction with *CLV1* and *WUS* which are known proteins involved in leaf initiation and leaf polarity (Francischini & Quaggio, 2009).
The region around marker C3_24041641 contains *MITOGEN-ACTIVATED protein kinase kinase 5* (*MKK5*). It regulates stomatal cell fate. Furthermore, it is regulating coordinated local cell proliferation which shapes morphology of plants (Wang *et al.,* 2007; Meng *et al.,* 2012).
In the region around Marker C4_4779806, *IRREGULAR XYLEM 9* (IRX9) was identified. *IRX9* is involved in the synthesis of hemicellulose, a component of secondary cell walls. It is probably plays a role in cell elongation (Brown *et al.,* 2005). Around the other marker on C04, C4_36909949, no genes of interest were identified.
The region around marker C5_2023603 contained two candidate genes. *GLOBAL TRANSCRIPTION FACTOR GROUP E4* (*GTE4*) is involved in the activation and maintenance of cell division in meristems (Della Rovere *et al.,* 2010). CLOTHO (CLO) is associated with the control of polarized cell growth and cell proliferation (Yagi *et al.,* 2009).
The region of marker C5_31650480 contained two candidate genes. *CLATHRIN HEAVY CHAIN1* (*CHC1*) is required for a correct polar distribution of PIN auxin transporters (Kitakura

et al., 2011) which play an important role in leaf initiation and thus leaf growth. *LOB domain-containing protein 21* (*LBD21*) is an *ASYMMETRIC LEAVES 2* (*AS2*) like protein. *AS2* is involved in leaf initiation and leaf polarity. Leaf polarity genes are important candidate genes involved in leafy head formation (Cheng *et al.,* 2016).
The region around marker C07, C7_3941239 contained a Squamosa promotor-binding-like protein 10 (SPL10). Based on the GO annotation of biological process, this gene is involved in leaf shaping (Shikata *et al.,* 2009)
The regions around the two markers in C08 in *table 4* did not contain candidate genes. Therefore, another marker was added (C8_3362427). The region around C8_3362427 contained *Phosphatidylinositol 4-phosphate 5-kinase 3* (*PIP5K3*). Based on GO annotation biological process, this gene is involved in the regulation of cell polarity and root growth (Stanislas *et al.,* 2015; Stenzel *et al.,* 2008).
Based on GO annotations and described functions of the above listed genes from *A. thaliana*, *TMK1/4*, *APUM5*, *MKK5*, *GTE4* and *CHC1* are most promising candidate genes for Head Weight as they are involved in cell expansion, cell proliferation, leaf initiation, leaf polarity and cell division

Genomic regions around some of the markers for Head Weight in *table 4* did not harbour clear candidate genes which may be an indication that this marker-trait association is a false positive. For all Head Length and Blistering associated markers, candidate genes were identified. This indicates a higher probability for a true positive. The false positives for Head Weight can be explained. The LOD threshold after FDR correction was low which resulted in a high number of significant marker-trait associations. It was expected that some of the markers were false positives.

6. Conclusion and recommendations

The aims which were stated in the beginning of this research are achieved, although improvements can be made. The analysis of phenotypic data in Companies2015 identified significant differences between cabbage types for all traits except Core Length. The results were all explainable. However, improvements in future research can be made, when companies are involved in gathering phenotypic data. Clear agreements have to be made about the traits to measure and harvesting time.

The collection of phenotypic data in ZonMW2016 can be further improved. When images are taken, the orientation of the cabbage head should be the same for all measurements. Furthermore, Both halves of the cabbage should be photographed from the cross section side to improve the measurements for Core Length and when 3D images are considered, perhaps Head Volume. A correction should be implemented for the height between the camera and the cabbage head because this length is varying per cabbage head size which can cause overestimation of cabbage size. The algorithm, which was used to analyse the images, has to be improved. Core Length is an important trait and is not correctly measured in white, pointed and savoy cabbage. When the image is split in different colour channels, the Core Length can be distinguished. Furthermore, Head Density and Head Volume still need to be analysed by the computer vision and robotics department as well as leaf images. Leaf blistering would be a good addition to the ZonMW2016 dataset and is easy to score based on images with a scale from one to nine. The analysis of ZonMW2016 resulted in logical differences between morphotypes per trait.

The population structure was calculated with STRUCTURE software and the results were logical. With the knowledge we have now, regarding computational time and parameter settings, the population structure should be recalculated with the un-thinned marker file of 1376 markers. Furthermore, iterations should be increased to at least five and the MCMC calculations should be increased to at least 100.000. The burn-in period of 100.000 can remain the same. The interpretation of the STRUCTURE results were challenging. It would be good to compare results from STRUCTURE to results of PCA/PCoA to check if the population structure is correct. Additionally, kinship can be included into the model but one could question the added value. LD analysis was not performed in this research but is advised to conduct in further research. Finally, genotypic data gathered on heading cabbage accessions, rather than all morphotypes, could improve the number of called SNPs and perhaps the quality of the population structure and subsequent association study.

The GWAS was performed with TASSEL software using a GLM. Results were analysed with the FDR which identified a significant marker-trait association threshold. For some traits, especially in WURField2015, a large number of markers was associated. Other traits did not identify any significant marker-trait associations at all. To decrease the number of significant marker-trait associations, the Bonferroni threshold could be implemented. When there is more time available, more interesting regions on the genome could be selected for candidate gene analysis. The allelic composition of the peak markers can give an indication of the quality of the marker and should be investigated for each peak-marker used in the research. The analysis for candidate genes by screening a region of 100 KB around a peak marker, identified multiple candidate genes for Head Length, Blistering and Head Weight. With more

time available, more significant marker-trait associations could be research which could lead to the identification of more candidate genes in the BolBase genome browser.

Candidate genes of Head Length (*CUC2*), Blistering (*CYCU2-1, EXP4/6* and *CUC1*) and Head Weight (*TMK1/4, APUM5, MKK5, GTE4* and *CHC1*) have known sequences in *A. thaliana*. Homologs of these genes might be identified in re-sequence data of the Brassica 1000 genome project. If the gene can be identified in *B. oleracea*, the sequences can be compared to identify different loci which might explain the phenotype.

Acknowledgement

I would like to thank Guusje for her support and feedback during the six months of this thesis. The discussions really improved the quality of the thesis. Furthermore, I would like to thank Johan for letting me use his computer for STRUCTURE, TASSEL and GenStat. I would also like to thank the *Brassica* people in the Growth and development group with harvesting and imaging the cabbage heads. I would like to thank Theo Borm for providing genotypic data for this research and Joao for giving advice with regard to population structure. I would like to thank Gerrit, Danijela and Toon for their work on the imaging software. Finally, I would like to thank my fellow students in the Breeders Hall which made this six months enjoyable.

References

Adenot, X., Elmayan, T., Lauressergues, D., Boutet, S., Bouché, N., Gasciolli, V., & Vaucheret, H. (2006). DRB4-dependent TAS3 trans-acting siRNAs control leaf morphology through AGO7. *Current Biology*, *16*(9), 927-932.

Aida, M., Ishida, T., & Tasaka, M. (1999). Shoot apical meristem and cotyledon formation during Arabidopsis embryogenesis: interaction among the CUP-SHAPED COTYLEDON and SHOOT MERISTEMLESS genes. *Development*, *126*(8), 1563-1570.

Anastasiou, E., Kenz, S., Gerstung, M., MacLean, D., Timmer, J., Fleck, C., & Lenhard, M. (2007). Control of plant organ size by KLUH/CYP78A5-dependent intercellular signaling. *Developmental cell*, *13*(6), 843-856.

Anderson, M., & ter Braak, C. T. (2003). Permutation tests for multi-factorial analysis of variance. *Journal of statistical computation and simulation*, *73*(2), 85-113.

Apweiler, R., Bairoch, A., Wu, C. H., Barker, W. C., Boeckmann, B., Ferro, S., ... & Martin, M. J. (2004). UniProt: the universal protein knowledgebase. *Nucleic acids research*, *32*(suppl 1), D115-D119.

Arias, T., Beilstein, M. A., Tang, M., McKain, M. R., & Pires, J. C. (2014). Diversification times among Brassica (Brassicaceae) crops suggest hybrid formation after 20 million years of divergence. *American journal of botany*, *101*(1), 86-91.

Autran, D., Jonak, C., Belcram, K., Beemster, G. T., Kronenberger, J., Grandjean, O., ... & Traas, J. (2002). Cell numbers and leaf development in Arabidopsis: a functional analysis of the STRUWWELPETER gene. *The EMBO Journal*, *21*(22), 6036-6049.

Bar, M., & Ori, N. (2014). Leaf development and morphogenesis. *Development*, *141*(22), 4219-4230.

Barkoulas, M., Galinha, C., Grigg, S. P., & Tsiantis, M. (2007). From genes to shape: regulatory interactions in leaf development. *Current opinion in plant biology*, *10*(6), 660-666.

Bayer, E. M., Smith, R. S., Mandel, T., Nakayama, N., Sauer, M., Prusinkiewicz, P., & Kuhlemeier, C. (2009). Integration of transport-based models for phyllotaxis and midvein formation. *Genes & development*, *23*(3), 373-384.

Belles-Boix, E., Hamant, O., Witiak, S. M., Morin, H., Traas, J., & Pautot, V. (2006). KNAT6: an Arabidopsis homeobox gene involved in meristem activity and organ separation. *The Plant Cell*, *18*(8), 1900-1907.

Benjamini, Y., & Hochberg, Y. (1995). Controlling the false discovery rate: a practical and powerful approach to multiple testing. *Journal of the royal statistical society. Series B (Methodological)*, 289-300.

Bonnema, G., Del Carpio, D. P., & Zhao, J. (2011). Diversity analysis and molecular taxonomy of Brassica vegetable crops. *Genetics, Genomics and Breeding of Vegetable Brassicas*, 81.

Bradbury, P. J., Zhang, Z., Kroon, D. E., Casstevens, T. M., Ramdoss, Y., & Buckler, E. S. (2007). TASSEL: software for association mapping of complex traits in diverse samples. *Bioinformatics*, *23*(19), 2633-2635.

Braybrook, S. A., & Kuhlemeier, C. (2010). How a plant builds leaves. *The Plant Cell*, *22*(4), 1006-1018.

Brown, D. M., Zeef, L. A., Ellis, J., Goodacre, R., & Turner, S. R. (2005). Identification of novel genes in Arabidopsis involved in secondary cell wall formation using expression profiling and reverse genetics. *The Plant Cell*, *17*(8), 2281-2295.

Browning, S. R., & Weir, B. S. (2010). Population structure with localized haplotype clusters. *Genetics*, *185*(4), 1337-1344.

Bus, A., Körber, N., Snowdon, R. J., & Stich, B. (2011). Patterns of molecular variation in a species-wide germplasm set of Brassica napus. *Theoretical and Applied Genetics*, *123*(8), 1413-1423.

Byrne, M. E., Simorowski, J., & Martienssen, R. A. (2002). ASYMMETRIC LEAVES1 reveals knox gene redundancy in Arabidopsis. *Development*, *129*(8), 1957-1965.

Cantor, R. M., Lange, K., & Sinsheimer, J. S. (2010). Prioritizing GWAS results: a review of statistical methods and recommendations for their application. *The American Journal of Human Genetics*, *86*(1), 6-22.

Carles, C. C., & Fletcher, J. C. (2003). Shoot apical meristem maintenance: the art of a dynamic balance. *Trends in plant science*, *8*(8), 394-401.

Cartea, M. E., Lema, M., Francisco, M., Velasco, P., Sadowski, J., & Kole, C. (2011). Basic information on vegetable Brassica crops. *Genetics, Genomics and Breeding of Vegetable Brassicas*, 1-33.

Cheng, F., Mandáková, T., Wu, J., Xie, Q., Lysak, M. A., & Wang, X. (2013). Deciphering the diploid ancestral genome of the mesohexaploid Brassica rapa. *The Plant Cell*, *25*(5), 1541-1554.

Cheng, F., Sun, R., Hou, X., Zheng, H., Zhang, F., Zhang, Y., ... & Liu, D. (2016). Subgenome parallel selection is associated with morphotype diversification and convergent crop domestication in Brassica rapa and Brassica oleracea. *Nature Genetics*.

Cheng, F., Wu, J., Fang, L., Sun, S., Liu, B., Lin, K., ... & Wang, X. (2012). Biased gene fractionation and dominant gene expression among the subgenomes of Brassica rapa. *PLoS One*, *7*(5), e36442.

Cheng, F., Wu, J., & Wang, X. (2014). Genome triplication drove the diversification of Brassica plants. *Horticulture Research*, *1*, 14024.

Conomos, M.P. (2017). Population Structure and Relatedness Inference using the GENESIS Package. [online] Available at: https://www.bioconductor.org/packages/devel/bioc/vignettes/GENESIS/inst/doc/pcair.html [Accessed 9-March-2017]

Dai, N., Wang, W., Patterson, S. E., & Bleecker, A. B. (2013). The TMK subfamily of receptor-like kinases in Arabidopsis display an essential role in growth and a reduced sensitivity to auxin. *PLoS One*, *8*(4), e60990.

Della Rovere, F., Airoldi, C. A., Falasca, G., Ghiani, A., Fattorini, L., Citterio, S., ... & Altamura, M. M. (2010). The Arabidopsis BET bromodomain factor GTE4 regulates the mitotic cell cycle. *Plant signaling & behavior*, *5*(6), 677-680.

Del Carpio, D. P., Basnet, R. K., De Vos, R. C., Maliepaard, C., Paulo, M. J., & Bonnema, G. (2011). Comparative methods for association studies: a case study on metabolite variation in a Brassica rapa core collection. *PLoS One*, *6*(5), e19624.

Dinneny, J. R., Yadegari, R., Fischer, R. L., Yanofsky, M. F., & Weigel, D. (2004). The role of JAGGED in shaping lateral organs. *Development*, *131*(5), 1101-1110.

Dkhar, J., & Pareek, A. (2014). What determines a leaf's shape?. *EvoDevo*, *5*(1), 1.

Earl, D. A. (2012). STRUCTURE HARVESTER: a website and program for visualizing STRUCTURE output and implementing the Evanno method. *Conservation genetics resources*, *4*(2), 359-361.

Eshed, Y., Izhaki, A., Baum, S. F., Floyd, S. K., & Bowman, J. L. (2004). Asymmetric leaf development and blade expansion in Arabidopsis are mediated by KANADI and YABBY activities. *Development*, *131*(12), 2997-3006.

Evanno, G., Regnaut, S., & Goudet, J. (2005). Detecting the number of clusters of individuals using the software STRUCTURE: a simulation study. *Molecular ecology*, *14*(8), 2611-2620.

FAOSTAT, 2015. Food and Agriculture Organisation of the United Nations – Statistical Division. [online] Available at: http://faostat3.fao.org/browse/Q/QC/E [Accessed 12 September 2016]

Fit&Nourished, (2016). Cauli-power: Viva the revolution of cauliflower. [online] Available at: http://fitandnourished.com.au/?p=854 [Accessed 16 September 2016]

FoodsWithJudes, (2013). Brussels Sprouts Spotlight. [online] Available at: http://blog.foodswithjudes.com/brussels-sprouts-spotlight/ [Accessed 3 October 2016]

Francischini, C. W., & Quaggio, R. B. (2009). Molecular characterization of Arabidopsis thaliana PUF proteins–binding specificity and target candidates. *Febs Journal*, *276*(19), 5456-5470.

FruttaWeb, (2016). Fruit&Vegetable-Fresh vegetables-Only made in Italy-White cabbage 1 piece. [online] Available at: http://www.fruttaweb.com/en/only-made-in-italy/1687-white-cabbage-1-piece-origin-italy.html [Accessed 3 October 2016]

Gaamouche, T., Manes, C. L. D. O., Kwiatkowska, D., Berckmans, B., Koumproglou, R., Maes, S., ... & Inzé, D. (2010). Cyclin-dependent kinase activity maintains the shoot apical meristem cells in an undifferentiated state. *The Plant Journal*, *64*(1), 26-37.

Gajardo, H. A., Wittkop, B., Soto-Cerda, B., Higgins, E. E., Parkin, I. A., Snowdon, R. J., ... & Iniguez-Luy, F. L. (2015). Association mapping of seed quality traits in Brassica napus L. using GWAS and candidate QTL approaches. *Molecular Breeding*, *35*(6), 143.

GardensOnline, (2016). Plantfinder: Brassica juncea. [online] Available at: http://www.gardensonline.com.au/GardenShed/PlantFinder/Show_2651.aspx [Accessed 16 September 2016]

Gattepaille, L. M., & Jakobsson, M. (2012). Combining markers into haplotypes can improve population structure inference. *Genetics*, *190*(1), 159-174.

Gómez-Campo, C., & Prakash, S. (1999). 2 Origin and domestication. *Developments in plant genetics and breeding*, *4*, 33-58.

Grillo Services, (2016). The Blog – best vegetables for a Connecticut garden with HD images. [onlinie] Available at: http://grilloservices.com/grillo-blog/best-vegetables-for-a-connecticut-ct-garden-with-hd-images/ [Accessed 3 October 2016]

Guenot, B., Bayer, E., Kierzkowski, D., Smith, R. S., Mandel, T., Žádníková, P., ... & Kuhlemeier, C. (2012). PIN1-independent leaf initiation in Arabidopsis. *Plant Physiology*, *159*(4), 1501-1510.

Gupta, P. K., Kulwal, P. L., & Jaiswal, V. (2013). Association mapping in crop plants: opportunities and challenges. *Advances in genetics*, *85*, 109-147.

Harper, A. L., Trick, M., Higgins, J., Fraser, F., Clissold, L., Wells, R., ... & Bancroft, I. (2012). Associative transcriptomics of traits in the polyploid crop species Brassica napus. *Nature biotechnology*, *30*(8), 798-802.

Halkier, B. A., & Gershenzon, J. (2006). Biology and biochemistry of glucosinolates. *Annu. Rev. Plant Biol.*, *57*, 303-333.

Hamblin, M. T., Close, T. J., Bhat, P. R., Chao, S., Kling, J. G., Abraham, K. J., ... & Hayes, P. M. (2010). Population structure and linkage disequilibrium in US barley germplasm: implications for association mapping. *Crop Science*, *50*(2), 556-566.

Hardy, O. J., & Vekemans, X. (2002). SPAGeDi: a versatile computer program to analyse spatial genetic structure at the individual or population levels. *Molecular ecology notes*, *2*(4), 618-620.

Higdon, J. V., Delage, B., Williams, D. E., & Dashwood, R. H. (2007). Cruciferous vegetables and human cancer risk: epidemiologic evidence and mechanistic basis. *Pharmacological Research*, *55*(3), 224-236.

Horiguchi, G., Kim, G. T., & Tsukaya, H. (2005). The transcription factor AtGRF5 and the transcription coactivator AN3 regulate cell proliferation in leaf primordia of Arabidopsis thaliana. *The Plant Journal*, *43*(1), 68-78.

Hu, Y., Xie, Q., & Chua, N. H. (2003). The Arabidopsis auxin-inducible gene ARGOS controls lateral organ size. *The Plant Cell*, *15*(9), 1951-1961.

Hu, Z., Xu, F., Guan, L., Qian, P., Liu, Y., Zhang, H., ... & Hou, S. (2014). The tetratricopeptide repeat-containing protein slow green1 is required for chloroplast development in Arabidopsis. *Journal of experimental botany*, *65*(4), 1111-1123.

Inzé, D., & De Veylder, L. (2006). Cell cycle regulation in plant development 1. *Annu. Rev. Genet.*, *40*, 77-105.

JodanSeeds, (2016). Vegetable seeds-Cabbage-Open Pollinated-Red Acre Cabbage. [online] Available at: http://jordanseeds.com/Red-Acre-Cabbage.html [Accessed 3 October 2016]

Jombart, T. (2008). adegenet: a R package for the multivariate analysis of genetic markers. *Bioinformatics*, *24*(11), 1403-1405.

Kalve, S., De Vos, D., & Beemster, G. T. (2014). Leaf development: a cellular perspective. *Frontiers in plant science*, *5*, 362.

Kitakura, S., Vanneste, S., Robert, S., Löfke, C., Teichmann, T., Tanaka, H., & Friml, J. (2011). Clathrin mediates endocytosis and polar distribution of PIN auxin transporters in Arabidopsis. *The Plant Cell*, *23*(5), 1920-1931.

Khwaja, F. S., Wynne, S., Posey, I., & Djakiew, D. (2009). 3, 3′-diindolylmethane induction of p75NTR-dependent cell death via the p38 mitogen-activated protein kinase pathway in prostate cancer cells. *Cancer Prevention Research*, *2*(6), 566-571.

Kidner, C. A., & Martienssen, R. A. (2004). Spatially restricted microRNA directs leaf polarity through ARGONAUTE1. *Nature*, *428*(6978), 81-84.

Kim, M. H., Kim, Y., Kim, J. W., Lee, H. S., Lee, W. S., Kim, S. K., ... & Kim, S. H. (2013). Identification of Arabidopsis BAK1-associating receptor-like kinase 1 (BARK1) and characterization of its gene expression and brassinosteroid-regulated root phenotypes. *Plant and Cell Physiology*, pct106.

Labana, K. S., & Gupta, M. L. (1993). Importance and origin. In *Breeding Oilseed Brassicas* (pp. 1-7). Springer Berlin Heidelberg.

Lan, T. H., & Paterson, A. H. (2001). Comparative mapping of QTLs determining the plant size of Brassica oleracea. *Theoretical and Applied Genetics*, *103*(2-3), 383-397.

LaoDong, (2016). Phương pháp điều trị xanh chống lại bệnh ung thư [online] Available at: http://laodong.com.vn/suc-khoe/phuong-phap-dieu-tri-xanh-chong-lai-benh-ung-thu-318485.bld [Accessed 3 October 2016]

Lawson, D. J., Hellenthal, G., Myers, S., & Falush, D. (2012). Inference of population structure using dense haplotype data. *PLoS genetics*, *8*(1), e1002453.

Li, J., Mo, X., Wang, J., Chen, N., Fan, H., Dai, C., & Wu, P. (2009). BREVIS RADIX is involved in cytokinin-mediated inhibition of lateral root initiation in Arabidopsis. *Planta*, *229*(3), 593-603.

Li, F., Wu, X., Lam, P., Bird, D., Zheng, H., Samuels, L., ... & Kunst, L. (2008). Identification of the wax ester synthase/acyl-coenzyme A: diacylglycerol acyltransferase WSD1 required for stem wax ester biosynthesis in Arabidopsis. *Plant physiology*, *148*(1), 97-107.

Li, Y., Zhang, T., Korkaya, H., Liu, S., Lee, H. F., Newman, B., ... & Sun, D. (2010). Sulforaphane, a dietary component of broccoli/broccoli sprouts, inhibits breast cancer stem cells. *Clinical Cancer Research*, *16*(9), 2580-2590.

Li, Y., Zheng, L., Corke, F., Smith, C., & Bevan, M. W. (2008). Control of final seed and organ size by the DA1 gene family in Arabidopsis thaliana. *Genes & Development*, *22*(10), 1331-1336.

Lischer, H. E. L., & Excoffier, L. (2012). PGDSpider: an automated data conversion tool for connecting population genetics and genomics programs. Bioinformatics, 28(2), 298-299.

Liu, S., Liu, Y., Yang, X., Tong, C., Edwards, D., Parkin, I. A., ... & Wang, X. (2014). The Brassica oleracea genome reveals the asymmetrical evolution of polyploid genomes. *Nature communications*, *5*.

Liu, D., Song, Y., Chen, Z., & Yu, D. (2009). Ectopic expression of miR396 suppresses GRF target gene expression and alters leaf growth in Arabidopsis. *Physiologia plantarum*, *136*(2), 223-236.

Liscum, E., & Reed, J. W. (2002). Genetics of Aux/IAA and ARF action in plant growth and development. In *Auxin Molecular Biology* (pp. 387-400). Springer Netherlands.

Lysak, M. A., Cheung, K., Kitschke, M., & Bureš, P. (2007). Ancestral chromosomal blocks are triplicated in Brassiceae species with varying chromosome number and genome size. *Plant Physiology*, *145*(2), 402-410.

Maggioni, L., von Bothmer, R., Poulsen, G., & Branca, F. (2010). Origin and domestication of cole crops (Brassica oleracea L.): linguistic and literary considerations1. *Economic botany*, *64*(2), 109-123.

Meng, X., Wang, H., He, Y., Liu, Y., Walker, J. C., Torii, K. U., & Zhang, S. (2012). A MAPK cascade downstream of ERECTA receptor-like protein kinase regulates Arabidopsis inflorescence architecture by promoting localized cell proliferation. *The Plant Cell*, *24*(12), 4948-4960.

Mouchel, C. F., Osmont, K. S., & Hardtke, C. S. (2006). BRX mediates feedback between brassinosteroid levels and auxin signalling in root growth. *Nature*, *443*(7110), 458-461.

MSU, (2016). Michigan State University – Michigan Fresh: Turnips (HNI46). [online] Available at: http://msue.anr.msu.edu/resources/michigan_fresh_turnips [Accessed 16 September 2016]

Nagaharu, U. (1935). Genome analysis in Brassica with special reference to the experimental formation of B. napus and peculiar mode of fertilization. *Jpn J Bot*, *7*, 389-452.

Nagpal, P., Ellis, C. M., Weber, H., Ploense, S. E., Barkawi, L. S., Guilfoyle, T. J., ... & Ecker, J. R. (2005). Auxin response factors ARF6 and ARF8 promote jasmonic acid production and flower maturation. *Development*, *132*(18), 4107-4118.

Nakata, M., Matsumoto, N., Tsugeki, R., Rikirsch, E., Laux, T., & Okada, K. (2012). Roles of the middle domain–specific WUSCHEL-RELATED HOMEOBOX genes in early development of leaves in Arabidopsis. *The Plant Cell*, *24*(2), 519-535.

Nikovics, K., Blein, T., Peaucelle, A., Ishida, T., Morin, H., Aida, M., & Laufs, P. (2006). The balance between the MIR164A and CUC2 genes controls leaf margin serration in Arabidopsis. *The Plant Cell*, *18*(11), 2929-2945.

Nordborg, M., & Tavaré, S. (2002). Linkage disequilibrium: what history has to tell us. *TRENDS in Genetics*, *18*(2), 83-90.

Nuruzzaman, M., Sharoni, A. M., Satoh, K., Karim, M. R., Harikrishna, J. A., Shimizu, T., ... & Kikuchi, S. (2015). NAC transcription factor family genes are differentially expressed in rice during infections with Rice dwarf virus, Rice black-streaked dwarf virus, Rice grassy stunt virus, Rice ragged stunt virus, and Rice transitory yellowing virus. *Frontiers in plant science*, *6*, 676.

OpenFotos, (2016). Free photos – Food – Kohlrabi. [online] Available at: http://www.openfotos.com/view/kohlrabi-6060 [Accessed 3 October 2016]

Pace, J., Gardner, C., Romay, C., Ganapathysubramanian, B., & Lübberstedt, T. (2015). Genome-wide association analysis of seedling root development in maize (Zea mays L.). *BMC genomics*, *16*(1), 47.

Palatnik, J. F., Allen, E., Wu, X., Schommer, C., Schwab, R., Carrington, J. C., & Weigel, D. (2003). Control of leaf morphogenesis by microRNAs. *Nature*, *425*(6955), 257-263.

Panjabi, P., Jagannath, A., Bisht, N. C., Padmaja, K. L., Sharma, S., Gupta, V., ... & Pental, D. (2008). Comparative mapping of Brassica juncea and Arabidopsis thaliana using Intron Polymorphism (IP) markers: homoeologous relationships, diversification and evolution of the A, B and C Brassica genomes. *BMC genomics*, *9*(1), 1.

Parkin, I. A., Gulden, S. M., Sharpe, A. G., Lukens, L., Trick, M., Osborn, T. C., & Lydiate, D. J. (2005). Segmental structure of the Brassica napus genome based on comparative analysis with Arabidopsis thaliana. *Genetics*, *171*(2), 765-781.

Peaucelle, A., Morin, H., Traas, J., & Laufs, P. (2007). Plants expressing a miR164-resistant CUC2 gene reveal the importance of post-meristematic maintenance of phyllotaxy in Arabidopsis. *Development*, *134*(6), 1045-1050.

Pike, N. (2011). Using false discovery rates for multiple comparisons in ecology and evolution. *Methods in Ecology and Evolution*, *2*(3), 278-282.

Pinterest, (2016). Mustard plants, fields… [online] Available at: https://www.pinterest.com/rid83/mustard-plants-fields/ [Accessed 16 September 2016]

Prakash, S., & Hinata, K. (1980). Taxonomy, cytogenetics and origin of crop Brassicas: a review. *Op. Bot*, (55), 1-57.

Pritchard, J. K., Stephens, M., & Donnelly, P. (2000). Inference of population structure using multilocus genotype data. *Genetics*, *155*(2), 945-959.

Rancour, D. M., Park, S., Knight, S. D., & Bednarek, S. Y. (2004). Plant UBX domain-containing protein 1, PUX1, regulates the oligomeric structure and activity of Arabidopsis CDC48. *Journal of Biological Chemistry*, *279*(52), 54264-54274.

REAL, (2016). Responsible Eating and Living. [online] Available at: http://responsibleeatingandliving.com/juiced-curly-kale-kills-melanoma-cancer-cells/ [Accessed 16 September 2016]

Risch, N., & Merikangas, K. (1996). The future of genetic studies of complex human diseases. *Science*, *273*(5281), 1516-1517.

Rodriguez, R. E., Mecchia, M. A., Debernardi, J. M., Schommer, C., Weigel, D., & Palatnik, J. F. (2010). Control of cell proliferation in Arabidopsis thaliana by microRNA miR396. *Development*, *137*(1), 103-112.

Russnak, R., Konczal, D., & McIntire, S. L. (2001). A family of yeast proteins mediating bidirectional vacuolar amino acid transport. *Journal of Biological Chemistry*, *276*(26), 23849-23857.

Sampedro, J., & Cosgrove, D. J. (2005). The expansin superfamily. *Genome biology*, *6*(12), 242.

Satina, S., Blakeslee, A. F., & Avery, A. G. (1940). Demonstration of the three germ layers in the shoot apex of Datura by means of induced polyploidy in periclinal chimeras. *American Journal of Botany*, 895-905.

Scheuring, D., Löfke, C., Krüger, F., Kittelmann, M., Eisa, A., Hughes, L., ... & Kleine-Vehn, J. (2016). Actin-dependent vacuolar occupancy of the cell determines auxin-induced growth repression. *Proceedings of the National Academy of Sciences*, *113*(2), 452-457.

Schoof, H., Lenhard, M., Haecker, A., Mayer, K. F., Jürgens, G., & Laux, T. (2000). The stem cell population of Arabidopsis shoot meristems is maintained by a regulatory loop between the CLAVATA and WUSCHEL genes. *Cell*, *100*(6), 635-644.

Schranz, M. E., Lysak, M. A., & Mitchell-Olds, T. (2006). The ABC's of comparative genomics in the Brassicaceae: building blocks of crucifer genomes. *Trends in plant science*, *11*(11), 535-542.

Scofield, S., & Murray, J. A. (2006). KNOX gene function in plant stem cell niches. *Plant molecular biology*, *60*(6), 929-946.

Sebastian, R. L., Kearsey, M. J., & King, G. J. (2002). Identification of quantitative trait loci controlling developmental characteristics of Brassica oleracea L. *Theoretical and Applied Genetics*, *104*(4), 601-609.

Senome Layang, (unknown). Lihatlah lebih dekat. [online] Available at: http://senomelayang.blogspot.nl/ [Accessed 3 October 2016]

Shannon, S., & Meeks-Wagner, D. R. (1991). A mutation in the Arabidopsis TFL1 gene affects inflorescence meristem development. *The Plant Cell*, *3*(9), 877-892.

Shikata, M., Koyama, T., Mitsuda, N., & Ohme-Takagi, M. (2009). Arabidopsis SBP-box genes SPL10, SPL11 and SPL2 control morphological change in association with shoot maturation in the reproductive phase. *Plant and Cell Physiology*, *50*(12), 2133-2145.

Siegfried, K. R., Eshed, Y., Baum, S. F., Otsuga, D., Drews, G. N., & Bowman, J. L. (1999). Members of the YABBY gene family specify abaxial cell fate in Arabidopsis. *Development*, *126*(18), 4117-4128.

Slob, F., (2016). *Genetic analysis of leaf morphology in Brassica oleracea.* (Unpublished MSc thesis, Wageningen University, Wageningen, The Netherlands)

Smyth, D. R. (1995). Flower Development: Origin of the cauliflower. *Current Biology*, *5*(4), 361-363.

Song, K., Osborn, T. C., & Williams, P. H. (1990). Brassica taxonomy based on nuclear restriction fragment length polymorphisms (RFLPs). *Theoretical and Applied Genetics*, *79*(4), 497-506.

Stanislas, T., Hüser, A., Barbosa, I. C., Kiefer, C. S., Brackmann, K., Pietra, S., ... & Grebe, M. (2015). Arabidopsis D6PK is a lipid domain-dependent mediator of root epidermal planar polarity. *Nature plants*, *1*, 15162.

Stenzel, I., Ischebeck, T., König, S., Hołubowska, A., Sporysz, M., Hause, B., & Heilmann, I. (2008). The type B phosphatidylinositol-4-phosphate 5-kinase 3 is essential for root hair formation in Arabidopsis thaliana. *The Plant Cell*, *20*(1), 124-141.

Su, Y. H., Liu, Y. B., & Zhang, X. S. (2011). Auxin–cytokinin interaction regulates meristem development. *Molecular plant*, *4*(4), 616-625.

Takii seed, (2016). Vegetable Recipe – Chinese cabbage and seafood soup. [online] Available at: http://www.takiiseed.com/recipe/leafcrops/chinese-cabbage-and-seafood-soup/ [Accessed 16 September 2016]

Team, R. C. (2014). R: A language and environment for statistical computing. R Foundation for Statistical Computing, Vienna, Austria. 2013.

Torres Acosta, J. A., de Almeida Engler, J., Raes, J., Magyar, Z., De Groodt, R., Inzé, D., & De Veylder, L. (2004). Molecular characterization ofArabidopsisPHO80-like proteins, a novel class of CDKA; 1-interacting cyclins. *Cellular and molecular life sciences*, *61*(12), 1485-1497.

Toxicologycentre, (2016). Ethiopian Mustard. [online] Available at: http://www.toxicologycentre.com/cenkatukue/ [Accessed 16 September 2016]

Tsuge, T., Tsukaya, H., & Uchimiya, H. (1996). Two independent and polarized processes of cell elongation regulate leaf blade expansion in Arabidopsis thaliana (L.) Heynh. *Development*, *122*(5), 1589-1600.

Tsukaya, H. (2013). Leaf development. *The arabidopsis book*, e0163.

UPOV (International Union For The Protection Of New Varieties Of Plants), (2016). *Cabbage: Guidelines For the Conduct Of Tests For Distinctness, Uniformity And Stability*. Geneva: UPOV [online] Available at: <http://www.upov.int/edocs/tgdocs/en/tg048.pdf> [Accessed: 2-2-2017]

VanBijOns, (2016). Groenten Van Bij Ons- Spitskool. [online] Available at: http://www.lekkervanbijons.be/groenten/groenten-van-bij-ons/spitskool [Accessed 3 October 2016]

VSN International (2015). Genstat *for Windows* 18th Edition. VSN International, Hemel Hempstead, UK. Web page: Genstat.co.uk

Waites, R., & Hudson, A. (1995). phantastica: a gene required for dorsoventrality of leaves in Antirrhinum majus. *Development*, *121*(7), 2143-2154.

Wang, H., Ngwenyama, N., Liu, Y., Walker, J. C., & Zhang, S. (2007). Stomatal development and patterning are regulated by environmentally responsive mitogen-activated protein kinases in Arabidopsis. *The Plant Cell*, *19*(1), 63-73.

Wang, X., Wang, H., Wang, J., Sun, R., Wu, J., Liu, S., ... & Huang, S. (2011). The genome of the mesopolyploid crop species Brassica rapa. *Nature genetics*, *43*(10), 1035-1039.

Warwick, S. I., Francis, A., & Al-Shehbaz, I. A. (2006). Brassicaceae: species checklist and database on CD-Rom. *Plant Systematics and Evolution*, *259*(2-4), 249-258.

Warwick, S. I., Mummenhoff, K., Sauder, C. A., Koch, M. A., & Al-Shehbaz, I. A. (2010). Closing the gaps: phylogenetic relationships in the Brassicaceae based on DNA sequence data of nuclear ribosomal ITS region. *Plant Systematics and Evolution*, *285*(3-4), 209-232.

Wikipedia, (2016). Rapeseed. [online] Available at: https://en.wikipedia.org/wiki/Rapeseed [Accessed 16 September 2016]

Wolf, S., Hématy, K., & Höfte, H. (2012). Growth control and cell wall signaling in plants. *Annual review of plant biology*, *63*, 381-407.

Xu, R., & Li, Y. (2011). Control of final organ size by Mediator complex subunit 25 in Arabidopsis thaliana. *Development*, *138*(20), 4545-4554.

Yagi, N., Takeda, S., Matsumoto, N., & Okada, K. (2009). VAJ/GFA1/CLO is involved in the directional control of floral organ growth. *Plant and cell physiology*, *50*(3), 515-527.

Yanai, O., Shani, E., Dolezal, K., Tarkowski, P., Sablowski, R., Sandberg, G., ... & Ori, N. (2005). Arabidopsis KNOXI proteins activate cytokinin biosynthesis. *Current Biology*, *15*(17), 1566-1571.

Yokoyama, R., & Nishitani, K. (2001). A comprehensive expression analysis of all members of a gene family encoding cell-wall enzymes allowed us to predict cis-regulatory regions involved in cell-wall construction in specific organs of Arabidopsis. *Plant and Cell Physiology*, *42*(10), 1025-1033.

Yu, J., Pressoir, G., Briggs, W. H., Bi, I. V., Yamasaki, M., Doebley, J. F., ... & Kresovich, S. (2006). A unified mixed-model method for association mapping that accounts for multiple levels of relatedness. *Nature genetics*, *38*(2), 203-208.

Yu, J., Zhao, M., Wang, X., Tong, C., Huang, S., Tehrim, S., ... & Liu, S. (2013). Bolbase: a comprehensive genomics database for Brassica oleracea. *BMC genomics*, *14*(1), 664.

Zhang, J., Mason, A. S., Wu, J., Liu, S., Zhang, X., Luo, T., ... & Yan, G. (2015). Identification of putative candidate genes for water stress tolerance in canola (Brassica napus). *Frontiers in plant science*, *6*, 1058.

Zhang, Y., Persson, S., & Giavalisco, P. (2013). Differential regulation of carbon partitioning by the central growth regulator Target of Rapamycin (TOR). *Molecular plant*, *6*(6), 1731-1733.

Zhu, C., Gore, M., Buckler, E. S., & Yu, J. (2008). Status and prospects of association mapping in plants. *The plant genome*, *1*(1), 5-20.

Appendix

In the appendix of this thesis all additional information that was not shown in the report will be presented.

Appendix 1: Measured traits in WURField2015, Companies2015 and ZonMW2016

In this paragraph, the measured traits in three datasets will be shown. A subset of WURField2015 and Companies 2015 was used for the association analysis. However, the potential of the datasets is higher because leaf traits can be analysed as well. The traits in *table 3* are all measured traits for heading cabbage in ZonMW2016. However, picture analysis still has to be performed on detached leaves and is not included in this thesis. Therefore, appendix 1.3 shows the quantification of qualitative trait Head Shape.

Appendix 1.1: Measured traits in WURField2015

Table 6: Traits for heading cabbage.

Trait	Abbreviation	Description	Unit
Head area	HA	Surface area of the midsection of the head (figure 9)	mm^2
Head volume	HV	Volume of a fitted spheroid	mm^3
Head height	HH	Maximum height of the head (figure 9)	mm
Head width	HW	Maximum width of the head (figure 9).	mm
Total above ground biomass	TW	Fresh weight of above ground biomass	g
Head weight	HWe	Fresh weight of the head	g
Head weight percentage	HWeP	HWe percentage of TW	%
Head density	HD	HWe/HV	g/mm^3
Head index	HI	Ratio of HH/HW	#
Head roundness	HR	4 x (HA/(π x length major axis of a fitted ellipse^2))	#
Head shape	HS	1= Transverse narrow elliptic 2= Transverse elliptic 3= Circular 4= Broad elliptic 5= Broad obovate 6= Broad ovate 7= Angular ovate	scale

Table 7: Measured traits for leaf morphology in *Brassica oleracea*

Trait	Abbreviation	Description	Unit
Leaf area	LA	Total leaf area, including petiole	mm^2
Leaf length	LL	Total leaf length: the sum of PL+LaL	mm
Lamina length	LaL	Length of the lamina, from tip to base of the lamina	mm
Lamina width	LaW	Maximum width of the lamina	mm
Petiole presence	PP	Percentage of leaves with petiole	%
Petiole length	PL	Length of petiole (when present) from base to lamina (figure 8).	mm

Lamina length / petiole ratio	LPI	Ratio of LaL/PL	#
Petiole/midvein width	PW	Maximum width of petiole or midvein in absence of the petiole	mm
Lamina index	LaI	Ratio of LaL/LaW	#
Leaf index	LI	Ratio of LL/LaW	#
Lobe presence	LBp	% of leaves with deep lobes	%
Number of lobes	LBn	Number of deep lobes (when present)	#
Cumulative lobe length	LBcl	Cumulative length of lobes (when present)	mm
Average lobe length	LBla	Result of LBcl/LBn	mm
Leaf margin shape	LMS	1= Entire 2= Crenate 3= Undulate 4= Dentate 5= Curly crenate 6=Curly dentate 7=Lacerate	scale
Lamina shape	LS	1= Transverse broad elliptical 2= Circular 3= Broad ovate 4= Obovate 5= Spathulate 6=Elliptical 7= Deltoid 8= Oblong 9= Others	scale
Leaf complexity	LC	1= Entire 2= Weak 3= Medium 4= Strong 5= Very strong 6= Compound	scale

Appendix 1.2: Measured traits in Companies2015

Table 8: List of measured traits by breeders for white/pointed cabbage (Rijk Zwaan), red cabbage (Hazera) and savoy cabbage (Syngenta). Many traits were not measured for all cabbage types. A subset of traits was analysed (*table 2*)

Trait	Description	Unit
Cabbage Type	E=early; I=Industry; S=storage; red	#
Growing Days	Number of days after transplanting till harvest	# days
Leaves/vigour	Weight of outer leaves	g
Uniformity	9=Very uniform 1=very heterogeneous (5 intermediate)	scale
Stem Length	measurement in cm, average of 5 plants	cm/plant (avg. 5 plants)
Lodging	9=Straight 1=Falling down	scale
Blister	9=Very fine highly blistered 1=Smooth	scale
Depth	9=Deep within wrapper 1=On top of the wrapper	scale
Overlap	9=You can only see 1 leave 1= Top of the head is like a	scale

	whole	
Outside	9=Very smooth 1=Very rough	scale
Outer Colour - red	9=very dark red; 1= pale red	scale
Outer Colour - green/white	9=Very green 1=very white ;	scale
Wax	9=Very waxy; 1=no wax.	scale
Shape	UPOV scale (UPOV, 2016)	scale
Weight Head	measurement in grams/plant , average of 5 plants	g/plant (avg. 5 plants)
Height Head	measurement in cm/plant , average of 5 plants	cm/plant (avg. 5 plants)
Width Head	measurement in cm/plant, average of 5 plants	cm/plant (avg. 5 plants)
Core Width	measurement in cm/plant, average of 5 plants	cm/plant (avg. 5 plants)
Core Length	measurement in cm/plant, average of 5 plants	cm/plant (avg. 5 plants)
Inside / Density	9=Solid build-up, leaves packed and nicely layered 1=Very open and going flat structured	scale
Inner Colour	9=Very yellow 1=very white	scale
Cracking	9: absent; 1 large cracks	scale
Pulling	9: absent; 1 large cracks	scale
Harvest Date	the date when the head is harvested for measurements	date
Plant Date	the date when the plant is transplanted into the field	date
Maturation time	the days of the head growing in field before being harvested for measurements	# days

Appendix 1.3: Definition of Head Shape parameters in ZonMW2016

1) Phi: Orientation of the ellipse fitted to the object. Ra is the main radius of the ellipse. Phi is the angle between the x-axis of the image and Ra.

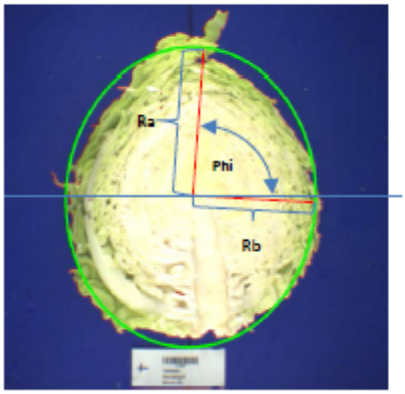

2) Anisometry: Anisometry = Ra/Rb.

3) Roundness:

If p is the center of the area, p_i the pixels and F the area of the contour.

$$\texttt{Distance} = \frac{1}{F}\sum \|p - p\_i\|$$

$$\texttt{Sigma}^2 = \frac{1}{F}\sum (\|p - p\_i\| - \texttt{Distance})^2$$

$$\texttt{Roundness} = 1 - \frac{\texttt{Sigma}}{\texttt{Distance}}$$

$$\texttt{Sides} = 1.4111\left(\frac{\texttt{Distance}}{\texttt{Sigma}}\right)^{0.4724}$$

4)

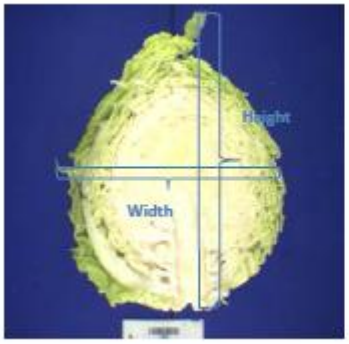

Height_over_width = Height/Width

- Ratio of areas under the cabbage widths function(IR=S1/S2):

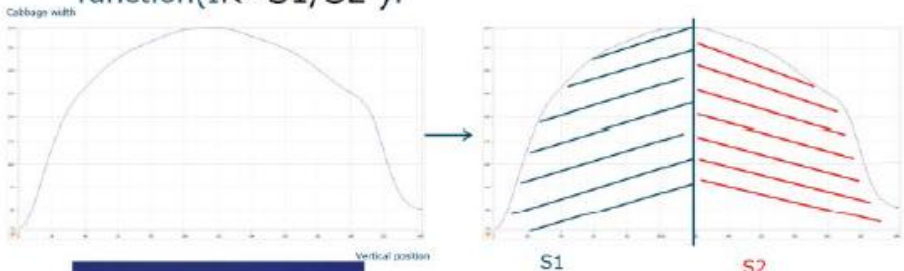

5) AreaRatio (IR)

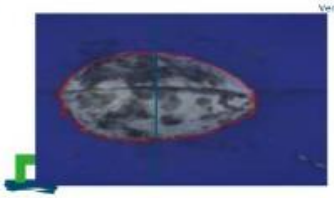

6) maxwidth_row_over_half_height

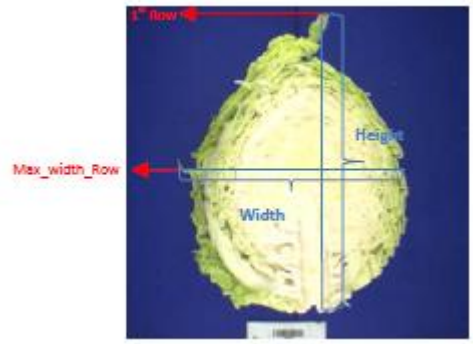

maxwidth_row_over_half_height =
Max_width_Row/(Height/2)

Appendix 2: Heading cabbage definition by UPOV

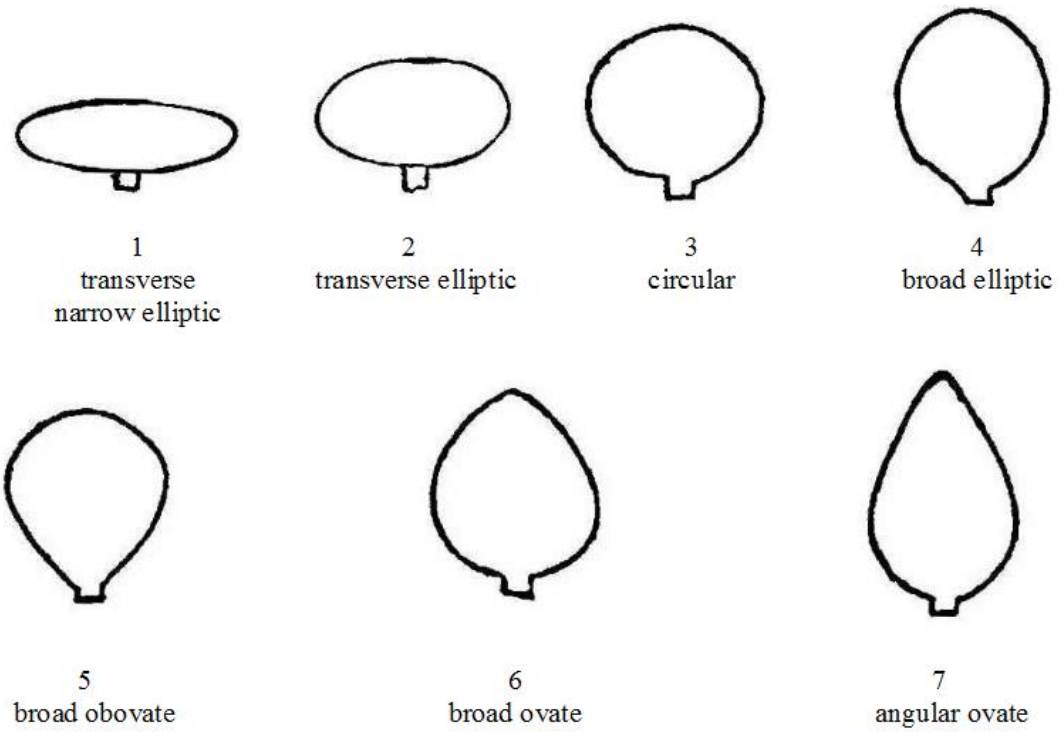

Figure 20: Heading cabbage definition by UPOV, 2016

Appendix 3: Morphotypes and identification code

Table 9: Overview of morphotypes and their identification code

(Sub-)Morphotype	Numerical code	Letter code
Broccoli (unknown)	1a	Bu
Broccoli (summer/autumn)	1b	Bs
Broccoli (winter)	1c	Bw
Cauliflower (unknown)	2a	Cu
Cauliflower (summer/autumn)	2b	Cs
Cauliflower (winter)	2c	Cw
Cauliflower (Romanesco)	2d	Cr
Cauliflower (tropical)	2e	Ct
Kale (unknown)	3a	Ku
Kale (bore and curly)	3b	Kb
Kale (marrow stem/palmy)	3c	Km
Kale (Chinese)	3d	Kc
Collard Greens	4a	Gu
Heading (unknown)	5a	Hu
Heading (white)	5b	Hw
Heading (red)	5c	Hr
Heading (savoy)	5d	Hs
Heading (pointed)	5e	Hp
Kohlrabi	6a	Ru
Ornamental	7a	Ou
Brussels sprouts	8a	Su
Tronchuda	9a	Tu
Wild *B. oleracea*	10a	Wu
13 Wild C9 species (not oleracea)	11a	9u
Off Types	12a	Xu

Appendix 4: Group definition population structure

Table 10: Amount of morphotypes per subpopulation (K). The definition of the group is based on the colour. K6 has multiple groups and is therefore a rest group. Missing values are defined as an accession does not have ≥50% in a certain K.

	K1	K2	K3	K4	K5	K6	K7	K8	Sum	Total	Missing
C9 species	0	24	0	0	0	14	0	2	40	44	4
Broccoli	0	0	2	57	0	8	0	0	67	87	20
Cauliflower	0	0	57	4	1	5	2	138	207	230	23
Collard Green	0	0	0	0	0	19	0	0	19	22	3
Heading	1	0	0	2	1	64	220	0	288	311	23
Kale	1	0	0	0	1	30	1	0	33	45	12
Ornamental	0	0	0	0	0	16	4	0	20	26	6
Kohlrabi	0	0	0	0	35	12	1	1	49	50	1
Sprouts	48	0	0	0	0	1	0	0	49	49	0
Tronchuda	0	0	0	0	0	23	0	0	23	25	2
Wild oleracea	0	0	0	0	0	8	3	0	11	16	5
Off types	0	0	0	2	1	2	2	1	8	8	0
Total	50	24	59	65	39	202	233	142	814	913	99

Appendix 5: Phenotypic data analysis ZonMW2016

In this appendix, the ANOVA results are shown based on the ZonMW2016 dataset. Pictures were taken from both sides of the cabbage heads in block A & B. This orientation (frontal side & cross section side) is tested in *section 5.1* and *5.2*. In *section 5.3*, the block effect is tested and significant results are tested for interaction in *section 5.4*. Significant effect are shown in red.

Appendix 5.1: ANOVA | Orientation effect block A

HL	Degrees of freedom	Sum of squares	Mean square	F-value	P-value
Orientation	1	75044.	75044.	38.54	<.001
Residual	617	1201434.	1947.		
Total	618	1276478.			

HWi	Degrees of freedom	Sum of squares	Mean square	F-value	P-value
Orientation	1	47163.	47163.	5.20	0.023
Residual	617	5597883.	9073.		
Total	618	5645046.			

HoW	Degrees of freedom	Sum of squares	Mean square	F-value	P-value
Orientation	1	0.0322	0.0322	0.28	0.600
Residual	617	72.1357	0.1169		
Total	618	72.1680			

AR	Degrees of freedom	Sum of squares	Mean square	F-value	P-value
Orientation	1	0.04922	0.04922	0.99	0.321
Residual	617	30.77664	0.04988		
Total	618	30.82585			

A	Degrees of freedom	Sum of squares	Mean square	F-value	P-value
Orientation	1	1.407	1.407	0.27	0.602
Residual	617	189.654	5.170		
Total	618	3191.060			

P	Degrees of freedom	Sum of squares	Mean square	F-value	P-value
Orientation	1	0.671	0.671	0.64	0.425
Residual	617	649.270	1.052		
Total	618	649.941			

R	Degrees of freedom	Sum of squares	Mean square	F-value	P-value
Orientation	1	0.000042	0.000042	0.00	0.945
Residual	617	5.358887	0.008685		
Total	618	5.358929			
M	**Degrees of freedom**	**Sum of squares**	**Mean square**	**F-value**	**P-value**
Orientation	1	0.00029	0.00029	0.01	0.939
Residual	617	30.63975	0.04966		
Total	618	30.64004			

Appendix 5.2: ANOVA | Orientation effect block B

HL	Degrees of freedom	Sum of squares	Mean square	F-value	P-value
Orientation	1	86324	86324	25.70	<.001
Residual	665	2233269	3358		
Total	666	2319594			

HWi	Degrees of freedom	Sum of squares	Mean square	F-value	P-value
Orientation	1	45515	45515	6.13	0.014
Residual	665	4935544	7422		
Total	666	4981059			

A	Degrees of freedom	Sum of squares	Mean square	F-value	P-value
Orientation	1	2.662	2.662	0.85	0.357
Residual	665	2083.374	3.133		
Total	666	2086.037			

AR	Degrees of freedom	Sum of squares	Mean square	F-value	P-value
Orientation	1	0.00602	0.00602	0.11	0.742
Residual	665	37.04934	0.05571		
Total	666	37.05536			

HoW	Degrees of freedom	Sum of squares	Mean square	F-value	P-value
Orientation	1	0.0317	0.0317	0.27	0.603
Residual	665	77.9393	0.1172		
Total	666	77.9710			

P	Degrees of freedom	Sum of squares	Mean square	F-value	P-value
Orientation	1	0.000	0.000	0.00	0.995
Residual	665	100.043	1.053		
Total	666	700.043			

R	Degrees of freedom	Sum of squares	Mean square	F-value	P-value
Orientation	1	0.001367	0.001367	0.19	0.664
Residual	665	4.814068	0.007239		
Total	666	4.815434			

M	Degrees of freedom	Sum of squares	Mean square	F-value	P-value
Orientation	1	0.01148	0.01148	0.26	0.613
Residual	665	29.76384	0.04476		
Total	666	29.77532			

Appendix 5.3: ANOVA | Block effect

HL	Degrees of freedom	Sum of squares	Mean square	F-value	P-value
Block	3	104500	34833	12.68	<.001
Residual	1282	3521642	2747		
Total	1285	3626141			

HWi	Degrees of freedom	Sum of squares	Mean square	F-value	P-value
Block	3	5430	1810	0.22	0.884
Residual	1282	10621168	8285		
Total	1285	10626598			

A	Degrees of freedom	Sum of squares	Mean square	F-value	P-value
Block	3	12.777	4.259	1.04	0.376
Residual	1282	5268.752	4.110		
Total	1285	5281.518			

AR	Degrees of freedom	Sum of squares	Mean square	F-value	P-value
Block	3	0.21100	0.07033	1.33	0.263
Residual	1282	67.85673	0.05293		
Total	1285	68.06773			

HoW	Degrees of freedom	Sum of squares	Mean square	F-value	P-value
Block	3	2.3488	0.7829	6.79	<.001
Residual	1282	147.9248	0.1154		
Total	1285	150.2936			

P	Degrees of freedom	Sum of squares	Mean square	F-value	P-value
Block	3	6.399	2.133	2.03	0.108
Residual	1282	1349.125	1.052		
Total	1285	1355.525			

R	Degrees of freedom	Sum of squares	Mean square	F-value	P-value
Block	3	0.042667	0.014222	1.80	0.146
Residual	1282	10.143720	0.007912		
Total	1285	10.186387			

M	Degrees of freedom	Sum of squares	Mean square	F-value	P-value
Block	3	0.19219	0.06406	1.36	0.253
Residual	1282	60.25320	0.04700		
Total	1285	60.44539			

CL	Degrees of freedom	Sum of squares	Mean square	F-value	P-value
Block	3	15026	5009	0.85	0.468
Residual	1282	3780646	5907		
Total	1285	3795671			

Appendix 5.4: ANOVA | Block*Genotype effect

HL	Df	Sum of squares	Mean square	F-value	P-value
Block	3	104500	34833	24.29	<.001
TKI_number	110	1696046	15419	10.75	<.001
Block*TKI_number	105	295688	2816	1.96	<.001
Residual	1067	1529908	1434		
Total	1285	3626141	2822		

HoW	Df	Sum of squares	Mean square	F-value	P-value
Block	3	2.34878	0.78293	15.70	<.001
TKI_number	110	77.55770	0.70507	14.14	<.001
Block*TKI_number	105	17.16043	0.16343	3.28	<.001
Residual	1067	53.20670	0.04987		
Total	1285	150.27361	0.11694		

Appendix 5.5: Pearson correlation matrix

The raw output of the Pearson correlation matrix for ZonMW2016. Correlations ≥ 0.50 are considered positive correlations and ≥ -0.50 considered negative correlations (both shown in red). The matrix was calculated with 86 heading cabbage accessions.

A	1	-											
AR	2	-0.48	-										
CL	3	-0.27	-0.18	-									
HL_A	4	-0.35	-0.24	0.58	-								
HL_B	5	-0.17	-0.15	0.55	0.65	-							
HWe	6	-0.27	0.07	0.52	0.35	0.53	-						
Hwi	7	0.54	-0.43	0.26	-0.05	0.21	0.52	-					
LoW_A	8	-0.25	0.04	-0.04	0.52	0.23	-0.36	-0.71	-				
LoW_B	9	0.08	0.01	-0.13	0.26	0.30	-0.41	-0.54	0.71	-			
M	10	0.59	-0.85	0.09	0.12	0.14	-0.04	0.53	-0.12	-0.03	-		
P	11	0.07	0.06	-0.20	0.10	0.00	-0.49	-0.48	0.55	0.60	-0.11	-	
R	12	-0.78	0.50	0.06	-0.01	-0.05	0.13	-0.46	0.00	-0.18	-0.61	-0.02	-
		1	2	3	4	5	6	7	8	9	10	11	12

Appendix 5.6: Q-Q plots ZonMW2016

The Q-Q plots of the measured traits in ZonMW2016 to check normality assumptions.

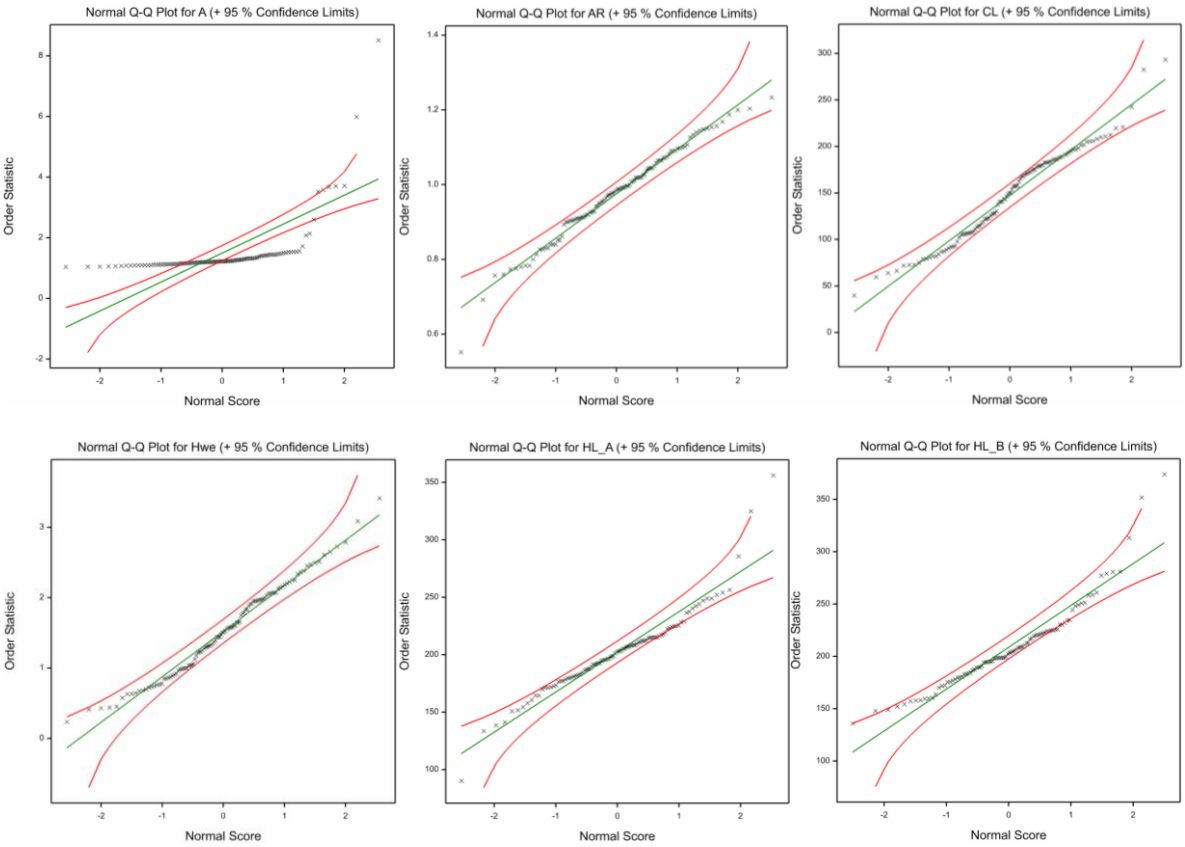

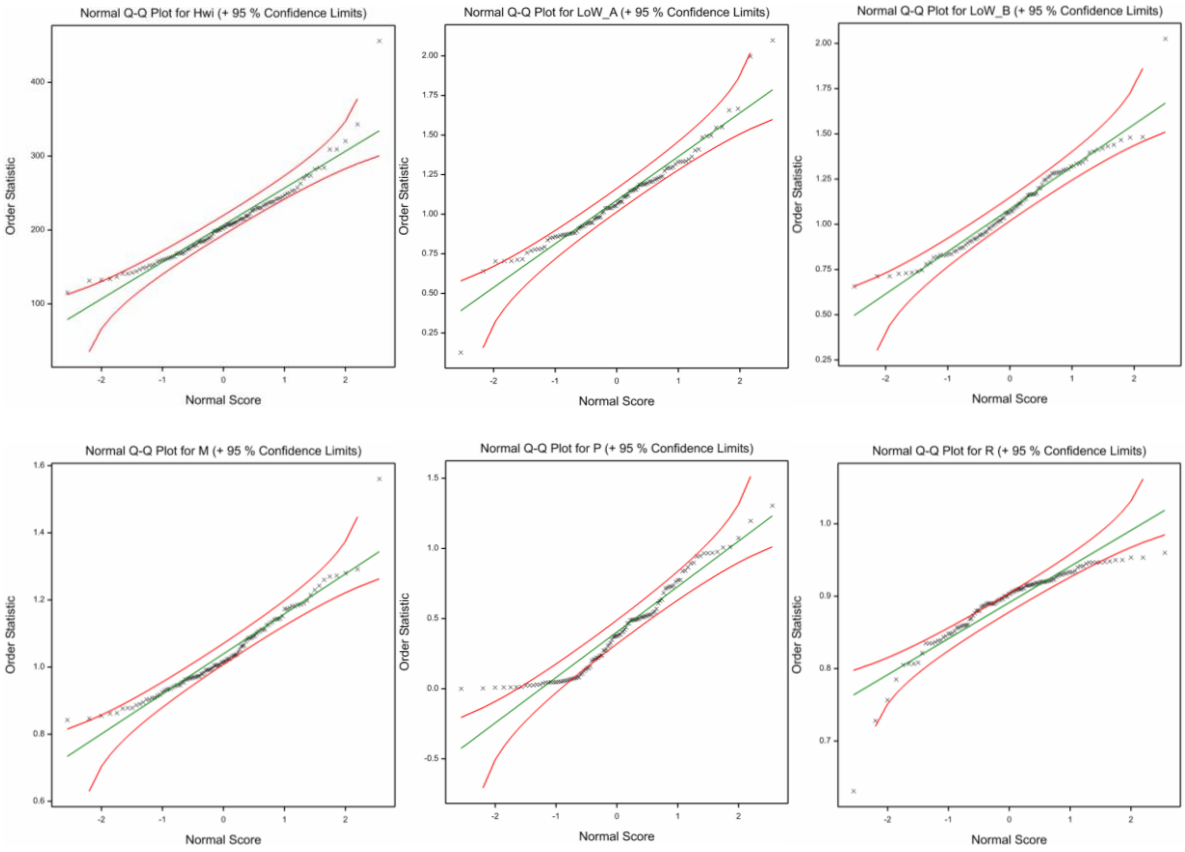

Appendix 5.7: ANOVA | Traits per morphotype

A	Degrees of freedom	Sum of squares	Mean square	F-value	P-value
Type	3	3.1078	1.0359	2.19	0.094
Residual	105	49.6696	0.4730		
Total	108	52.7772			

Type:	Mean	Score
Pointed	-	-
Red	-	-
Savoy	-	-
White	-	-

AR	Degrees of freedom	Sum of squares	Mean square	F-value	P-value
Type	3	0.19510	0.06503	4.94	0.003
Residual	106	1.39449	0.01316		
Total	109	1.58959			

Type:	Mean	Score
Pointed	0.7850	a
Red	0.9997	b
Savoy	0.9384	b
White	0.9884	b

CL	Degrees of freedom	Sum of squares	Mean square	F-value	P-value
Type	3	127495	42498	32.10	<0.001
Residual	106	140320	1324		
Total	109	267815			

Type:	Mean	Score
Pointed	236.7	d
Red	96.4	a
Savoy	128.8	b
White	167.1	c

HL	Degrees of freedom	Sum of squares	Mean square	F-value	P-value
Type	3	36056	12019	9.21	<0.001
Residual	90	117448	1305		
Total	93	153505			

Type:	Mean	Score
Pointed	292.2	c
Red	198.0	ab
Savoy	187.3	a
White	211.5	b

HWe	Degrees of freedom	Sum of squares	Mean square	F-value	P-value
Type	3	17.0814	5.6938	20.17	<0.001
Residual	106	29.9177	0.2822		
Total	109	46.9991			

Type:	Mean	Score
Pointed	1.606	bc
Red	1.229	b
Savoy	0.875	a
White	1.849	c

HWi	Degrees of freedom	Sum of squares	Mean square	F-value	P-value
Type	3	31519	10506	6.56	<0.001
Residual	104	166465	1601		
Total	107	197984			

Type:	Mean	Score
Pointed	196.8	ab
Red	178.4	a
Savoy	187.3	a
White	217.2	b

LoW	Degrees of freedom	Sum of squares	Mean square	F-value	P-value
Type	3	1.38719	0.46240	10.69	<0.001
Residual	90	3.89336	0.04326		
Total	93	5.28054			

Type:	Mean	Score
Pointed	1.418	b
Red	1.235	b
Savoy	1.032	a
White	1.003	a

M	Degrees of freedom	Sum of squares	Mean square	F-value	P-value
Type	3	0.11781	0.03927	3.42	0.020
Residual	105	1.20402	0.01147		
Total	108	1.32183			

Type:	Mean	Score
Pointed	1.151	b
Red	1.016	a
Savoy	1.083	b
White	1.020	a

P	Degrees of freedom	Sum of squares	Mean square	F-value	P-value
Type	3	1.24147	0.41382	4.16	0.008
Residual	106	10.53573	0.09939		
Total	109	11.77720			

Type:	Mean	Score
Pointed	0.7575	c
Red	0.5298	bc
Savoy	0.4075	ab
White	0.3299	a

R	Degrees of freedom	Sum of squares	Mean square	F-value	P-value
Type	3	0.028061	0.009354	3.95	0.010
Residual	106	0.250862	0.002367		
Total	109	0.278926			

Type:	Mean	Score
Pointed	0.8310	a
Red	0.8745	ab
Savoy	0.8918	bc
White	0.9014	c

Appendix 5.8: Boxplots ZonMW2016

Visualisation of the ANOVA output in *appendix 5.7*. The traits A, AR, LoW, M, P and R are depicted here. The remainder, HL, HWi, HWe and CL are depicted in *section 4.1.2.*

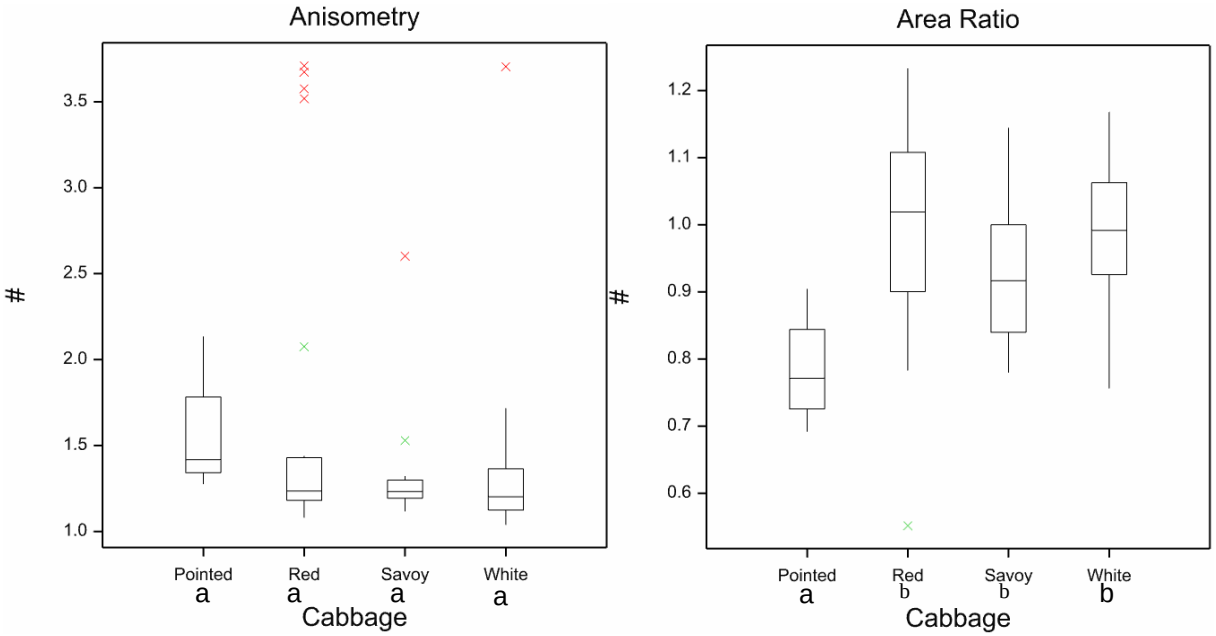

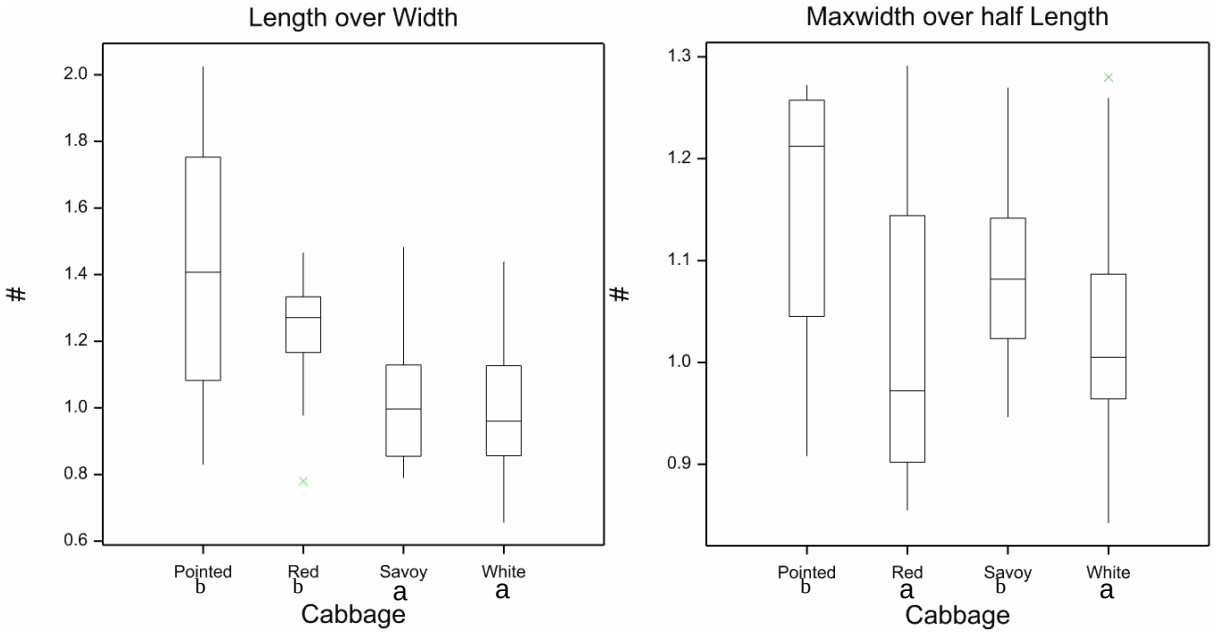

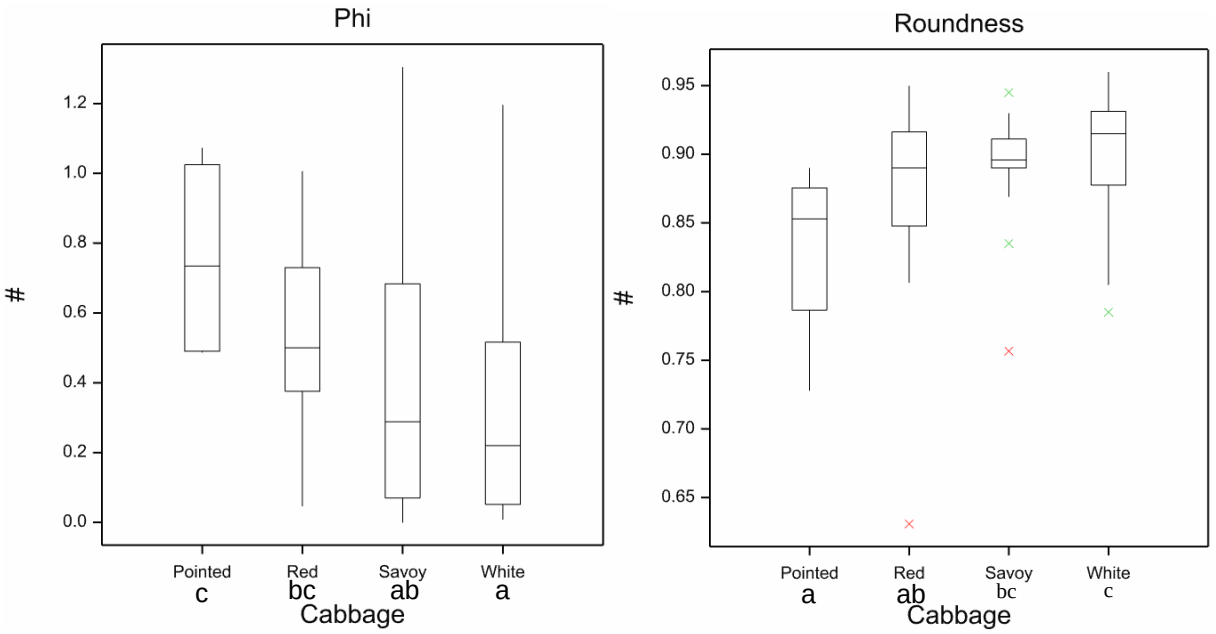

Appendix 6: Phenotypic data analysis Companies2015

This appendix contains the statistical analysis of phenotypic data originating from the Companies2015 dataset. Trait correlation can be seen in *appendix 6.1*, normality control in *appendix 6.2* and the statistical analysis visualized in Boxplots in *appendix 6.3*. The raw ANOVA output can be seen in *appendix 6.4*.

Appendix 6.1: Pearson correlation matrix Companies2015

A red/orange colour means a positive correlation between two traits. A blue colour means a negative correlation between these traits (*figure 21*). HWe and HWi are positively correlated. Other correlations were not found (> 0.50)

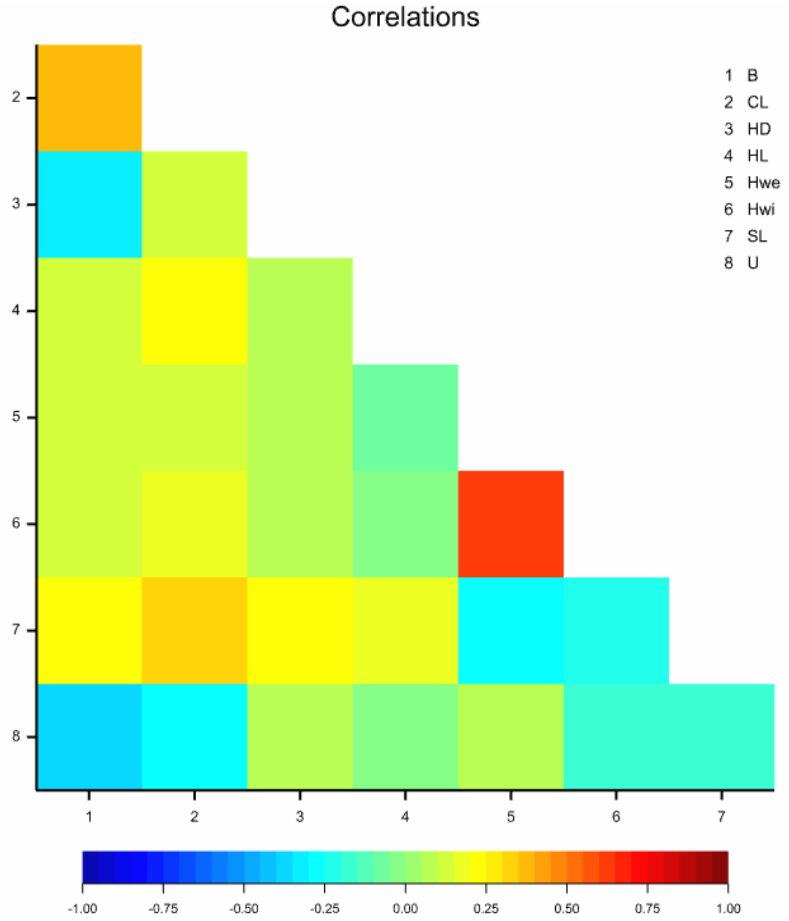

Figure 21: Pearson correlation test for traits in Companies2015 (n=46). A red/orange colour indicates a positive correlation whereas a blue colour indicates a negative correlation.

B	1	-						
CL	2	0.3625	-					
HD	3	-0.3486	0.1109	-				
HL	4	0.1371	0.2055	0.0741	-			
HWe	5	0.1031	0.1262	0.0914	-0.0856	-		
HWi	6	0.1420	0.1829	0.1000	-0.0413	0.6446	-	
SL	7	0.2123	0.3123	0.2418	0.1749	-0.2843	-0.2381	-
U	8	-0.3540	-0.2523	0.0798	-0.0246	0.0767	-0.1934	-0.1577
		1	2	3	4	5	6	7

Appendix 6.2: Q-Q plots Companies2015

The Q-Q plots of traits in Companies2015 are made to check normality assumptions.

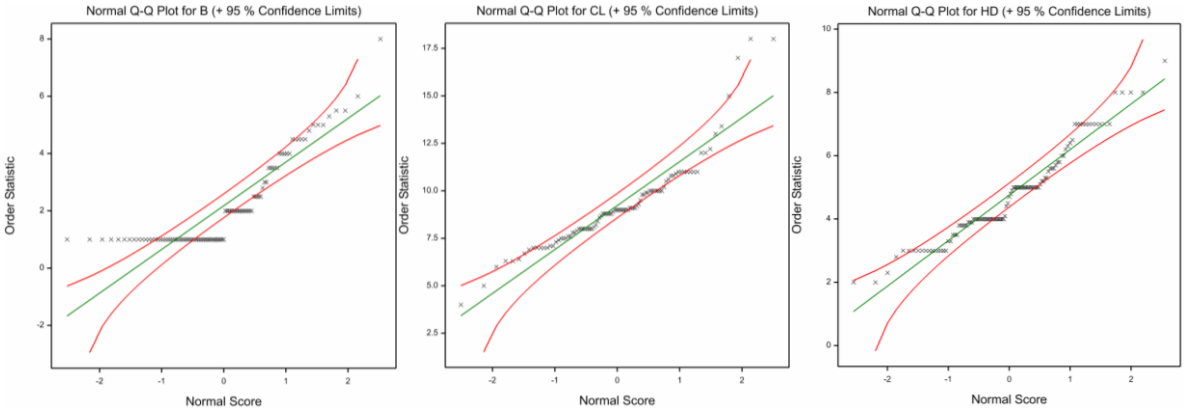

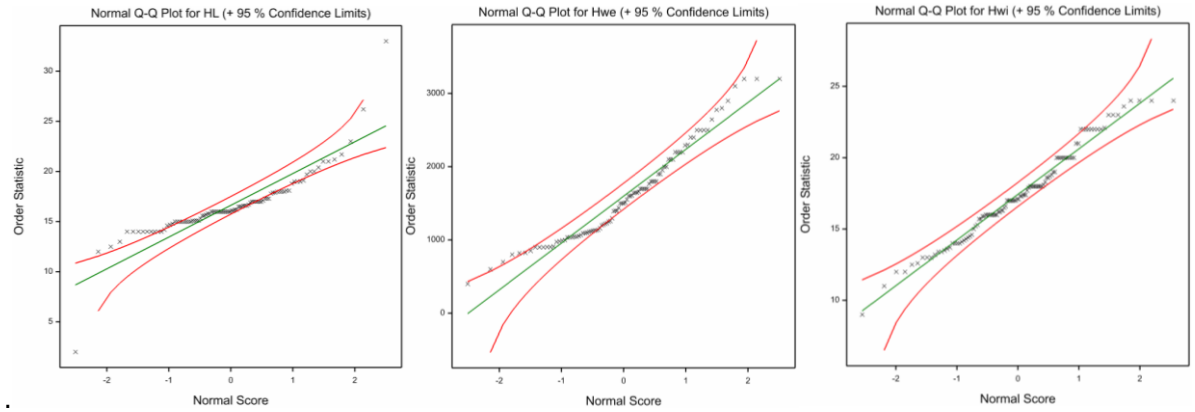

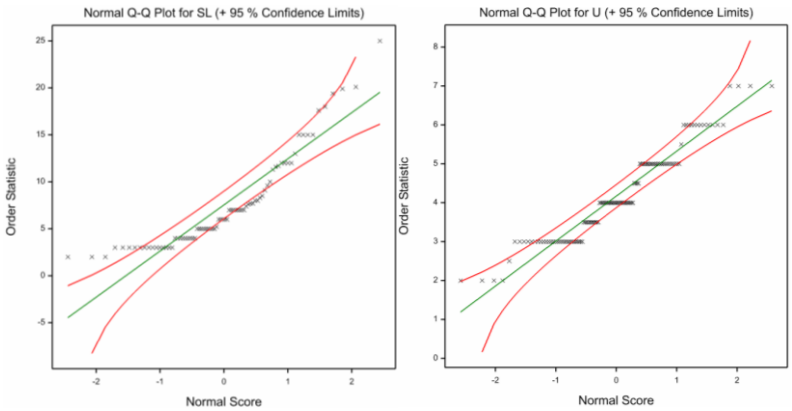

Appendix 6.3: ANOVA | Traits per morphotype

B	Degrees of freedom	Sum of squares	Mean square	F-value	P-value
Type	2	163.6182	81.8091	109.16	<.001
Residual	96	71.9436	0.7494		
Total	98	235.5618			

Type:	Mean	Score
Pointed	1.000	a
Red	-	-
Savoy	4.077	b
White	1.328	a

CL	Degrees of freedom	Sum of squares	Mean square	F-value	P-value
Type	3	17.382	5.794	1.05	0.375
Residual	90	497.144	5.524		
Total	93	514.526			

Type:	Mean	Score
Pointed	-	-
Red	-	-
Savoy	-	-
White	-	-

HD	Degrees of freedom	Sum of squares	Mean square	F-value	P-value
Type	3	17.611	5.870	2.90	0.039
Residual	105	212.657	2.025		
Total	108	230.269			

Type:	Mean	Score
Pointed	4.250	ab
Red	5.382	b
Savoy	4.223	a
White	4.895	b

HWe	Degrees of freedom	Sum of squares	Mean square	F-value	P-value
Type	3	11838725.	3946242.	12.88	<.001
Residual	91	27871640.	306282.		
Total	94	39710365.			

Type:	Mean	Score
Pointed	1500	ab
Red	1627	b
Savoy	1114	a
White	1913	b

HL	Degrees of freedom	Sum of squares	Mean square	F-value	P-value
Type	3	298.602	99.534	13.43	<.001
Residual	90	666.775	7.409		
Total	93	965.377			

Type:	Mean	Score
Pointed	33.00	b
Red	16.11	a
Savoy	17.21	a
White	16.04	a

HWi	Degrees of freedom	Sum of squares	Mean square	F-value	P-value
Type	3	207.505	69.168	7.82	<.001
Residual	104	919.858	2.845		
Total	107	1127.363			

Type:	Mean	Score
Pointed	14.50	a
Red	15.12	ab
Savoy	16.94	a
White	18.59	c

SL	Degrees of freedom	Sum of squares	Mean square	F-value	P-value
Type	2	407.466	203.73	10.02	<.001
Residual	75	1524.98	20.33		
Total	77	1932.44			

Type:	Mean	Score
Pointed	4.750	a
Red	11.806	b
Savoy	-	-
White	6.456	a

U	Degrees of freedom	Sum of squares	Mean square	F-value	P-value
Type	3	13.586	4.529	3.51	0.018
Residual	112	144.386	1.286		
Total	115	157.972			

Morphotype:	Mean	Score
Pointed	4.500	ab
Red	4.882	b
Savoy	3.790	a
White	4.141	a

Appendix 6.4: Boxplots Companies 2015

Visualisation of the ANOVA output in *appendix 6.3*. Traits B, CL, HL, HWi, SL and U are depicted here. HD and HWe in *section 4.1.1.*

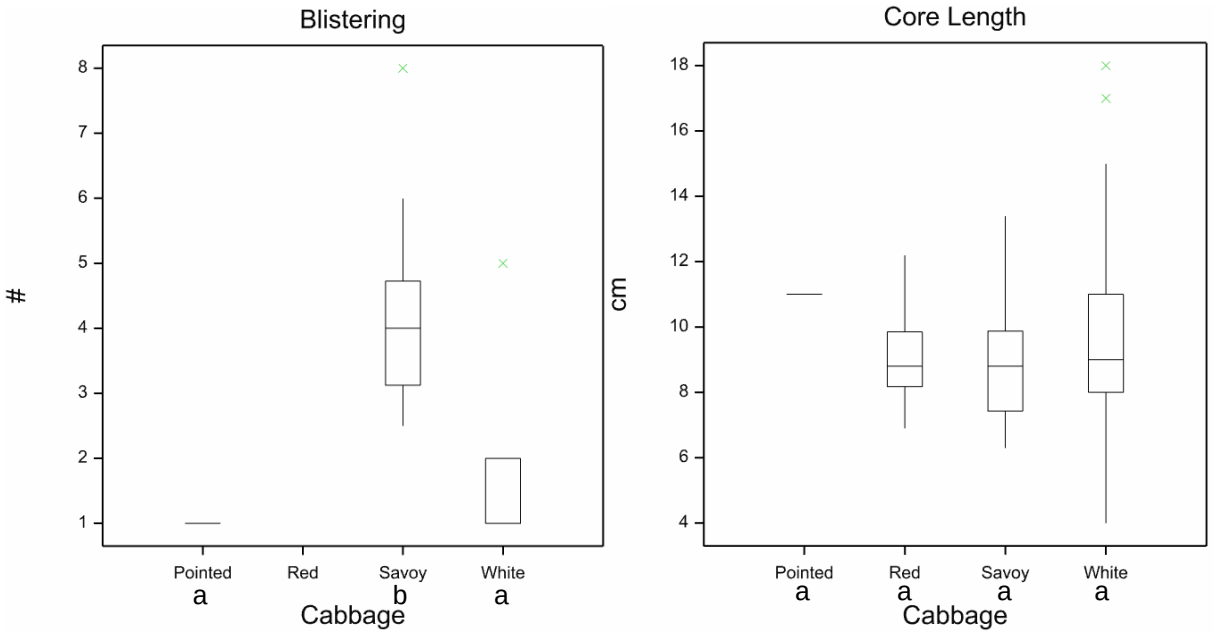

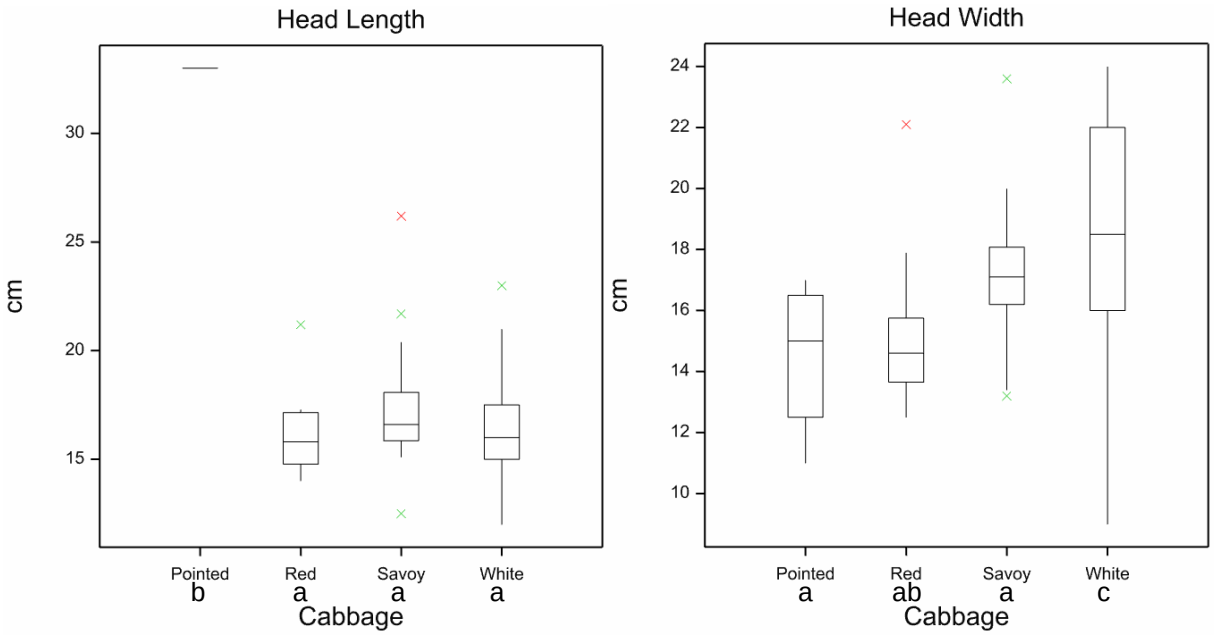

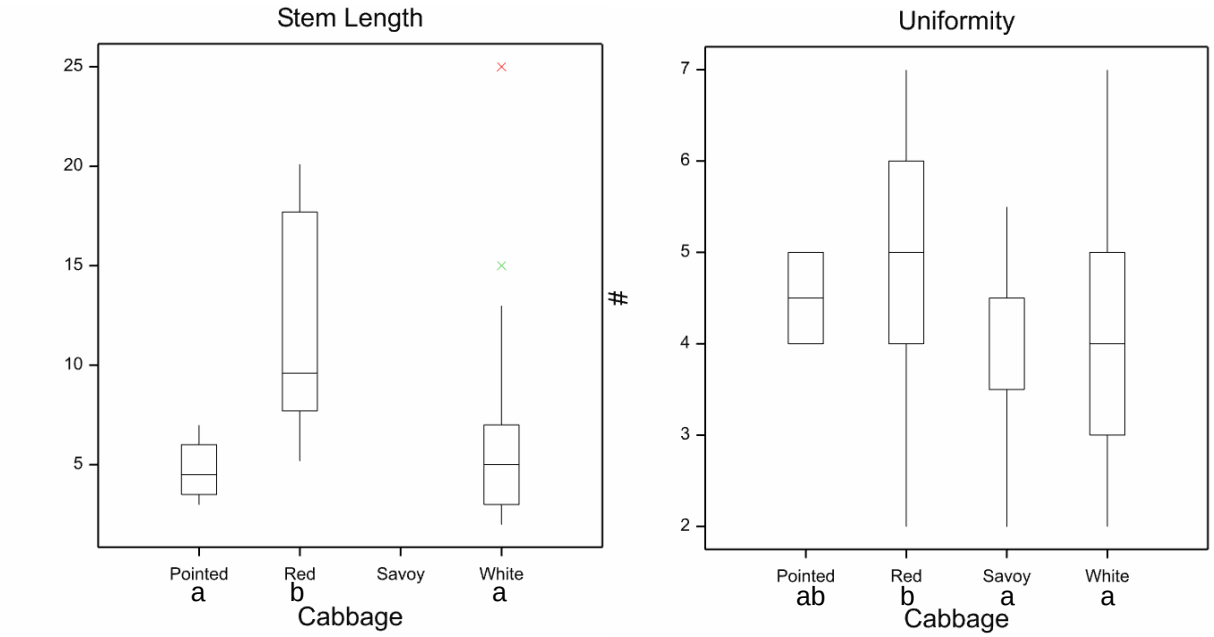

Appendix 7: GWAS

Appendix 7.1: Thresholds for GWAS per trait

In this table, an overview is given for the thresholds linked to a significant marker-trait association. Three sets are shown: No population structure (NoPS), K8 and K11. Each trait is tested for significance with the FDR method. Furthermore, not all traits are present in each dataset (WURFiled2015, Companies2015 and ZonMW2016). For each trait the significant P-value is given with the corresponding LOD score: $LOD = -\log^{10}(P - value)$.

Set	Trait	Threshold WURField2015		Threshold Companies2015		Threshold ZonMW2016	
		LOD	P-value	LOD	P-value	LOD	P-value
NoPS	A	*	*	*	*	4.384	0.000041318
NoPS	B	*	*	3.465	0.000342838	*	*
NoPS	CL	*	*	*	*	3.171	0.000674280
NoPS	HA	3.778	0.000166533	*	*	*	*
NoPS	HD	3.893	0.000127872	*	*	*	*
NoPS	HI	3.209	0.000618639	*	*	*	*
NoPS	HL	4.131	0.000074015	4.503	0.000031398	5.278	0.000005270
NoPS	HR	4.795	0.000016037	*	*	*	*
NoPS	HS	4.219	0.000060445	*	*	*	*
NoPS	HV	3.485	0.000327403	*	*	*	*
NoPS	HWe	3.709	0.000195522	5.943	0.000001139	4.200	0.000063145
NoPS	HWeP	4.034	0.000092518	*	*	*	*
NoPS	HWi	3.246	0.000567446	*	*	4.919	0.000012051
NoPS	LoW_B	*	*	*	*	3.902	0.000125300
NoPS	R	*	*	*	*	5.127	0.000007460
NoPS	SL	*	*	4.379	0.000041739	*	*

NoPS	TW	3.873	0.000133843	*	*	*	*
K8	A	*	*	*	*	4.501	0.000031567
K8	B	*	*	4.133	0.000073546	*	*
K8	CL	*	*	*	*	3.163	0.000686449
K8	HA	3.687	0.000205500	*	*	*	*
K8	HD	4.954	0.000011126	*	*	*	*
K8	HI	3.341	0.000456060	*	*	*	*
K8	HL	4.340	0.000045668	4.480	0.000033111	5.454	0.000003514
K8	HR	5.909	0.000001234	*	*	*	*
K8	HS	5.909	0.000001234	*	*	*	*
K8	HV	3.440	0.000362820	*	*	*	*
K8	HWe	3.454	0.000351760	6.244	0.000000570	3.785	0.000164082
K8	HWeP	3.926	0.000118490	*	*	*	*
K8	HWi	3.242	0.000573320	*	*	5.011	0.000009757
K8	LoW_B	*	*	*	*	4.172	0.000067346
K8	R	*	*	*	*	5.065	0.000008609
K8	SL	*	*	4.425	0.000037565	*	*
K8	TW	3.619	0.000240680	*	*	*	*
K11	A	*	*	*	*	4.485	0.000032715
K11	B	*	*	4.318	0.000048088	*	*
K11	CL	*	*	*	*	3.315	0.000484417
K11	HA	3.909	0.000123430	*	*	*	*
K11	HD	5.255	0.000005563	*	*	*	*
K11	HI	3.764	0.000172180	*	*	*	*
K11	HL	4.678	0.000020982	4.424	0.000037678	5.387	0.000004099
K11	HR	6.210	0.000000617	*	*	*	*
K11	HS	5.608	0.000002468	*	*	*	*
K11	HV	3.665	0.000216330	*	*	*	*
K11	HWe	3.664	0.000216610	*	*	4.003	0.000099239
K11	HWeP	4.188	0.000064799	*	*	*	*
K11	HWi	3.467	0.000341270	5.944	0.000001137	5.127	0.000007461
K11	LoW_B	*	*	*	*	5.454	0.000003514
K11	R	*	*	*	*	4.986	0.000010331
K11	SL	*	*	4.373	0.000042335	*	*
K11	TW	4.048	0.000089484	*		*	*

Appendix 7.2: Manhattan plots WURField2015

WURField2015-NoPS

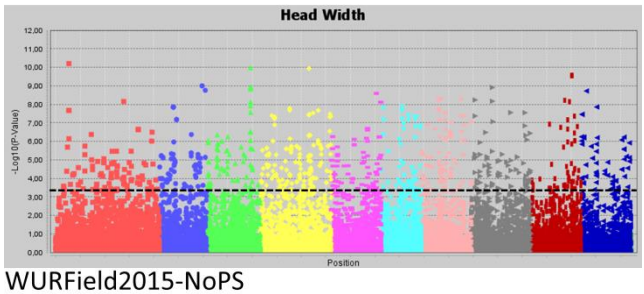

WURField2015-NoPS

WURField2015-K8

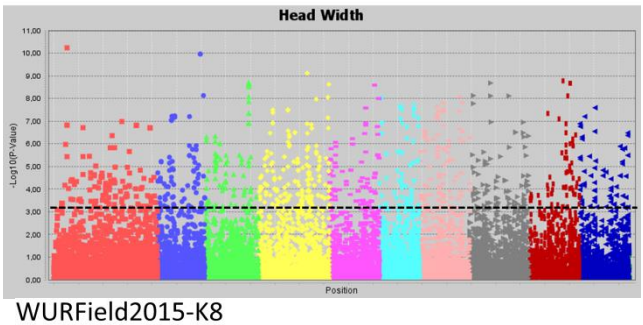

WURField2015-K8

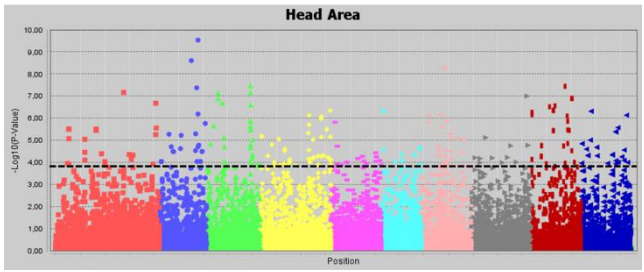

WURField2015-NoPS

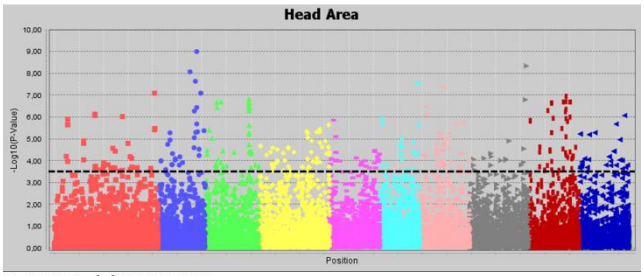

WURField2015-K8

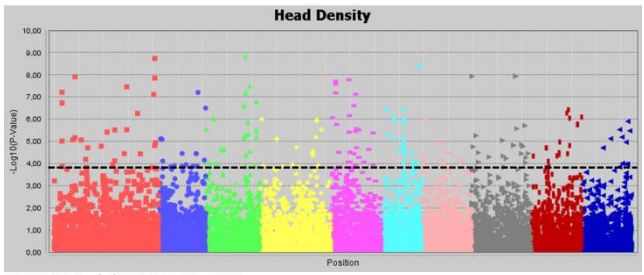

WURField2015-NoPS

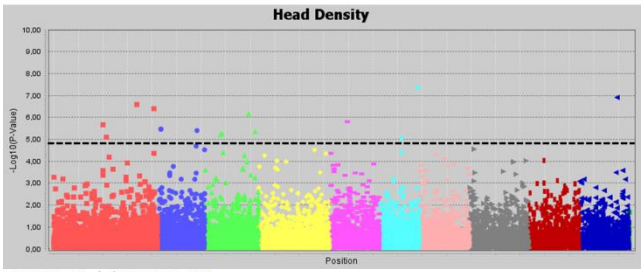

WURField2015-K8

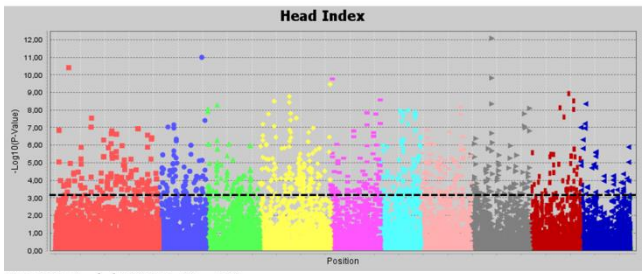

WURField2015-NoPS

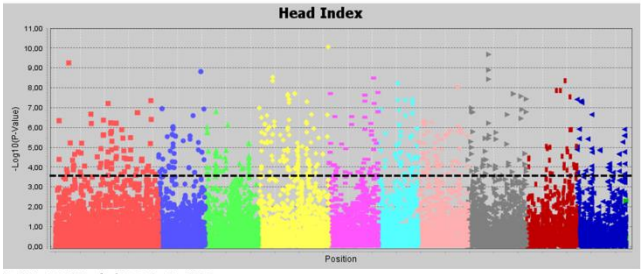

WURField2015-K8

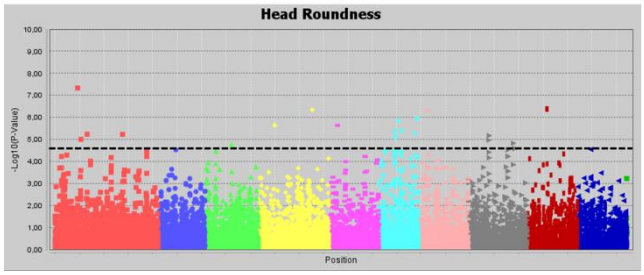

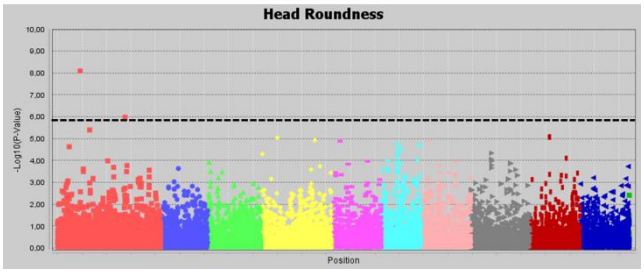

WURField2015-NoPS

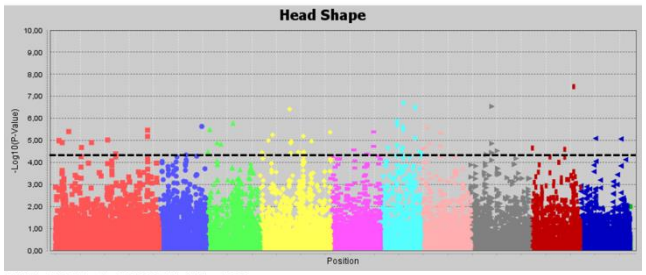

WURField2015-K8

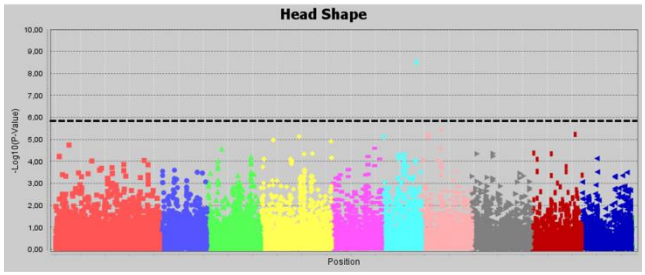

WURField2015-NoPS

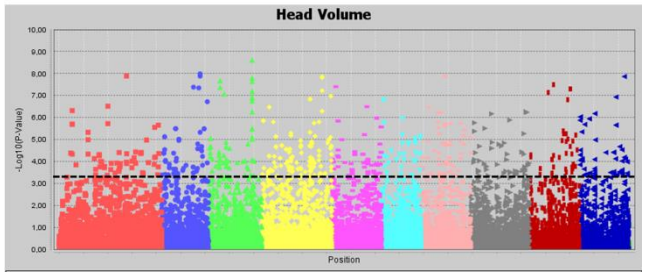

WURField2015-K8

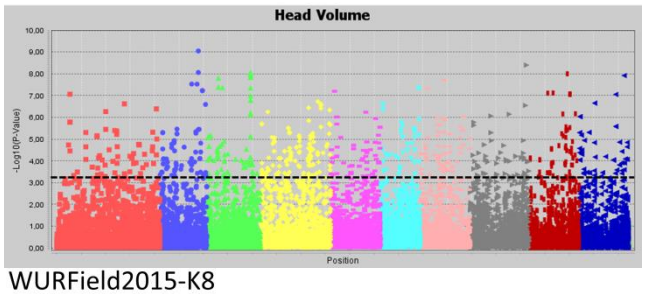

WURField2015-NoPS

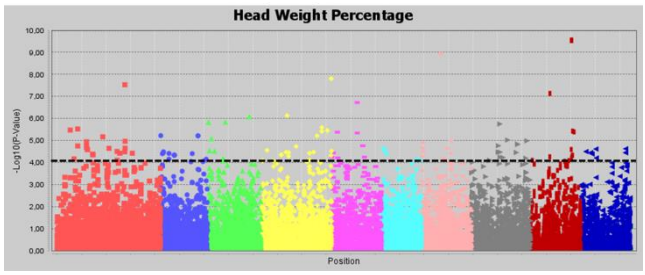

WURField2015-K8

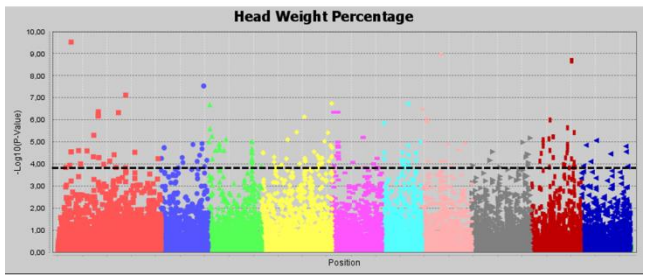

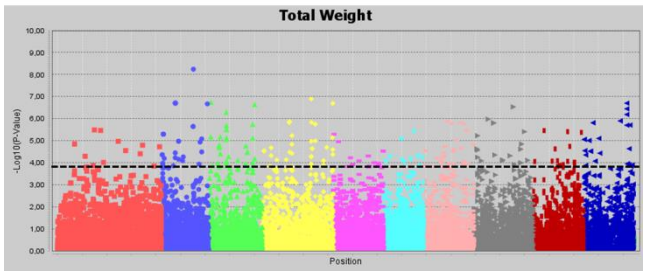

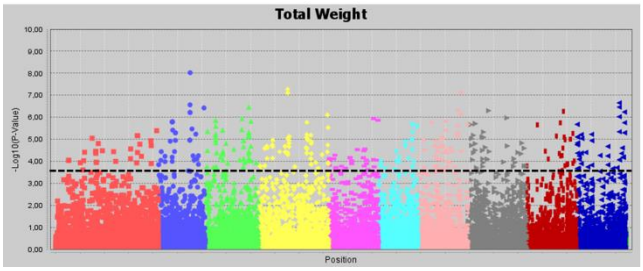

Appendix 7.3: Manhattan plots Companies2015

Companies2015-NoPS

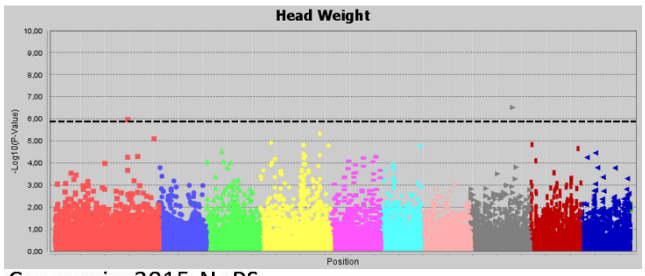

Companies2015-K8

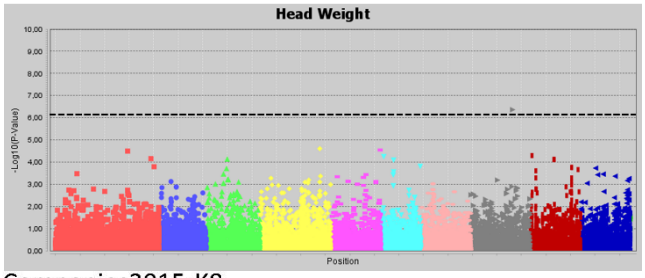

Companies2015-NoPS

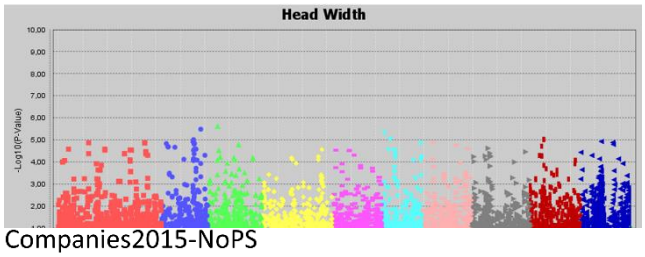

Companies2015-K8

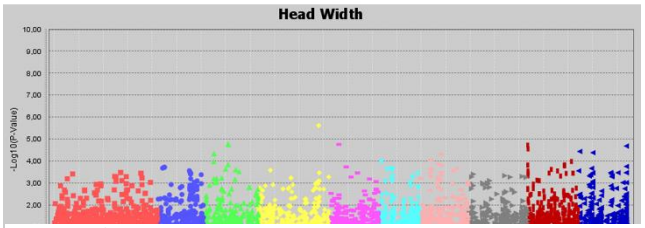

Companies2015-NoPS

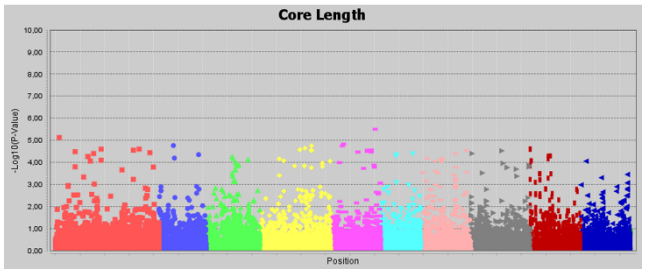

Companies2015-K8

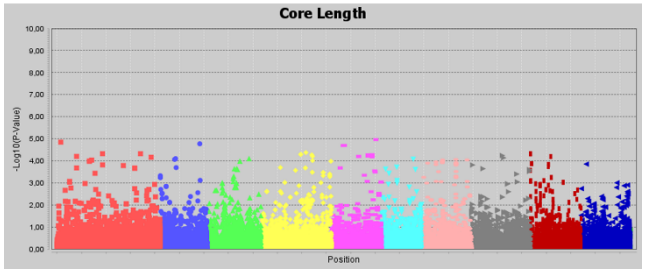

Companies2015-NoPS

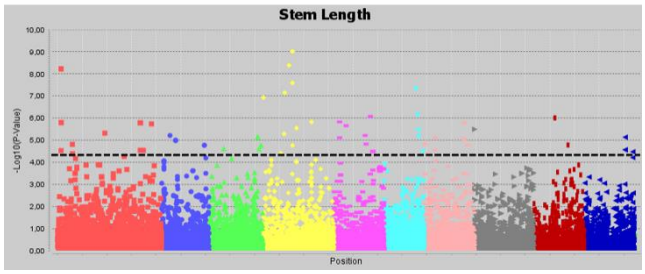

Companies2015-K8

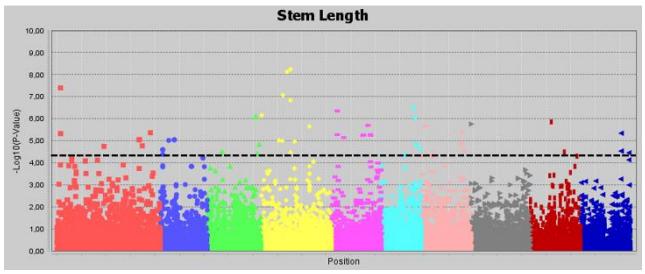

Companies2015-NoPS

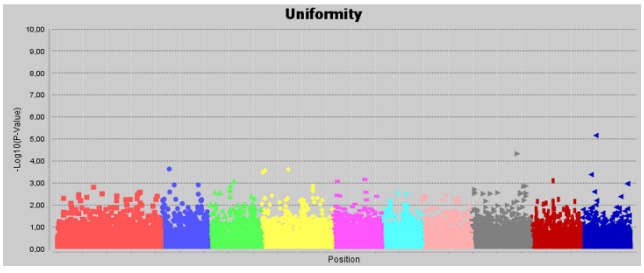

Companies2015-K8

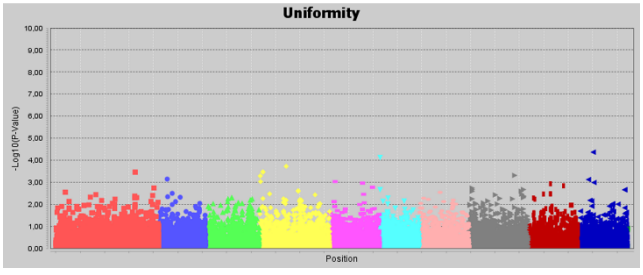

Companies2015-NoPS

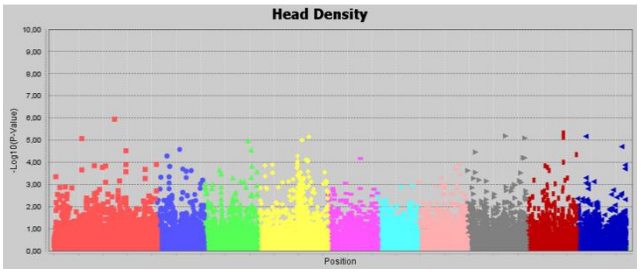

Companies2015-K8

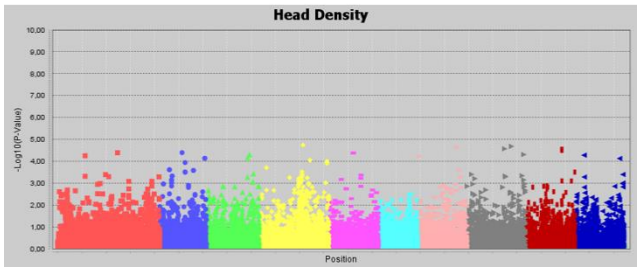

Appendix 7.4: Manhattan plots ZonMW2016

ZonMW2016-NoPS

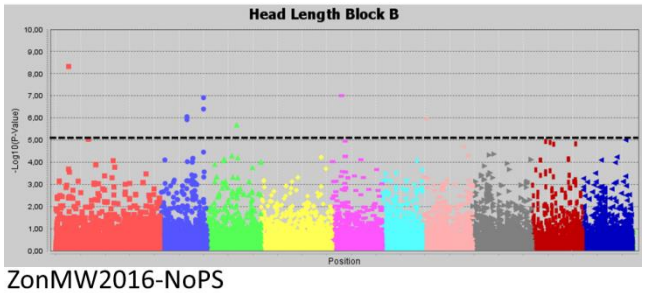

ZonMW2016-NoPS

ZonMW2016-K8

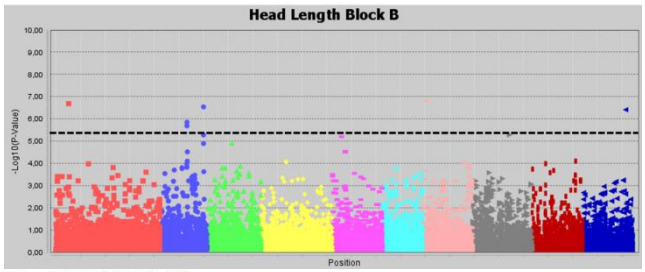

ZonMW2016-K8

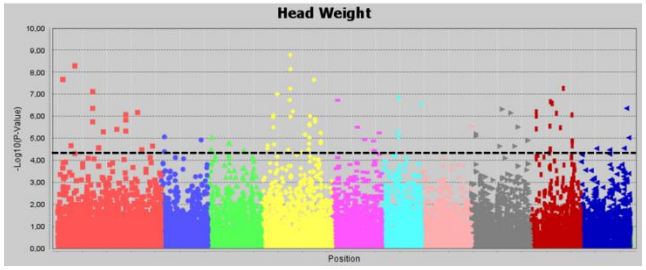

ZonMW2016-NoPS

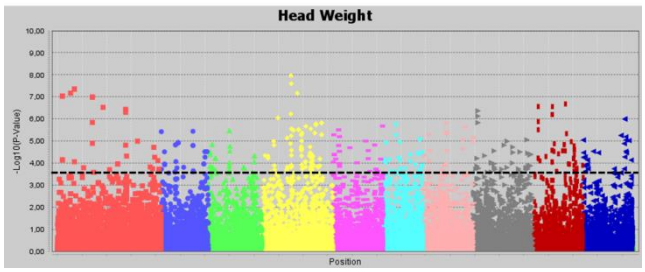

ZonMW2016-K8

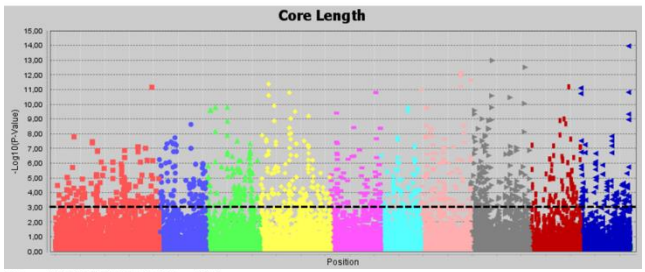

ZonMW2016-NoPS

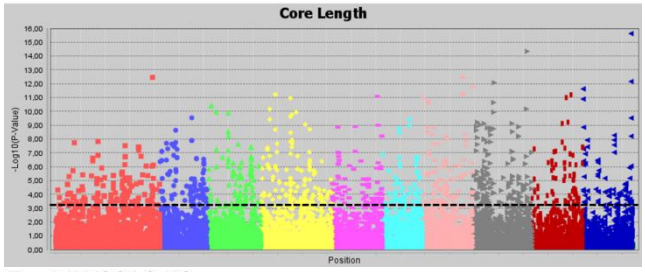

ZonMW2016-K8

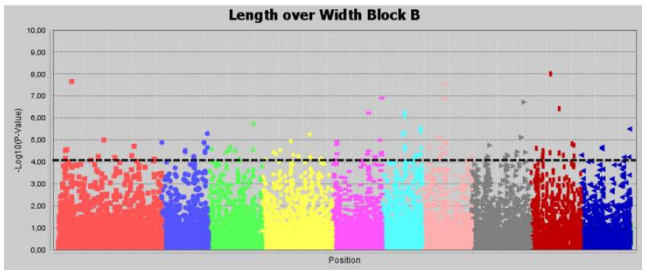

ZonMW2016-NoPS

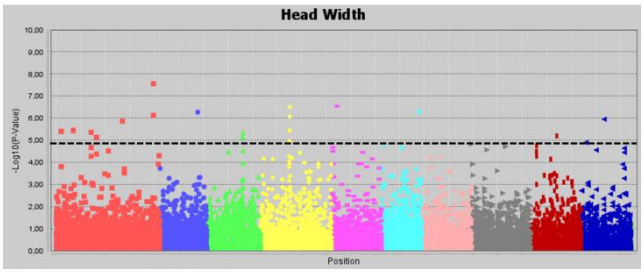

ZonMW2016-K8

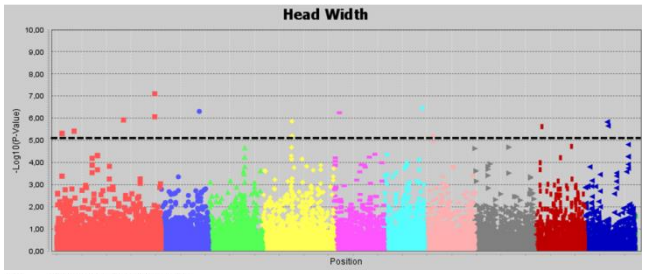

ZonMW2016-NoPS

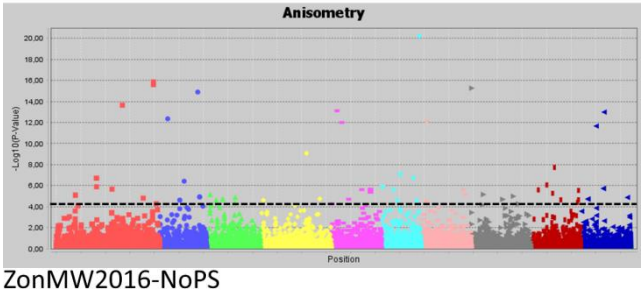

ZonMW2016-K8

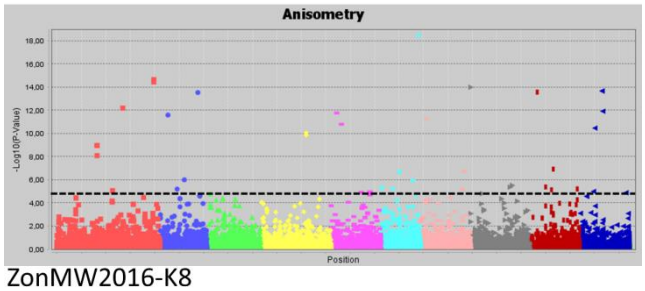

ZonMW2016-NoPS

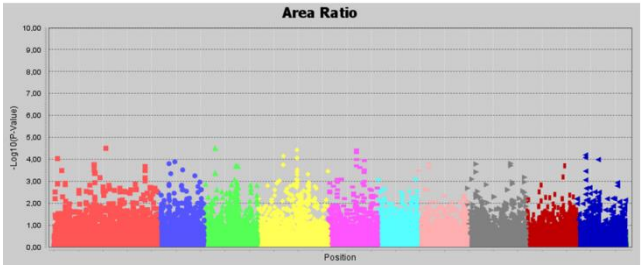

ZonMW2016-K8

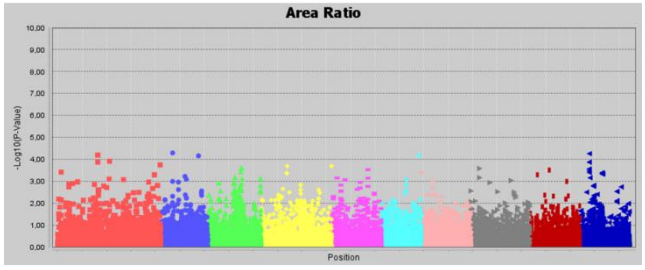

ZonMW2016-NoPS

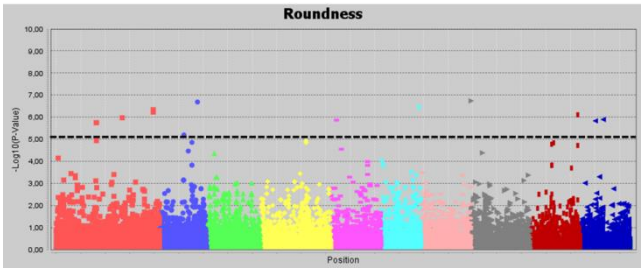

ZonMW2016-K8

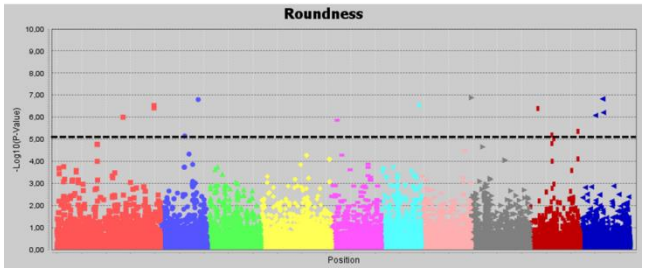

ZonMW2016-NoPS

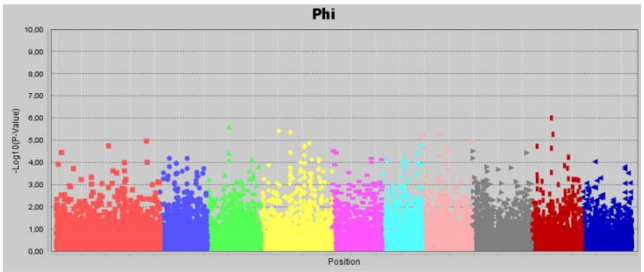

ZonMW2016-K8

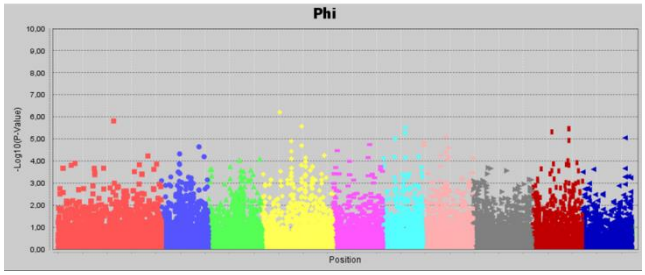

ZonMW2016-NoPS

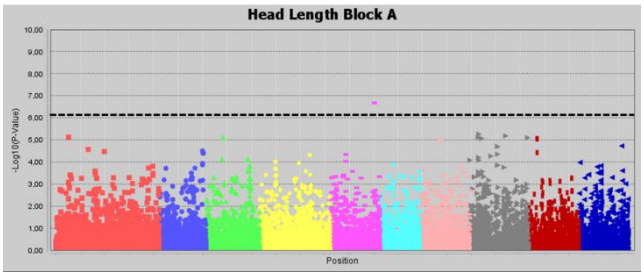

ZonMW2016-K8

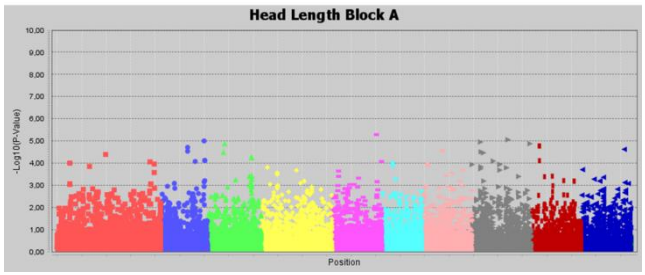

ZonMW2016-NoPS

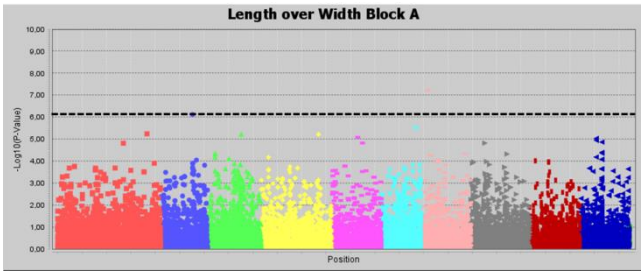

ZonMW2016-K8

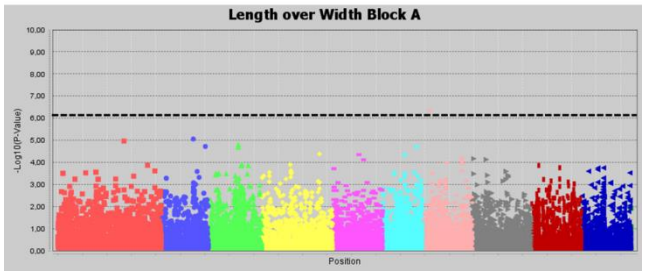

ZonMW2016-NoPS

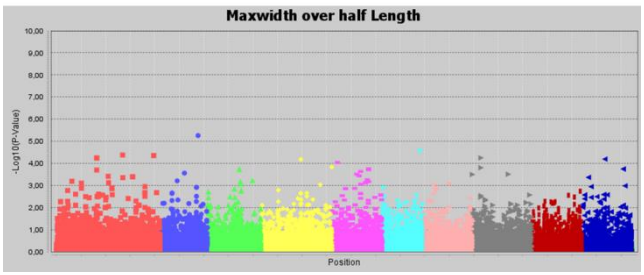

ZonMW2016-K8

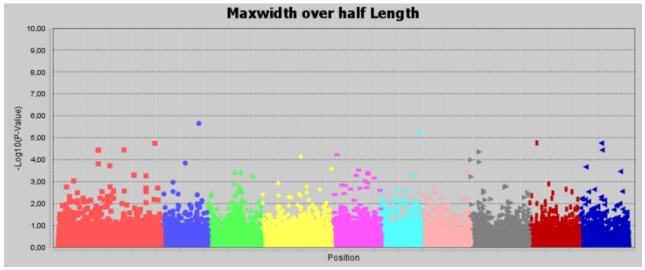

Appendix 7.5: Marker density

The distribution of SNPs over the genome. The marker distribution is low on the upper and lower part of C02. The upper part of C07 also has a low density as well as the upper part of C09.